CHALMERS

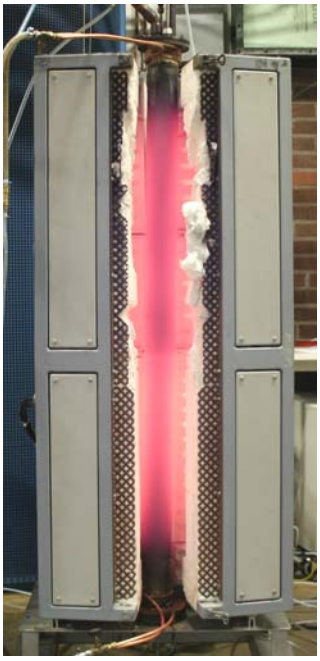

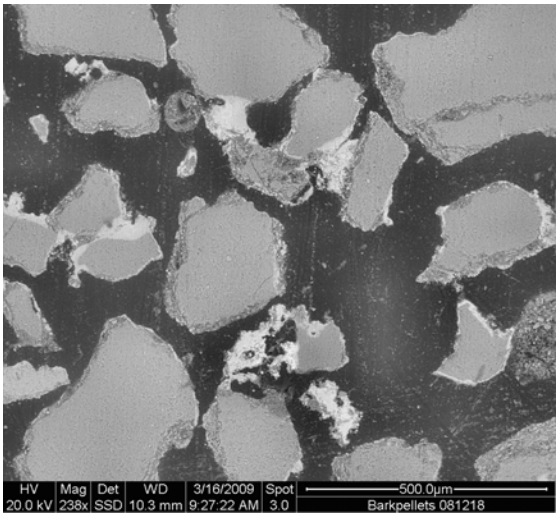

Prevention of Bed Agglomeration Problems in a Fluidized Bed Boiler by Finding the Trigging Value of Sewage Sludge Dosage Added to Combustion of Biofuels

Master of Science Thesis in Innovative and Sustainable Chemical Engineering

KAJSA ANDERSSON

PERNILLA GERVIND

Department of Energy and Environment
Division of Energy Technology
CHALMERS UNIVERSITY OF TECHNOLOGY
Göteborg, Sweden 2009
T2009-327

Prevention of Bed Agglomeration Problems in a Fluidized Bed Boiler by Finding the Trigging Value of Sewage Sludge Dosage Added to Combustion of Biofuels

KAJSA ANDERSSON
PERNILLA GERVIND

Department of Energy and Environment
CHALMERS UNIVERSITY OF TECHNOLOGY
Göteborg, Sweden 2009

Abstract

Agglomeration of bed sand is a common problem during combustion of biofuels with high ash content in fluidized bed boilers. Former studies have shown that co-combustion of biofuels with sewage sludge increases the agglomeration temperature. Sewage sludge has a low heating value and high ash content. It would therefore be better to use sludge as an additive to the combustion than as a co-combusted biofuel.

In this study the trigging value of sludge addition to the combustion of some biofuel was investigated. The effect of adding sludge with different precipitation chemicals, iron sulphate and aluminium sulphate, was investigated. The biofuels used for the experiments were bark, refused derived fuel (RDF) and a mixture of wood and straw, 75/25 % on energy basis. All experiments were carried out in a laboratory scale fluidized bed reactor.

Analyses of chemical composition of bed sand and SEM/EDX analyses were performed after the combustion. Eventually agglomeration tests were performed in order to find the agglomeration temperature of the samples. Some of the samples sintered during the combustion and were not tested for the agglomeration temperature.

SEM/EDX showed that all samples of bed sand contained sand particles with more or less coatings. In some cases the coatings seemed to consist of one dense inner layer and one more porous outer layer.

From SEM/EDX and chemical composition analyses it was found that the total amount of phosphorous in the bed sand samples was increased with an increased addition of sludge in all experiments. The concentration of phosphorous was especially higher in the outer layers/coatings. It was also found that elements from the sludge seem to get caught by a sticky layer at the bed sand surface and form a non-sticky or less sticky layer that prevents agglomeration.

The total amount of aluminium was increased with an increased addition of sludge for the wood/straw samples, while it increased with an increased amount of combusted fuel for the RDF cases. A tendency of a higher concentration of aluminium in the bed sand could be seen in the samples precipitated with aluminium sulphate than the samples precipitated with iron sulphate. The total amount of potassium in the bed sand was only little increased during the combustion for all experiments.

The experiments showed that for the wood/straw samples an addition of 2wt% sludge was enough to increase the bed agglomeration temperature with about 100°C and an addition of 6wt% sludge gave an even better effect. For RDF an addition of 6wt% sludge was necessary to give any effect. Sludge precipitated with aluminium sulphate gave a better effect than sludge precipitated with iron sulphate.

Table of content

Introduction 1

1.1 Objective 3

2 Background 4

2.1 The fluidized bed boiler 4

2.1.1 Bed material 7

2.2 Combustion of solid fuels 8

2.3 Biofuels 9

2.3.1 Ash in biofuels 10

2.4 Agglomeration 12

2.4.1 Mechanisms of agglomeration 12

2.4.2 Melt induced agglomeration 13

2.4.3 Reaction introduced agglomeration 14

2.4.4 Melting behaviour of different components 14

2.4.5 Prevention of bed agglomeration 15

2.5 Additives 16

2.6 Sewage sludge 16

2.6.1 Zeolites 17

2.6.2 Phosphates 19

2.7 Ash elements that influence bed agglomeration 19

3 Method 22

3.1 Fuels used in the experiments 22

3.2 Experimental design 24

3.3 Combustion equipment 25

3.3.1 The laboratory scale reactor 25

3.3.2 The carousel feeder 26

3.4 First experiments and parameter settings 26

3.5 Chemical analysis of bed sand composition 27

3.6 SEM/EDX analysis 28

3.7 Agglomeration test 29

4 Results and discussion 30

4.1 Combustion results 30

4.2 Analyses of the bed sand samples 31
4.2.1 Bed sand samples after combustion 31
4.2.2 Results and discussion regarding the chemical analysis of the bed material after combustion 34
4.2.3 Results and discussion from the SEM/EDX analysis 37
4.2.4 Results and discussion regarding the agglomeration temperatures 51
4.2.5 Summary of the agglomeration discussion 52
4.2.6 Bed sand samples after agglomeration tests 53
5 Discussion and suggestions for further investigation 54
6 Conclusions 57
7 References 58
Appendix 63
A. Fuel analyses I
B. Pelletized fuel III
C. Calculation of air factor, m IV
D. Combustion temperature, pressure drop and concentrations of CO and CO2 V
E. Samples of bed sand after combustion XV
F. Result from Chemical analysis of bed sand composition XVI
G. Result agglomeration test XVII
H. Agglomerated Bed sand samples XX
I. SEM/EDX – element quantification XXII

Acknowledgement

This master thesis is the result of the friendly cooperation between the Department of Energy technology at SP Technical Research Institute of Sweden in Borås and the Department of Energy and Environment at Chalmers University of Technology in Göteborg. The master thesis is a part of the frame work *"Measures for simultaneous minimization of alkali related operating problems"* which is funded by Värmeforsk Service AB.

For friendly assistance and support we would like to express our gratitude to our supervisors Lars-Erik Åmand, Chalmers, and Linda Bäfver, SP. We would also like to express our gratitude to Britt-Marie Steenari at the Department of Environmental Inorganic Chemistry at Chalmers University, who helped us with the SEM-EDX analyses and Fredrik Niklasson, SP, who never got tired of answering our questions. At last we would like to thank all colleagues at SP who helped us out and encouraged us.

Introduction

In the last years wood and wood residues have become attractive fuels for new possible use e.g. for production of biodiesel. The combustion industry is therefore looking at alternative fuels such as straw, hemp, red canary grass and refused derived fuels. The new fuels are often problematic because of their high content of ash and alkali. Examples of problems are agglomeration in the fuel bed, deposits and corrosion on heat transfer surfaces. These problems can lead to unwanted shutdowns in boiler operation and need for additional maintenance stops which are very costly and it is therefore of large interest to find a way to minimize these problems.

This master thesis is part of a larger research program. The program is the third phase in the frame work “Measures for simultaneous minimization of alkali related operating problems”, hereinafter referred to as *Agglobelägg* (1) (2). The overall scope of the frame work is to “characterise the operational problems and to study measures to minimize them” (1).

In phase one and two of the Agglobelägg project change of bed material, use of additives and co-combustion with sewage sludge were studied. The additives used were kaolin, zeolite, ammonium sulphate and elemental sulphur. One of the conclusions from the second phase was that co-combustion with sewage sludge had the best overall effect on reducing the studied problems that were bed agglomeration, alkali chloride content in the flue gases, deposits and corrosion (1). In contrary to the good effects, the dosage of sewage sludge gave an unwanted increase of ash in the bed.

Phase three of the Agglobelägg project is primarily oriented towards deposits and corrosion, but agglomeration is also studied. The dosage of sewage sludge should be optimized so that the increase of ash content in the bed could be minimized. Sewage sludge should therefore rather be regarded as an additive than a co-combusted fuel. In this master thesis laboratory scale experiments was performed to find the trigging value of the dosage of sludge. The effect of using sludge that are precipitated with different chemicals as additives to the combustion of different fuel mixtures was studied. The experiments should be seen as a complement to the experiments within the Agglobelägg project that are performed at the research boiler at Chalmers University of Technology, which is a 12MW circulating fluidized bed boiler.

1.1 Objective

It has been found in previous projects using the fluidized bed boiler at Chalmers, that the co-combustion of sewage sludge with biofuels has a positive effect on reducing the agglomeration tendency of bed material. However the addition of sewage sludge increases the ash concentration of the bed significantly and should rather be seen as an additive to the biofuel than an additional fuel. One objective of this master thesis was to find the trigging value of the dosage of sewage sludge so that the increasing ash concentration in the bed could be minimized at the same time as the advantages against bed agglomeration were maintained.

It was also to be investigated whether sewage sludge could give the same positive synergy effect on reducing bed agglomeration when combusting refused derived fuels (RDF).

Since different waste water treatment plants use different purification methods the composition of sewage sludge can differ between the plants. The third objective was to compare the effect of two different sewage sludge where phosphorous was precipitated with different chemicals to investigate if the effect on agglomeration tendencies differs between the sludge.

The experiments are performed in a laboration scale fluidized bed reactor. The results should be comparable with earlier results from the *Agglobelägg projects* therefore similar conditions and methods are used. The bed material is combusted with the different compositions of fuel and sludge that is to be studied. After the combustion the bed sand samples were analysed with chemical analysis and a scanning electron microscope (SEM) equipped with an energy dispersive x-ray detector (EDX). Eventually the bed agglomeration temperature was investigated using a standard method that will be explained in the report.

2 Background

Bed agglomeration occurs mainly during combustion of alkali rich solid fuels in fluidized beds. This chapter gives an introduction to the background theory. The fluidized bed boiler is described followed by the mechanisms of combustion of solid fuels. A short description of common biofuels and their structure is given. Finally the mechanisms of agglomeration and theories around prevention of the agglomeration tendency are more thoroughly described.

2.1 The fluidized bed boiler

The fluidized bed boiler is one of the most common boilers used for the combustion of biofuels. A fluidized bed boiler produces hot water used for district heating, but can be combined to also produce steam for turbine generation of electricity. There are two different types of fluidized bed combustors, bubbling fluidized bed and circulating fluidized bed, referred to as BFB and CFB respectively. The fuel that is to be combusted is mixed into a hot sand bed fluidized by a powerful fan. The combustion temperature is normally around 850 °C, which is low compared to the temperature in conventional burners using pulverized fuels. The fuel is well mixed with combustion gas and only a small excess of oxygen is needed. This together with the low combustion temperature, results in lower emissions of NO_x. Even SO_x emissions can be prevented since the bed easily can be mixed with limestone that binds the sulphur as calcium sulphate (3).

Heat transfer

The bed material is used to transfer heat from the fuel to the heat exchanger areas of the boiler. Biofuels in general have a lower heating value than traditionally used fuels, e.g. coal, and therefore require a boiler with more efficient heat transfer. Bed material has a higher convective heat transfer value than flue-gases which for a CFB makes the transfer of heat from the hot flue gases to the heat transfer surfaces in the combustor more efficient (4) (5). In a pulverized coal boiler a larger part of the heat is transferred through radiation.

The primary mechanism of heat transfer originates from the turbulent motion of bed particles towards the wall. This overall process is called particle convection and occurs in different ways. Heat can be transferred at areas where bed particles form comparatively dense clusters, groups or strands in contact with the wall, but the dominating part of the heat transfer takes place through the gas film layer that separates the bed particles from the wall (5). At elevated temperatures even a radiation effect that acts at uncovered surfaces as well as surfaces covered by particles, becomes relevant (5). This is the case at the top of the combustion chamber where the solids concentration of bed material is fairly low even in a CFB boiler.

The degree of heat transfer varies with different factors. In cases with a lower heating value of the fuel, bed material of a coarser size is preferably used. With the same amount of primary air this results in a poorer fluidization with a lower bed and less heat transfer (4). The height of the bed can be adjusted by changing the amount of bed material used and thus changing the heat transfer from the bed. The amount of bed material is an important operating parameter. Less amount of bed material used results in less number of bed particles transferring heat to the boiler walls and a higher bed temperature.

Start up

Before starting the combustion in the bed, the bed material and combustion chamber has to be heated to an appropriate ignition temperature. The furnace can be heated by start-up burners installed at the front or side walls in the furnace (3) (6). As an alternative to wall mounted burners the primary air can be pre-heated by a duct burner located at the entrance to the wind box (6). Both types of burners use oil or gas as fuel (6).

Feeder

Fuel is transported from storage to the boiler via a transport system that can be constructed of different kind of feeders, e.g. screw feeder, scrape feeder or a cell feeder. The fuel is fed to the bottom of the combustion chamber (see 2 in Figure 1).

Air distributor

Primary air is used to fluidize the bed. Flue gas can be recirculated to the bed to control the temperature in the combustion chamber. This gas mixture contains a shortage of oxygen which means that the bed is operated at sub- stoichiometric conditions. The remaining part of oxygen needed to achieve complete combustion is added as secondary air through nozzles at different heights in the lower parts of the combustor (see 4 in Figure 1). By adding air at different levels of the combustion chamber the combustion occurs in stages and minimizes the formation of NO_x-gases (6).

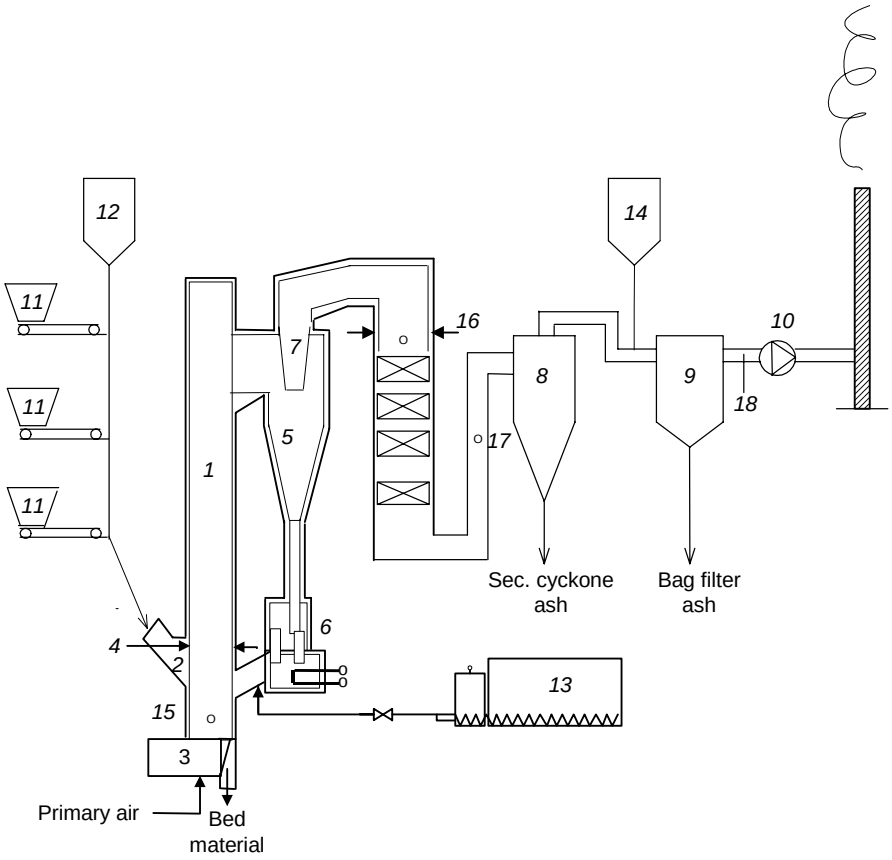

Figure 1. The 12-MW_{th} FBC boiler at Chalmers University of Technology.

(1) combustion chamber; (2) fuel feed chute; (3) air plenum; (4) secondary air inlet at 2.1m; (5) hot primary cyclone; (6) particle loop seal; (7) cyclone exit duct; (8) cold secondary cyclone; (9) bag house filter; (10) flue gas fan; (11) fuel bunkers; (12) sand bin; (13) sludge pump; (14) hydrated lime bin; (15) bed ash sampling hole; (16) measurement spot (before convection pass) IACM instrument, deposit probe and FTIR; (17) measurement spot (after convection pass) FTIR; (18) measurement spot (stack) FTIR.

Return and separation system

The high gas velocities created by the powerful fluidization carries sand and ash-particles from the bed. These particles have to be prevented from leaving the system. Different CFB processes have got different solid return systems. In circulating fluidized bed combustion the return system is simple, basically consisting of a cyclone (see 5 in Figure 1), some kind of particle seal (see 6 in Figure 1) (e.g. an overflow standpipe) and a return leg (7) (8).

Cyclone separators (see 5 in Figure 1) are used to separate sand and ash particles from the exiting flue gas. The separation mechanism used is radial centrifugal forces acting at the particles (9). The particles hits the cyclone wall where they slide to the downcomer of the cyclone and are collected in the particle seal to be restored to the bed. The finest particles follow the flue gas stream and are separated by bag filters or electrostatic precipitators. In some installations a secondary cyclone (see 8 in Figure 1) is located before the final device for fly ash removal.

The standpipe is a length of a pipe situated at the bottom of the cyclone, used to transfer solids from lower to higher pressure. The pressure in the bottom of the cyclone is much lower compared to the pressure in the bottom of the bed of the main combustion chamber to which the solids are to be returned. The solids can flow through the pipe in either dense or dilute phase. Most common for the CFB combustion is the overflow standpipe, where an upward gas flow relative the downcomming solids makes it possible to transfer solids by gravity. The overflow standpipe acts as a particle seal (see 6 in Figure 1) and hinders back flow of gas (8). The fluidization of particles in both the particle seal and the bed (of the main combustion chamber) make the particles flow like a liquid fluid against an adverse pressure gradient (7).

A baghouse filter (9 in Figure 1) or electrostatic filters are used for collecting the finest particles. The fine ash is pneumatically transported to ash silos, where it is stored. In some applications this ash is re-injected to the combustion chamber for increased burnout efficiency of the char fraction of the fly ash.

In a full scale fluidised boiler the bed sand is continuously taken out from the bottom of the bed via an ash drain system and replaced with new sand (6). The bed renewal can be in the range of 5 - 40 % of the total amount of bed material during a period of 24 hours (10). The particles are classified from their superficial velocity and the largest particles are removed in order to keep the bed pressure constant and maintain a good bed quality (6). Agglomeration makes it necessary with a more frequent bed renewal. This results in increased operation costs (10).

2.1.1 Bed material

No additional bed material has to be added to the bed when combusting e.g. coal or petcoke since the ash from these fuels gives good heat transfer due to a sufficient amount of inert material with an appropriate size. During combustion of biofuels it is however necessary to add extra material in the form of sand in order to achieve sufficient heat transfer.

Natural sand is the most commonly used bed material in fluidized bed combustion (4). This sand is a mixture of different minerals mostly quartz (SiO_2), but also feldspar ($KAlSi_3O_8$, $NaAlSi_3O_8$ or $CaAl_2Si_2O_8$) and biotite ($K(MgFe)_3(AlSi_3O_{10})(OH)_2$). The concentration of the different minerals differs depending on the origin of the sand. The bed sand must withstand the high temperatures in the boiler and all types of sand used have a melting point between 1100˚C and 1450˚C (4).

Since SiO_2 is one of the substances that are believed to have an impact on bed agglomeration, alternatives to natural sand have been investigated in phase 1 and 2 of the Agglobelägg projects. Sintered magnesite ($MgCO_3$) and calcined dolomite ($CaMg(CO_3)_2$) are examples of bed materials that have been tested (2). These materials are more expensive and lead to an increased operating cost unless the sand consumption is decreased. However this cost can be justified when using fuels known to cause severe agglomeration problems, e.g. straw.

2.2 Combustion of solid fuels

There exist a large number of different solid fuels such as peat, coal, lignite, petcoke, biomass and various types of solid combustible wastes (wood, plastics, paper, rubber, textiles, and sewage sludge). Different fuels burn in different ways and the combustion facility have to be designed to suit the chosen fuels. However the three main combustion mechanisms are the same for all types of solid fuels:

- Drying
- Devolatilization
- Char combustion

Drying

During drying the moisture in the fuel is vaporized and forced out of the particle. If the particle is small (e.g. pulverized coal) the drying is completed before the devolatilization starts. For larger fuels such as wood pellets the devolatilization starts before the core of the pellet is completely dry. The gas that is driven out during this second stage forces the vapour to the centre of the chip.

Devolatilization

When the fuel particle (or part of it) is completely dry the temperature rises and the fuel starts to decompose due to the heat. All oxygen is forced out of the particle during the devolatilization. When no external oxygen is present this process is called pyrolysis (11). During this process there are many reactions involved that forms CO, CO_2, CH_4, tar and other substances (12). The reactions are both endothermic and exothermic and the net heat of the devolatilization is said to be zero (11). The produced gases flow to the surface of the particle where they ignite in contact with air. Since all the oxygen is consumed at the surface of the particle the char combustion cannot start until the devolatilization has ended.

Char combustion

Char and ashes are left after the devolatilization. In the main reaction the char reacts with oxygen forming CO. This results in a partial oxidation of the char. There are other, slower, reactions present but these can be neglected when looking at main combustion reactions forming CO (11). To obtain complete combustion all CO has to be further oxidized by oxygen forming CO_2.

2.3 Biofuels

Biofuels are fuels that in contrary to fossil fuels can be re-created within a reasonable time period (13). They originate from relatively recently dead biomaterials and exist in solid, liquid or gaseous form.

All biomaterials have the same fundamental way of growth and reprocessing which make them very similar in main structure. However there are also major differences such as the content of lignin and ash. Sewage sludge and RDF can be classified as a biofuel and will be referred to that hereinafter (14).

Biomass is built up of cellulose, hemi-cellulose, lignin, organic substances with low molecular weight (e.g. lipids, terpenes) and ash (15). The main components in these parts are carbon, oxygen and hydrogen. The content of these substances in the combustible matter do not vary much between different biofuels, see Figure 2.

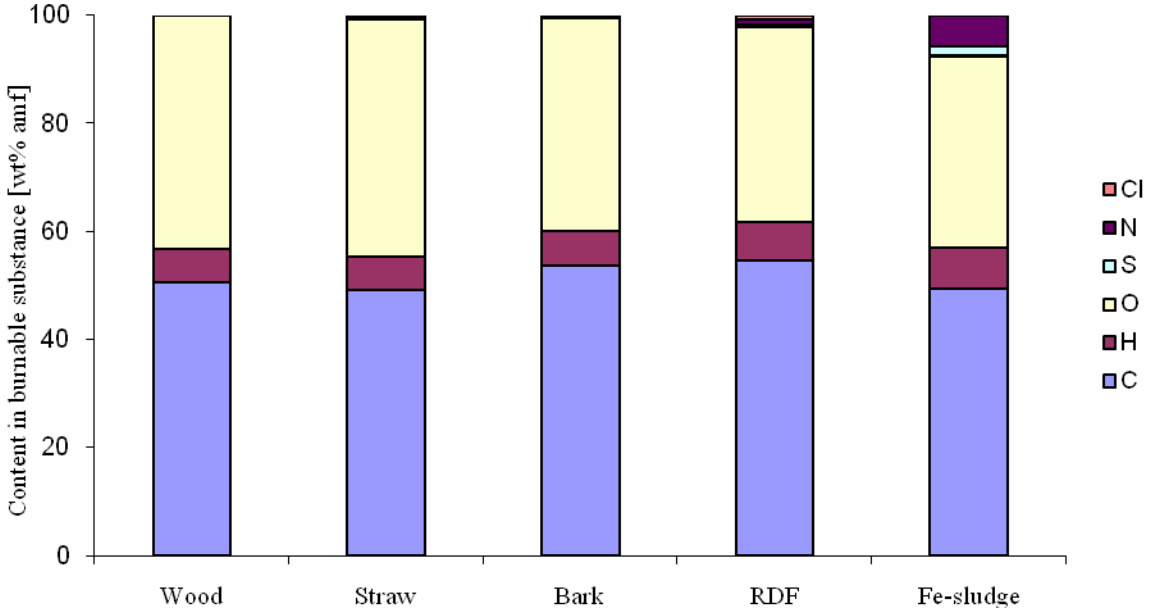

Figure 2. The content of elementary substances in some biofuels (18) (19) (20) (21). * amf = ash and moisture free. Rya is municipal sewage sludge from the municipal water treatment plant Ryaverket in Gothenburg.

Ash is the component that has the largest influence on bed agglomeration and therefore this is where the emphasis of this chapter will be.

2.3.1 Ash in biofuels

Ash is an umbrella term for the inorganic substances that do not take part in the combustion reactions. In a fluidized bed boiler part of the ash is accumulated in the bed, either as coarse ash particles or as components that have reacted with the bed material. The ash that is not captured in the bed is either vaporized or consists of so small particles that they can be carried away by the gas flow. Carried away ash that is not caught in the primary cyclone is referred to as fly ash.

The total amount of ashes differs between plant species. It varies from below 1% for wood to >18 % for straw (16), the difference can be seen in Figure 3, where the ash content for some biofuels is presented. Other biofuels that are rich in mineral matter are bark (17), energy crops and wood residues (18). The ash content differs widely within species of the same kind, for straw it can vary from 2 to >18 %.

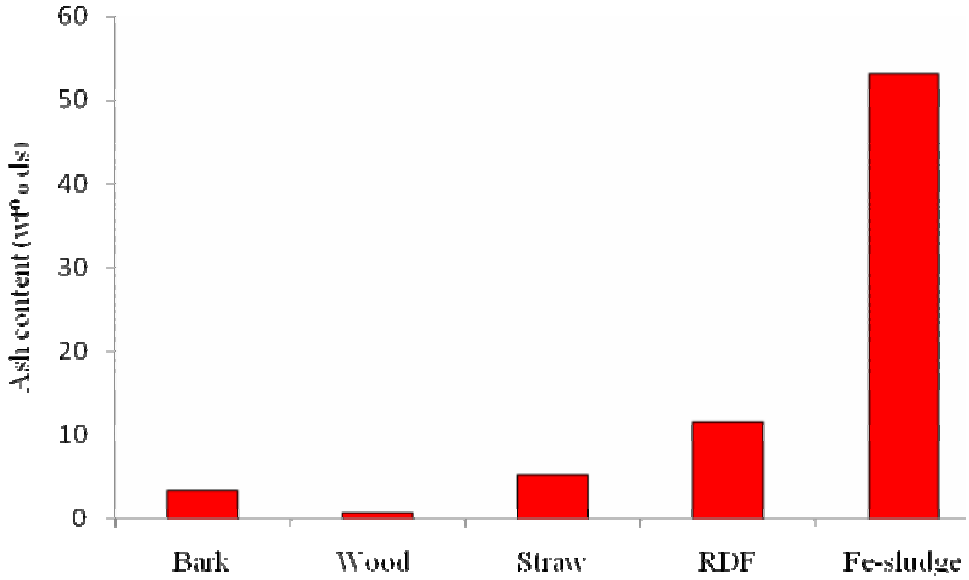

Figure 3. The ash content in various biofuels (18) (19) (20) (21). ds = dry substance. Fe is sewage sludge from the municipal waste water treatment plant Ryaverket in Gothenburg.

In the waste water treatment plant large amounts of the organic substance is digested by active bacteria in two steps, one aerobe and one anaerobe (22). The bacteria thus increase the concentration of ash in the sewage sludge by decreasing the organic content. The sludge from Ryaverket has an ash content of approximately 50% (ds).

The most common elements in biomass ashes are Ca, K, Mg, P, Si, Mn, Fe, Al, Na, S and Cl (15)-(18). The mineral concentration depends on plant species and what part of the plant that ends up in the fuel. The concentration of K is very high in annual growth materials such as straw, grass and leaves. In Figure 4 it is clearly seen that the concentration of K is higher in

straw than in wood and very low in RDF and sewage sludge. The content of Ca, P and Mg is also substantial in these parts (18). In the stem wood the situation is the opposite, these parts contain mostly Ca and lower concentrations of K, P, Mg and Si (18). In RDF the concentration of Na is significantly higher than for the other fuels. Magnesium is bound to the chlorophyll and can be found in all green parts of biomaterial (15). The high content of Fe and Al in the sewage sludge from Ryaverket originates from the chemicals used to precipitate phosphorous.

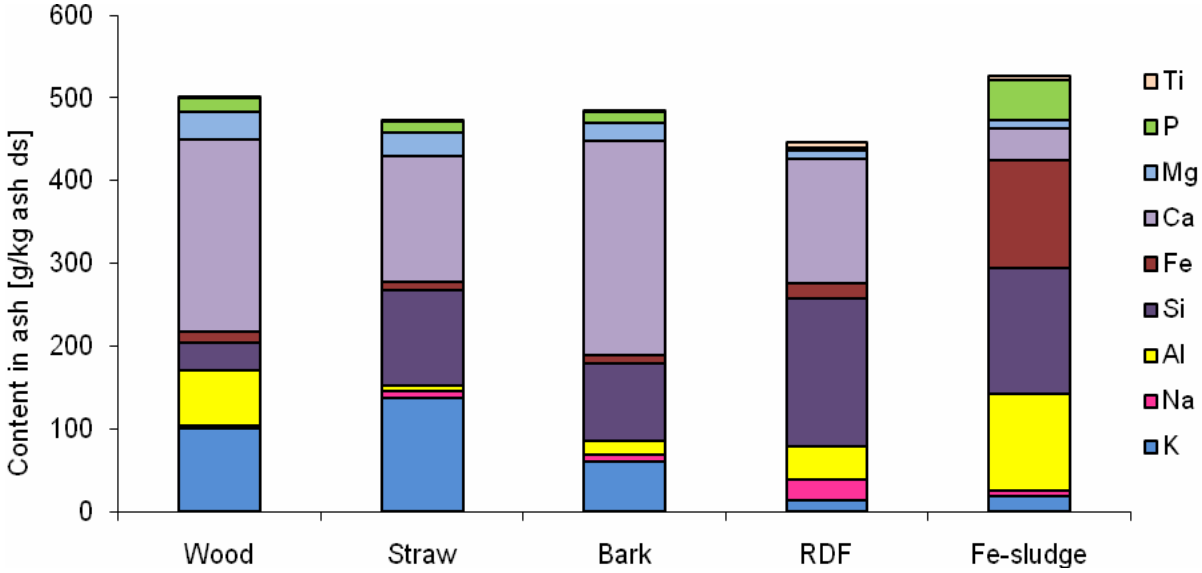

Figure 4. The content of the most common elements of some biofuel ashes. (18) (19) (20) (21). ds = dry substance. Fe-sludge is sewage sludge from the municipal waste water treatment plant Ryaverket in Gothenburg.

Inorganic matter is either associated with the water soluble compounds or the organic matter (24). The alkali and alkali earth metals are found either as salts or associated with the carboxylic group of the carbohydrates (16). Si is mostly present as amorphous silicic acid (18) or in esters linkage to carbohydrates (16). Si is found in large concentration especially in cereal straw (16). P can be found in esters whereas Cl is always found as water soluble salts (17), (18).

Contaminations such as soil (carried away during harvest of growth) and additives (e.g. lignin in the production of wooden pellets) are also ranked as ashes (18). What plant species that is used is however considered to be the factor that influences the mineral content of the fuel the most.

During combustion of biofuels the alkali and chlorine are volatilized and can react with the surrounding elements (25). In coal much of the alkali metals are bound in stable aluminium silicates and are never released into the gas phase at fluidized bed combustion conditions.

The alkali metals are therefore hindered from taking part in any reactions or melting (26), (27). This explains why biofuels cause agglomeration problems and coal does not.

2.4 Agglomeration

Agglomeration is an ash generated problem that occurs due to sticky ash which is related to the alkali loading and the combustion temperature in the boiler. The particles of the bed sand are stuck together forming new larger particles, so called agglomerates. This phenomenon is called adhesion. Agglomeration occurs mainly in fluidized beds since the bed sand is a key factor for trigging the agglomeration process. Slagging of fuel ash can also occur during combustion on a grate (without any presence of bed sand).

A fluidized bed containing small or just a few agglomerated particles has negligible disturbances and can be operated at normal conditions. Stable agglomerates start to form at a critical point, where the uniting forces of the bed sand particles overcome the separating ones. The critical point can e.g. be when a critical fraction of alkali containing ashes is obtained. When agglomerates are formed the total surface of the bed material is decreased which leads to different fluidization behaviour and decreased mass and heat transport. The decreased heat transport causes an uneven temperature distribution and local over-heating which increase the amount of ash melting and results in accelerated agglomeration (18).

When the agglomerates get too large the bed defluidizes which can result in a sintered bed and shutdowns in boiler operation. A sintered bed is a bed that is fully agglomerated and defluidized. It can take days before the boiler is back in operation. This is very expensive in full-scale boilers since the heat and power has to be substituted by other boilers using a more expensive fuel.

The agglomeration tendency is very dependent upon temperature sensitive interactions between ash and bed material. Ashes that have high alkali content (primarily K and Na) have lower melting points, which increase the interaction between bed particles resulting in more severe agglomeration problems. The melting point of the ash is thus fuel dependent since the alkali content differs between the fuels (28). The most common melt that causes bed agglomeration is some kind of potassium silicate (29).

2.4.1 Mechanisms of agglomeration

Agglomeration occurs in different steps which are described below. The mechanisms are complicated and it is unknown exactly what happens. To summarize these steps several different mechanisms have been discussed in literature. The mechanisms can be classified in

many different ways. One way is to divide them into melt induced and reaction introduced agglomeration (18), (30). Figure 5 presents the reaction mechanisms schematically.

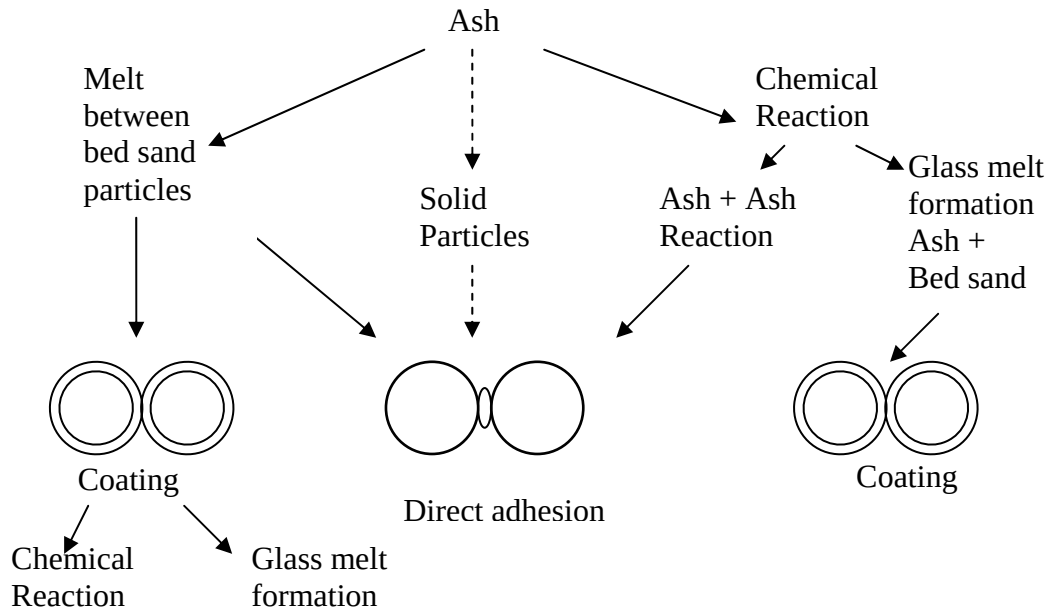

Figure 5. The mechanisms behind agglomeration. The dashed line shows a mechanism that is unlikely and is therefore not further discussed [5].

The mechanisms lead either to direct adhesion of the particles or a coating that glue the particles together. In commercial fluidized boilers most agglomeration is believed to be coating introduced (31).

2.4.2 Melt induced agglomeration

Accumulated ash can be totally or partly melted in a wide range of temperatures. The melting is present especially in hot areas of the bed, e.g. around burning particles and consists mainly of alkali and earth alkali salt components (32) (33).

The melted ash can coat sand particles forming a sticky film or be a drop of melt between two particles. The sticky film acts as glue and adhere colliding bed sand particles together which results in formation of agglomerates. The melt can also react with the bed sand particle or with surrounding substances. Solid ash particles can cover coated surfaces which hinder bed sand particles from adhesion, thus acting against the agglomeration. Additives like calcium and kaolin can give the same effect.

The mechanism is mainly dependent on K and Na salts but also on salts that contain Ca and Mg. The salt forming counter ions are S, P, Cl and C with different kinds of ionic bonds (18) (34). The mechanism has a local temperature maximum of about 600-800°C, but can occur

at even lower temperatures. At higher temperatures ash that is rich in salt reaches a saturation where melt no longer is formed with an increasing temperature, instead the melt gets less viscous and less sticky (18).

2.4.3 Reaction introduced agglomeration

Reactions can occur either between ash and bed sand or between ash particles. Solid-gas phase reactions are the most commonly suggested for bed agglomeration (30). Reactive alkali (mainly K_2O, Na_2O, KOH and NaOH) and acids (mainly SiO_2) from the ash can react and form low temperature melting phases. The reactive alkali can also be directly reacted with free silicic acid on the free surface of quarts sand (SiO_2) bed material. The forming product is a particle coated or partly coated by a sticky melt that gives the same effect as the salt melt. Melting phases that includes SiO_2 is referred to as glass melt since the phases are known from the production of glass where Na is the active component. During combustion of woody biomass the concentration of K is normally 10 times higher than Na and K becomes more important but the chemistry is similar. When this reaction occurs during the usage of quartz sand the presence of SiO_2 in biomass can be neglected (18).

An increased temperature increases the number of potential reactions and hence the number of possible kinds of melt. At a high temperature the formation of salt melt reaches a maximum, this is not the case for reaction introduced agglomeration. The viscosity and hence the stickiness of the glass melt increases with the increasing temperature. Reaction introduced agglomeration thus has to be prevented by keeping the combustion at a lower temperature.

2.4.4 Melting behaviour of different components

Skrifvars et al. divided ash components into three different groups depending on melt behaviour (34).

- Simple alkali salts. Potassium and sodium salt with carbonates, sulphates and chlorides can solute in each other both in solid and liquid state.
- Silicates. Oxides of calcium, magnesium, potassium, sodium, aluminium and silicon form silicates that can melt together into a liquid. This liquid is insoluble with the liquid of simple alkali salts.
- Rest. Compounds like phosphates, calcium carbonates, iron oxides and unknown ash compositions belong to this group. These compounds are assumed not to melt or interact with any compound of the two first groups.

2.4.5 Prevention of bed agglomeration

To avoid the adhesion of sand particles the combustion temperature can either be increased or decreased. The latter alternative prevents salt melt to form but might result in difficulty to reach a good combustion. The former alternative requires such high temperatures that salt forming no longer occurs and that existing salt melt has such low viscosity that it will not be a technical problem (2 in Figure 6) (18). However increasing the temperature results in an enhanced risk of reaction introduced adhesion (4 in Figure 6) and it is not guaranteed that the two mechanisms do not overlap. To avoid that reaction introduced adhesion occurs at higher temperature the bed material can be replaced with a material that is resistant to high temperatures and the formation of glass melt (18).

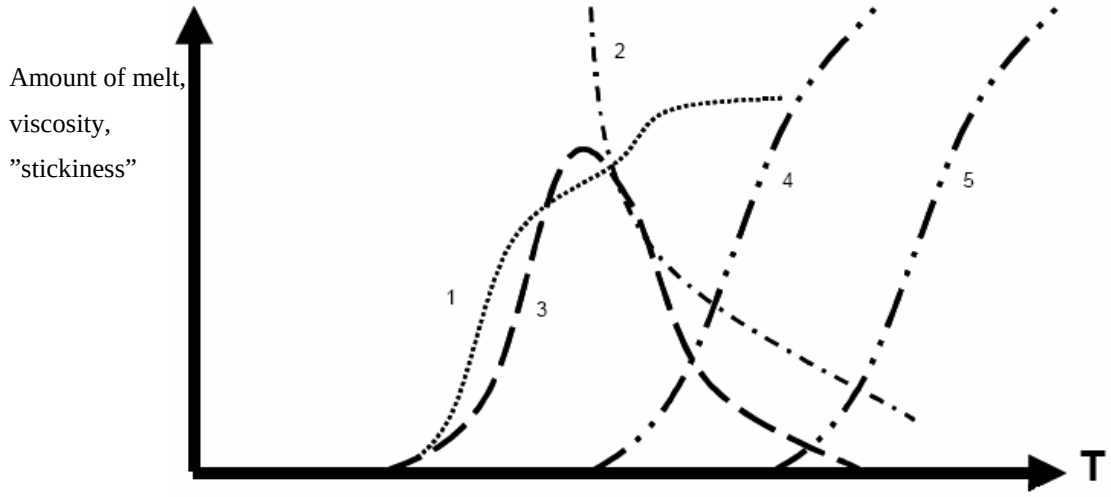

Figure 6. Stickiness related to temperature. (1) Formation of salt melt. (2) The viscosity (stickiness) of salt melt. (3) Risk of sintering due to salt melt. (4) Formation of glass melt at reaction with a pure bed material. (5) Formation of salt melt at reaction with a good bed material [18].

Agglomeration cannot be prevented in the same way when combusting fuels that are melt forming in itself, e.g. straw. The ash from these fuels will form melt independent of what kind of bed material that is used. Additives can be used to shift the ash composition towards more low melting phases thus avoiding the formation of eutectics (33). Another alternative is to co-combust problematic fuels with fuels containing ash that capture the alkali and forms an ash mixture that will not melt at the operating temperature of a fluidized bed (1).

An increased flow of fluidization gas can prevent or at least delay agglomeration since a higher flow causes more particle movement and more collisions between particle-particle and particle-walls.

2.5 Additives

Additives can be used to prevent bed agglomeration in fluidized bed boilers. Examples of additives that can be used are limestone ($CaCO_3$), dolomite ($CaMg(CO_3)_2$), kaolin, zeolite and several rest products (2).

One of the most commonly suggested additives is kaolin which consist mostly of a mineral called kaolinite ($Al_2Si_2O_5(OH)_4$). Kaolin is the most effective additive when it comes to enhancing the melting point during combustion of straw (35). The potassium is adsorbed on the surface of the kaolin, it can then diffuse into and react with the aluminium silicate structure (35). The compounds formed are $KAlSiO_4$ and $KAlSi_2O_6$ (35).

Dolomite has also shown to increase the melting temperature of the ashes. The formed products are calcium-magnesium-silicates. No chemical reactions between dolomite and potassium are believed to take place (35).

By adding limestone to the system the concentration of Ca increases which can hinder agglomeration, see chapter 2.7.

Zeolites are a group of aluminium silicates with porous structure. They have good features as ion exchangers and are believed to take up K during combustion, more about zeolites can be found in chapter 2.6.1.

Instead of using pure additives, rest products from the industry can be used. Examples of these products are waste water from the pulp and paper industry (contains e.g. kaolin and lime), coal ashes (contains kaolin and sulphur) and municipal sewage sludge (contains zeolites, sulphur, iron and phosphorous) (2).

2.6 Sewage sludge

Sewage water is purified in municipal waste water treatment plants to get rid of substances that can affect the environment negatively. These substances are e.g. ammonium, phosphates and organic matter. The cleaning is done in several steps with mechanical, chemical and biological cleaning.

To precipitate phosphates from the sewage water different chemicals can be used, e.g. iron sulphate ($FeSO_4$), iron chloride ($FeCl_3$), aluminium sulphate ($Al_2(SO_4)_3$) or limestone ($CaCO_3$). In Swedish municipal waste water treatment plants $FeSO_4$ is the most commonly used chemical during operation at normal water flows. $FeSO_4$ is added to the waste water in

basins where it reacts with the phosphates and form flocculates that grow larger and eventually settles to the bottom where it is mixed with the rest of the sludge (36).

During heavy raining when the flow of water into the treatment plant increases, the waste water is led out to the recipient without complete purification. At Ryaverket in Gothenburg phosphates are precipitated directly in the pre-sedimentation basins with poly aluminium chlorides (PAC) during these periods, the composition of the sludge can therefore vary between periods (36). PAC is a more effective but more expensive precipitation chemical and is therefore not part of the ordinary waste water cleaning (37).
Today the waste water treatment plants have to engage a sludge treatment company to get rid of the sewage sludge. There are different ways to treat the sludge e.g. construction soil, production of soil, cultivation of Salix, fertilization, and incineration (38). The sludge has a low heating value due to its high water content; it can therefore be discussed if incineration is a good alternative. It is however possible to pre-dry the sludge in order to increase its heating value and thus combust the sludge with a higher degree of heat recovery.

From March 2008 it is no longer allowed to sell laundry detergents containing phosphate in Sweden in an attempt to reduce the eutrophication of our waters (38). Zeolites are used as softener as replacement for phosphates. The zeolites follow the waste water and parts will end up in the sewage sludge in waste water treatment plants. Even though phosphates now are forbidden in laundry detergents, sewage sludge still contains phosphates, e.g. in wastewater from toilets.

There are different theories on what substance in the sludge that prevents the agglomeration tendency when co-firing biofuels and sewage sludge in a fluidized bed. The positive effect can be explained by the capture of alkali by zeolites, the capture of alkali by phosphates or a mix of both (39) (40). Phosphorous can also give negative effects, the addition of phosphorous rich fuels can contribute to the formation of low temperature melting calcium alkali phosphates. This chemistry has been seen in the CFBB at Chalmers when co-combusting rapeseed cake pellets, that is a biomaterial rich in phosphorous, with wood chips (41). Agglomeration problems due to melting of calcium/alkali phosphates has also been seen when adding a mixture of sewage sludge and industrial sludge to a FBC incinerator (42). It is possible that the phosphorous from the sludge can react with potassium and calcium from the base fuels, but no such chemistry has been seen in the CFBB at Chalmers.

2.6.1 Zeolites

Zeolites are a group of aluminium silicates with porous structure (43). Its chemical formula can be written $M_{x/n}[Al_xSi_yO_{2(x+y)}]\cdot_wH2O_y$, where M is a positive ion with the charge n (43). Most commonly this ion is Na, Ca or K (43). In laundry detergents two different synthetic

zeolites are used; *NaA zeolite* and *MAP* (44) (45). Both zeolites have Na as the positive ion (44) (39)

It is the feature as ion exchanger that makes zeolites useful as softeners in detergents. The positive ions of the zeolites are exchanged to the Ca or Mg ions of the tap water and increase the efficiency of the detergent used in washing machines (44).

The selectivity for different ions depends on the structure, amount of aluminium and Al:Si ratio of the zeolite (46) (47). The zeolites used as softeners shall possess selectivity to Ca and Mg over Na. This is the case for both NaA zeolites and MAP (46). Studies have also shown that MAP has a marked selectivity to K over Na (47).

The two zeolites have different structure which gives them different properties (48). MAP has a Gismondine structure which is built up from two dimensional crankshaft chains (48). The chains are built up of SiO_2 and AlO_4 tetrahedra which are linked together forming a porous system. The crankshaft chains make the structure more flexible compared to that of LTA which is built up in a cubic arrangement (48). The structures can be seen in Figure 7 and Figure 8.

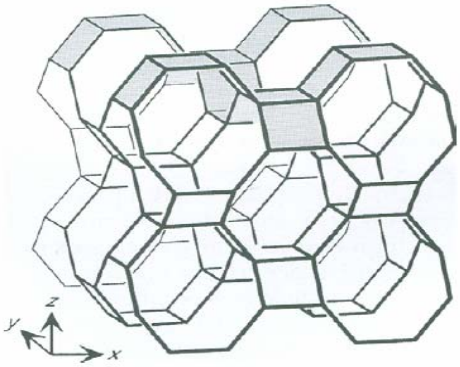

Figure 7. Gismondine structure (GIS) (48).

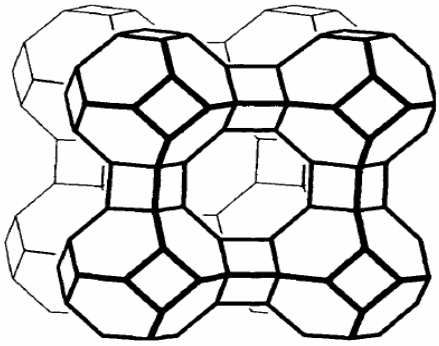

Figure 8. Linde type A (LTA) Structure NaA zeolites (48).

It is unknown what form the zeolites take in the sewage sludge after the water treatment process. Part of the zeolites probably maintain their original structure, part of it has been ion exchanged with Ca and Mg and parts might have taken up other metals (even heavy metals) from the sewage water (39). The composition and hardness of tap water in the area that provides water to the municipal waste water treatment plant effects what sort and amount of ions that is exchanged. It is therefore difficult to predict the behaviour of zeolites when added to the furnace.

Möller has in her master thesis studied the behaviour of zeolites when heated (39). The studied zeolite was MAP, both with original structure and ion-exchanged with Ca. The zeolites were heated together with an addition of KCl. The result showed that both zeolites had an uptake of K and Cl.

2.6.2 Phosphates

Phosphates are believed to have an impact on the agglomeration behaviour of the bed materials. Sewage sludge contains a substantial part of phosphates but so does the ash from the biofuel itself. More information about the impact of phosphates on agglomeration can be found in chapter 2.7.

2.7 Ash elements that influence bed agglomeration

Several elements and compounds are believed to influence the bed agglomeration in different ways. This chapter is an attempt to review the most commonly interactions suggested in literature.

Alkali elements (K and Na)

Inorganic alkali components, mainly K and Na are known to have large impact on the agglomeration. K compounds tend to be accumulated in the bed at normal bed temperatures (800-900°C) (49). The presence of both alkali (mainly hydroxides or salts) and silicates in the bed can lead to the formation of eutectics and low temperature melting phases (28) (18). Lin et al identified the coating layer at sand particles as the melt of K_2O-SiO_2 which agrees with the thermodynamic equilibrium calculations of which molten phase potassium compound that is most stable (49). K is likely to be volatized with organic species during combustion and can be released as KCl if Cl is present (28). Alkali that has reacted with silicates is considered to be stable and non- volatile and is retained in the ash particles (50).

Silicates

Quartz (SiO_2) from the bed sand is found to interact with ash forming low temperature melting phases. Shao et al found that during sludge combustion eutectics of Fe_2O_3 and SiO_2 play an important role in bed agglomeration causing sand particles to glue together resulting in melt induced agglomeration (51). They also found sludge combustion to form coating introduced agglomeration with a layer enriched in Si, P and Ca. Fryda et al showed that total melt of silicate ash forms highly viscous liquid that causes the main defluidization mechanism (52).

When using silica rich bed material the bed silica interacts with K forming low temperature melting potassium silicates thus enriching potassium in the bottom ash (53) (16). However, if using silica rich fuel the reaction between potassium and fuel originated quartz or silicates dominate over the reaction with the bed material (16).

Yan et al found Na_2SiO_3 to be a low temperature melting specie using TPCE calculations (54). An inner coating layer of agglomerated particles has in studies been found to mainly consist of calcium silicates (and to less extent magnesium silicates and some phosphorous) (55).

Phosphates

It is discussed whether phosphorous has a positive or negative effect on agglomeration. Shao et al concluded that alkali phosphates (KPO_3 and $NaPO_3$) highly contribute to mainly melt induced agglomeration by forming low temperature melting eutectics during combustion of sludge (51). Melt point decrease due to phosphates is rarely seen during combustion of biofuels. The explanation is that formation of low temperature melting phosphates (different kinds of oligophosphates) does not occur when the presence of phosphates and other salt forming materials (Cl, S) is in shortage compared to alkalis, which often is the case for biofuels (18). Instead of binding to alkali the phosphorous binds to orthophosphates (PO_3^-) which has high melting points.

K will bind to phosphates in the bed sand rather than to S due to that phosphorous has high affinity to K. Therefore large amount of sulphur will be available for the sulphation of KCl higher up in the combustion chamber. KCl is formed during the combustion (56) if there is an excess of Cl added with the fuel. The potassium phosphates are either bound to coarse particles or form fine particles (40).

The presence of lime can shift the formation of low temperature melting potassium phosphates towards the higher temperature melting calcium rich potassium phosphates (e g. $CaKPO_4$ and $Ca_{10}K(PO_4)_7$) and pure calcium phosphates ($Ca_5(PO_4)_3(OH)$) (57). Zeuthen et al added monocalcium phosphates to the boiler to capture alkali metals as phosphates and thus reduce chlorine content in the deposits (40).

Sulphates

Yan et al used TPCE[1] calculations to predict that sulphates, especially $Al_2(SO_4)_3$, $Fe_2(SO_4)_3$ and Na_2SO_4, should be among the most common low temperature melting point species (54). Valmari concluded that SO_3 and SO_2 from the fuel may react with (primarily) alkali, such as hydroxides and chlorides, or calcium compounds forming condensed phases consisting of either K_2SO_4 or $CaSO_4$ (16) (18).

Calcium

Limestone can be added to the combustion since Ca has a positive effect on reducing agglomeration. As long as the relation K/Ca<1 is valid for the system, high temperature melting calcium- potassium-phosphate and sulphate phases are predominately formed, but if the opposite relation prevails low temperature melting eutectics forms instead (18). Normally the calcium fraction in biofuels is higher than the critical one and the presumptions are good for that a calcium addition will prevent the agglomeration (33).

Ca also coats silica and prevents the reaction between potassium phosphate and silica particles that forms low temperature melting potassium (calcium) silicates (41). However, there are observations where attacks of alkali and calcium cause extensive interactions between ash forming elements and bed material forming low melting layers (30). Shao et al found that stone as a sorbent, in contrary to the good effects, lime results in a sharp increase in aerosol formation (51).

Chlorides

Chlorides are highly volatile at high temperatures and are only slightly involved in high temperature bed sintering (18). Skrifvars et al found chlorine to escape from the bed regardless of sort of fuel (34). The alkali chlorides formed during combustion are condensed at about 600°C and is therefore harmful at heat exchanging areas rather than in the prevailing bed temperature (16).

[1] Thermodynamic multi-phase multi-component equilibrium calculations that leads to better understanding of which phases could form and which composition of the phases that leads to possible agglomerates (51).

3 Method

Nine different compositions of fuels were combusted in a laboratory scale fluidized bed reactor. The bed samples were analysed with three different methods. The methods were SEM/EDX, chemical analysis and finally a test in order to find the agglomeration temperature. The concept of the experimental design and the fuels that were used is presented in this chapter, followed by a description of the equipment and analysing methods.

3.1 Fuels used in the experiments

All fuels that were used in the experiments can be classified as biofuels apart from the plastic material and metal content of the RDF (14). The ash content of the materials can be found in Figure 9 and the complete fuel analyses can be found in appendix A.

Bark

Since bark will be main base fuel in the other experiments of the frame work of phase three in the Agglobelägg project one experiment was performed to be able to relate laboratory scale results to results from the CFB-boiler at Chalmers. This project involves fuel with high ash content; therefore bark, with its higher ash content than ordinary wood pellets, is suitable for pre-studies. The bark used came from Södra SkogsEnergi:s pulp & paper plant in Mönsterås Sweden. The pellets have an effective heating value of 17.77 MJ/kg (ds), the wet content is 9.1 % and the ash content is 3.4 % (ds).

Wood

Ordinary commercial wood pellets were used for the experiments. The present ones originated from a pellets factory in Ulricehamn and are made from saw dust of mainly spruce and pine. The pellets have an effective heating value 19.13 MJ/kg (ds), the wet content is 6.5 % and the ash content is 0.3% (ds).

Straw

The ash content in straw differs a lot between different species and origin. To be able to relate results to previous studies, wheat straw pellets with the same origin as in the previous Agglobelägg project were used. The pellets were delivered from a pellet factory in Køge in Denmark. The pellets have an effective heating value of 17.57 MJ/kg (ds), the wet content is 8.3% and the ash content is 4.1 % (ds).

RDF

Refuse Derived Fuel (RDF) is made from office disposals. It contains mostly paper, wood and mixed plastics, but also traces of metal. The pellet used for the experiments were

imported from Icopower in Amsterdam in the Netherlands. The pellets have an effective heating value of 19.82 MJ/kg (ds), the wet content is 5.3 % and the ash content is 15.4 % (ds).

Municipal sewage sludge

Two different municipal sewage sludge (MSS), where phosphorous has been precipitated with two different precipitation chemicals, were used for the experiments. The sludge used were collected at two different waste water treatment plants; Ryaverket in Gothenburg and Nolhaga in Alingsås. During normal conditions at Ryaverket, iron sulphate ($FeSO_4$) is used to precipitate phosphates (55), this explains the high concentration of Fe in the sludge from Ryaverket. At high working loads polyaluminium chlorides (PAC) can be added as a complement. At Nolhaga waste water treatment plant, aluminium sulphate ($Al(SO_4)_3$) is used as precipitation chemical. The use of the precipitation chemicals increases the concentration of Fe and Al in the sludge, see Figure 9. Therefore sludge from Ryaverket is referred to as Fe-sludge and sludge from Nolhaga as Al-sludge.

Fe-sludge has an effective heating value of 10.1 MJ/kg (ds), the wet content is 72.4 % and the ash content is 48.8 % (ds). Al-sludge has an effective heating value of 11.5 MJ/kg (ds), the wet content is 77.5 % and the ash content is 42.6 % (ds).

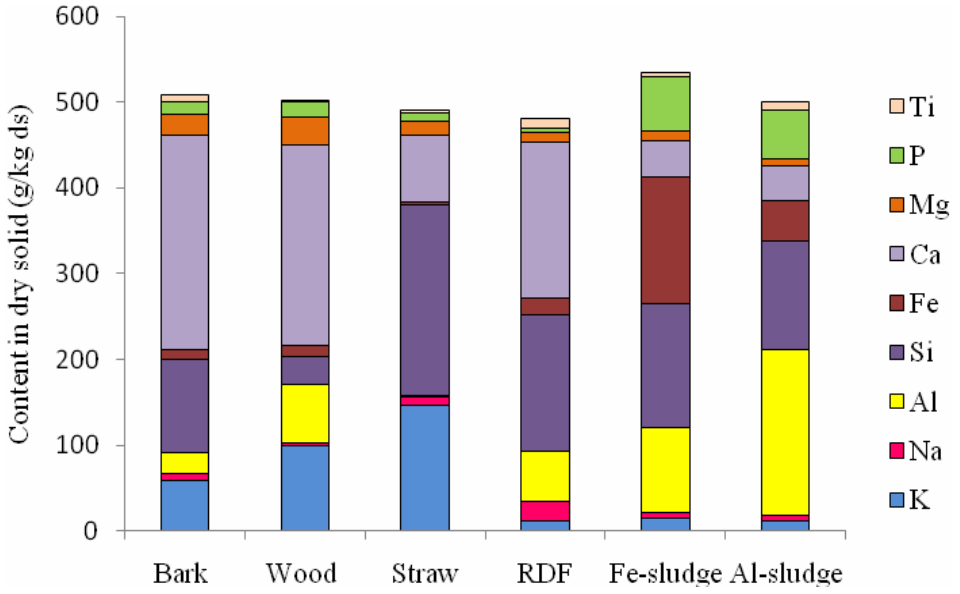

Figure 9. The ash content in the materials used in the experiments.

3.2 Experimental design

Nine combustion experiments were performed with three base fuels. The base fuels were bark, RDF and a mixture of wood and straw (wood/straw). Sewage sludge was added to wood/straw and RDF respectively in two different concentrations. The complete experimental matrix can be seen in Table 1. The percentage of sludge used in the combustion experiments refers to dry substance of the fuel (ds).

The same composition of wood and straw as in *Agglobelägg 2* was used, 75%/25% on energy basis. This mix is considered to give a fuel that is problematic enough in order to study measures to prevent alkali related problems (18).

Table 1. Experimental matrix. Weight percentage on dry substance.

Wood/straw	**RDF**	**Bark**
- 0% sludge	- 0% sludge	- 0% sludge
- 2% Fe-sludge	- 2% Fe-sludge	
- 6% Fe-sludge	- 6% Fe-sludge	
- 2% Al-sludge		
- 6% Al-sludge		

Wood/straw fuel without any addition of sludge is used as a reference case. The reference case is supposed to be comparable with the reference case in Agglobelägg 2, *Ref12h_BB*. *Ref12h_BB* was performed in the Chalmers bed boiler and used 77% wood and 23% straw, calculated on energy basis. The sample was taken in the bottom bed (BB) after 12 hours of combustion (1). The aim was to obtain the same concentration of ashes remaining in the bed after combustion of wood/straw0%MSS as for *Ref12h_BB*. Calcium is a relatively non-volatile substance and is therefore considered to be a good marker for the concentration of ash originating from the fuel that will remain in the bed material. The concentration of Ca in *Ref12h_BB* was 3.28 wt% (1). The theoretical amount of fuel that had to be combusted to reach this concentration of Ca in the bed was 2.00 kg of wood/straw pellets (ds). The relation fuel to bed sand was kept constant throughout the entire experimental matrix. 2.00 kg (ds) of each fuel was to be combusted in the laboratory scale reactor containing 95g sand.

The sewage sludge was dried and grinded at SP. Pellets of wood, straw and RDF was grinded at TPS in Nyköping. The wood- and straw pellets were easily grinded to the original fragment size. RDF was more problematic to grind due to the presence of pieces of metals and plastics, but was nevertheless grinded to a size of 1mm. To obtain an even distribution of ash addition over time pellets with the right composition of fuel and additives were pelletized. The pelletizing was done at SPC in Ljungby.

Due to a computational mistake the amount of bark pellets was too small, only 1.72 kg dry pellets were added during combustion. This mistake was considered to not affect the agglomeration temperature too much and it was therefore not necessary to redo this experiment.

"Baskarpsand" consisting of pure quartz (SiO_2) was used as bed sand in all experiments. The same sand is used in the CFBB at Chalmers.

3.3 Combustion equipment

A description of the equipment used for the experiments is described in this chapter.

3.3.1 The laboratory scale reactor

A laboratory scale fluidized bed reactor was used for the experiments, see Figure 10. The reactor is a 1.4 m vertical steel tube with an inner diameter of 0.07 m. A bed bottom filter made of sintered metal works as an air distributor. It is situated inside the tube at a height of 0.63 m, see Figure 11. The bed sand is placed upon this filter. The reactor is encapsulated in a furnace where the heating is divided into three different zones; the gas inlet zone, the bed bottom zone and the upper zone. All zones can be set to individual temperatures. The fluid gas inlet is placed at the bottom of the reactor and is connected to mass flow controllers where the gas flows can be adjusted.

To imitate a real combustion environment and still be able to do measurements inside the reactor a specially made lid was placed on the top. The lid is provided with four pipes; one for the fuel feed, one for exhaust gas outlet, one for the control of emissions and the last one for the control of bed temperature and pressure drop. The last pipe runs to the bottom of the bed and contains a thermocouple that measures the temperature and a pressure sensor that measures the pressure drop over the bed. To protect the sealings from being overheated the reactor is provided with water cooling around the top, close to the lid and around the bottom, close to the reactor inlet.

The pipe used for the exhaust gas control is connected to an IR-detector that measures the CO/CO_2 concentration. The results are computer logged using the software EasyView. Also the temperature and pressure drop are logged in EasyView.

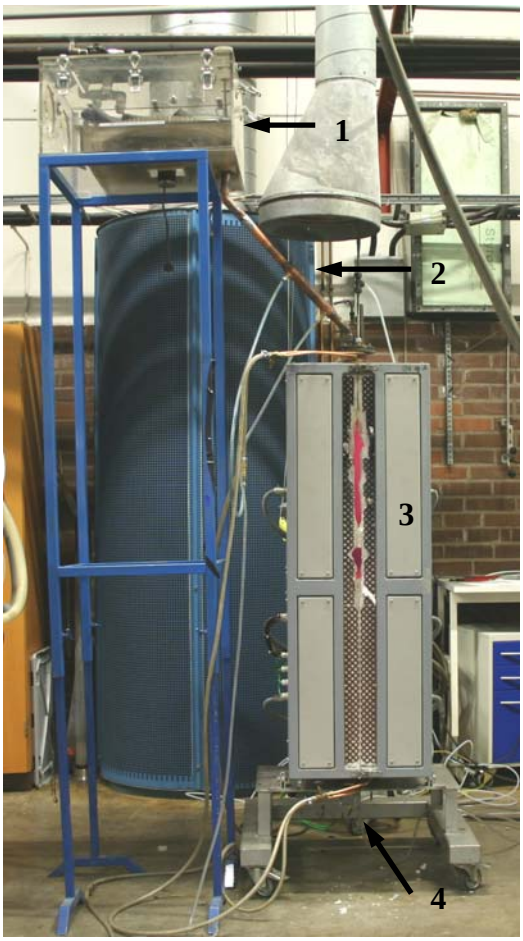

Figure 10. The equipment (1) carousel feeder, (2) fuel feeding pipe, (3) oven, (4) gas inlet.

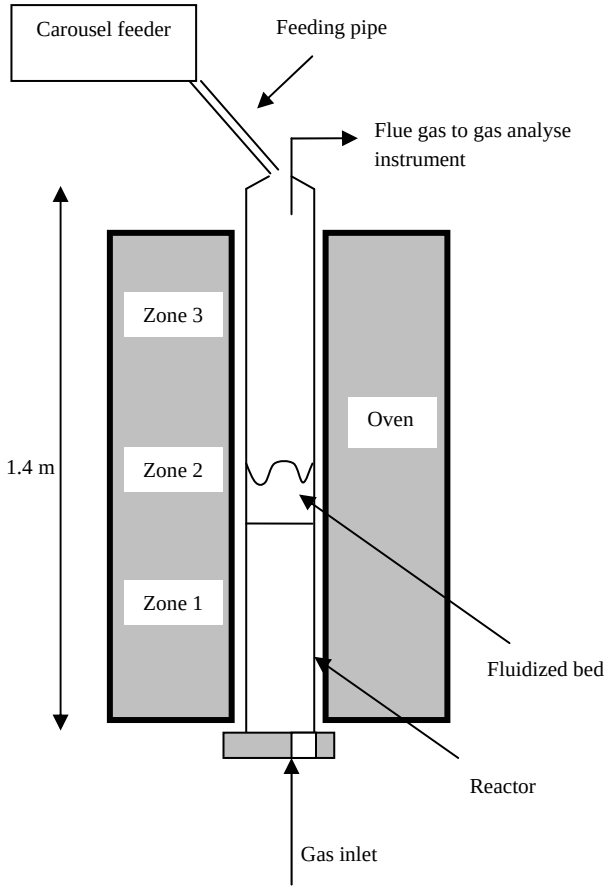

Figure 11. Cross-section of the equipment.

3.3.2 The carousel feeder

A carousel feeder was used to continuously provide fuel to the reactor. The feeder is a sealed box containing a wheel with 72 small bottomless containers for the pellets. The wheel is rotated stepwise with a rate adjusted to fit the required amount of fuel addition. Every time the wheel moves one pellet is dropped into the fuel feeding pipe that is connected to the reactor. The carousel feeder is fed with nitrogen gas to prevent the fuel from igniting. Gloves sealed at one side of the box are used to fill up the containers with pellets without letting any air in. Pellets are taken from storage inside the box using a pincer. The wheel is connected to an electric motor speed controlled by the software EasyTool.

3.4 First experiments and parameter settings

The combustion conditions should resemble the ones in the CFBB at Chalmers. In these first experiments, parameters such as furnace temperature, gas flow and gas compositions were studied to decide settings for the main tests. The fuel used was bark pellets.

The bed temperature should be close to normal combustion conditions, 850 °C. Too low temperature does not give an acceptable combustion while too high temperature increases the risk of agglomeration of the bed material. The three different temperature zones of the reactor were controlled individually in order to achieve a suitable and even bed temperature. The bed filter is situated in Zone 2. This temperature was set well above the ignition temperature. The bed temperature can be controlled by changing the temperature of the air pre-heating zone, zone 1. To get a good oxidation of the combustion gases the temperature in zone 3 should be high. The starting temperature of the different zones was set to:

Zone 1	600°C
Zone 2	750°C
Zone 3	900°C

The air factor (excess air ratio) in the CFBB at Chalmers during *Agglobelägg 2* was 1.21. The required airflow to achieve stoichiometric conditions for the different fuels was calculated from the fuel analyses data (Appendix A). This is the theoretical air flow needed to reach complete combustion. A small excess of air has to be used to get an air factor of 1.21. The total flue gas flow was set constant during all experiments, 25.5 l/min. The air was mixed with N_2 to achieve the required gas flow.

To avoid accumulation of fuel in the bed, the fuel must be combusted in the same rate as fed to the reactor. The fuel feed rate was considered suitable when the temperature of the bed was stable and did not increase when the feeding of fuel stopped. The appropriate fuel feed rate was set to 4 g/min (ds).

With a given mass of fuel and a constant feeding rate the theoretically duration of combustion is equal for the entire matrix, 8.5 hours. The fuel feed should proceed until the desired fuel batch was combusted, alternatively until the bed sintered. If the bed sintered the fuel feeding was interrupted. Regardless if the entire batch was combusted or not, the composition of the bed sand material was analysed with SEM/EDX and chemical analysis. Agglomeration tests were only performed on bed sand that was not sintered during the combustion.

3.5 Chemical analysis of bed sand composition

Major and minor elements in the bed sand can be recognized with chemical analysis. To analyze the main elements (Si, Al, Fe, Mn, Mg, Ca, Ti, Ba, P, K and Na) the bed sand is first ignited in air at 750 °C to constant weight[2] in order to remove any combustible particles from

[2] Mod. ASTM D 3682, Swedish standard method

the bed material. The sample is then fused within lithium tetra borate ($Li_2B_4O_7$), followed by dissolution of the melt in either hydrochloric acid (HCl) or dilute nitric acid (HNO_3). The solution is eventually analyzed by atomic absorption/emission. To quantify the content of S, a sample of bed sand is combusted in a gas stream of oxygen in a high temperature furnace[3]. Moist and solid particles are removed before the gas passes through an infra red detector that measure at the specific wavelength of sulphur dioxide. The over time integrated detector signal is a measure of the total content of S. The Cl content of the bed sand can be quantified by ion chromatograph spectroscopy.

3.6 SEM/EDX analysis

Detailed pictures of a cross-section of the bed sample can be taken with a scanning electron microscope (SEM). The sample was prepared by embedding a few bed sand particles in epoxy. The epoxy was polished to get an even cross sectional surface of the sample. The sample was placed inside the electron microscope. The pressure was lowered to 0.13 kPa, which is necessary to prevent interactions with the air molecules from disturbing the analysis. Total vacuum cannot be used since the surface of the sample then can become charged.

An electron beam is scanned over the surface of the sample. Different detectors can be connected to the microscope depending on what analysis that is to be performed. A backscattered electron (BSE) detector can be used to distinguish differences in the density of the sample. This detector registers the backscattered electrons from the sample. Backscattered electrons are electrons from the electron beam that are not absorbed by the sample but are instead reflected to the detector. Denser parts reflect more of the electrons and appear as brighter areas on the screen. The ash is denser than the bed sand and can be seen as bright areas in the pictures.

To decide the distribution of elements over the cross-section of the surface an energy dispersive x-ray fluorescence detector (EDX) can be used. The electron beam excites the electrons of an element. When the electron is relaxed the atom will send out x-ray fluorescence, this gives a spectrum that is characteristic for each element.

From the EDX both a quantitative and qualitative analysis can be given. A qualitative mapping over the sample area gives a number of pictures, each one showing the distribution of one element. Brighter areas indicate higher concentrations of the analysed element. The pictures are normalized individually and do not give any information about the concentrations

[3] SS 18 71 86, Swedish standard method

of the elements. As a complement to the mapping a quantitative analysis in small specific points can be made, this is called element quantification.

3.7 Agglomeration test

The agglomeration temperatures of the bed samples from the combustion experiments were determined with a method similar to the one used in previous works (2). 70g of the bed sample was placed in the reactor. The reactor was heated to 700°C where the temperature was stabilized. A small gas flow was passed through the bed during the heating period. The pressure drop over the bed was continuously logged while the temperature was increased by 3.5°C/minute to a maximum temperature of 1100°C. Bed agglomeration is indicated by a decreased pressure drop. Some samples showed a clear agglomeration temperature while other samples had more prolonged agglomeration behaviour. The agglomeration can be divided into three steps:

- Partial agglomeration – where the pressure drop starts to decrease.
- Distinct agglomeration – where the pressure drop decreases significantly with 4 Pa/minute or more.
- Total agglomeration – where the decrease in pressure drop declines.

The bed was fluidized with gas consisting of 15% CO_2 and 85% N_2. A gas flow of 18 l/min was enough to get a good fluidization of the bed material.

4 Results and discussion

To give a better understanding the discussion is weaved in to the presentation of the results.

4.1 Combustion results

The temperature, pressure drop and CO/CO_2-concentrations of the experiments were logged in EasyView; the results are presented in appendix D. An average of these data is presented in Table 2**.** All presented CO/CO_2-concentrations are compensated for the dilution of nitrogen used in the flue gas. The concentration of CO was generally high while the concentration of CO_2 was low compared to conditions in the CFBB at Chalmers. This can be seen as an indicator of an incomplete burnout. The air factors, presented in Table 2, were calculated from the theoretical and actual CO_2 concentration, see appendix C.

Table 2. Average combustion data.

	Average temp [°C]	**Max temp [°C]**	**Average $(CO)_t$ [ppm][a]**	**Average $(CO_2)_t$ [%][a]**	**Air factor[c]**
Bark	823	898	1100	11.5	1.7
Wood/straw0%MSS no.1	790	857	-	-	-
Wood/straw0%MSS no.2	752	827	25800	14.1	2
Wood/straw2%Fe	833	876	16500	17.5	1.6
Wood/straw6%Fe	820	888	11300	15.8	1.7
Wood/straw2%Al	838	872	-	*15.5*[b]	-
Wood/straw6%Al	823	862	-	*13.4*[b]	-
RDF0%MSSno.1	798	895	9700	10.1	1.8
RDF0%MSSno.2	819	856	7500	13	1.4
RDF2%Fe	827	876	11000	14.2	1.3
RDF6%Fe	817	884	6900	13.2	1.4

[a] Some data is missing due to instrumental problems. [b] These results are estimations since the pipe to the CO/CO_2 instrument was blocked. [c] When the combustion was extremely poor the air flow was adjusted to improve the condition.

In *wood/straw0%MSSno.1* the bed material sintered already after 22 minutes, which was surprisingly early. The experiment was repeated to make sure that the result was correct. During combustion of *RDF0%MSSno.1*, the bed sintered at a temperature above 880°C. The experiment was repeated to investigate whether the high bed temperature was the reason for the early sintering. Also *RDF2%Fe* sintered early, this time the experiment was not repeated since the combustion bed temperature was kept below 880°C.

The time of fuel feeding for the completed experiments varied between 7.5 and just over 9 hours, see
Table 3. The main reasons to the variation are the effect of blockings in the fuel feeding pipe and variance of weight between individual pellets.

Table 3. Description of the combustion.

	Time of fuel feeding [h]	Sintered during combustion	Combusted fuel [kg ds]
Bark	07:30		1.73
Wood/straw0%MSSno.1	00:22	X	0.12
Wood/straw0%MSSno.2	00:38	X	0.17
Wood/straw2%Fe	09:19		2.00
Wood/straw6%Fe	08:48		2.00
Wood/straw2%Al	07:55		2.00
Wood/straw6%Al	08:40		2.00
RDF0%MSSno.1	02:03	X	0.51
RDF0%MSSno.2	05:13	X	1.14
RDF2%Fe	02:57	X	0.62
RDF6%Fe	08:01		2.00

4.2 Analyses of the bed sand samples

The bed samples were taken from the reactor after the combustion experiments were finished. The samples were ocular inspected before agglomeration tests were performed. A more proper analysis was performed by taken one fraction of the samples to be used for chemically analysis at SP and one fraction for analysis with the SEM/EDX method at Chalmers. After the performance of the agglomeration test the bed samples were taken from the reactor and were again ocular inspected. The results from all the analyses are presented and discussed in this chapter.

4.2.1 Bed sand samples after combustion

After combustion the bed sand was taken out from the reactor. All samples contained a varying fraction of small, black particles. The dominating part of these was magnetic and probably originated from welding from the equipment used to measure the pressure drop in the bed sand. Parts of the black particles can also be coke from the fuel ash. A selection of photos of these samples is presented here. Pictures of the samples that are not presented in this

chapter can be found in appendix E. The bed weight of all wood/straw samples decreases during the combustion compared to the initial bed weight of 95 g. The reason is that the fluidisation gas carries sand and ashes from the bottom bed. The bed weight of RDF increases instead, which probably is due to the high ash content in combination with heavy fragments of metals in the RDF pellets.

Bark

Combustion of bark resulted in that the sand particles have started to form small stable agglomerates, which can be seen in Figure 12. A few of those have started to grow bigger. The sample has a black-brown colour.

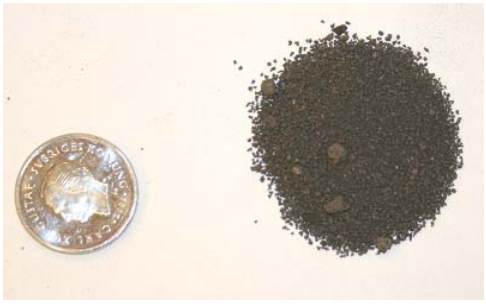

Figure 12. Bed sand sample after combustion of *bark.*

Wood/straw0%MSS

The two bed samples of *wood/straw0%MSS* sintered during combustion and resulted in large porous agglomerates, see Figure 13. The bed samples also contained a lot of smaller agglomerates, similar to those of the bark sample. The sand has a colour that resembles salt and pepper.

Figure 13. Bed sand sample after combustion of *wood/straw0%MSSno.1.*

Wood/straw2%Fe

The sample contains sand particles that are still shaped as the initial ones and flake shaped particles that seem to be sand covered by an unknown substance, see Figure 54. The flakes are porous and clearly red coloured from the Fe- ions of the sludge. A few sand particles show an indefinite agglomeration tendency.

Wood/straw6%Fe

The sample has a homogeneous red colour that can be compared to the colour of classical red brick. To a large extent it consists of red flakes looking like those in the sample of *wood/straw2%Fe,* see Figure 55.

Wood/straw2%Al

A few sand particles show an indefinite agglomeration tendency. The sample has a grey-brown colour, see Figure 56.

Wood/straw6%Al

Some of the sample particles tend to form flakes. The sample has a beige-brown colour, see Figure 57.

RDF0%MSS

The two bed samples of RDF pellets sintered during combustion and resulted in large porous agglomerates. The bed sample also contains a lot of small agglomerates. Since RDF contains large fractions of different materials, larger segments of e.g. metals are found in the ash. The sample has a grey-brown colour, see Figure 58.

RDF2%Fe

The sample sand sintered during combustion and formed large porous agglomerates. Large segments of different material originating from the fuel were found in the sample. The colour is similar to the colour of the *RDF0%MSS* samples, see Figure 59.

RDF6%Fe

A large fraction of this sample consists from rest segments of RDF, which can be seen in Figure 14. Some sand particles have formed smaller agglomerates. The flake structure that was seen for *wood/straw6%Fe* is not clearly seen here. The sample has a red-brown colour.

Figure 14. Bed sand sample after combustion of *RDF6%Fe.*

4.2.2 Results and discussion regarding the chemical analysis of the bed material after combustion

All results from the chemical analysis are presented in Table 8, Appendix F. In this chapter different samples are presented in groups; Bark, ref 12_12BB and wood/straw with Fe-sludge, wood/straw with Al-sludge and RDF. The figures present elements that either is present in large concentrations or are believed to have impact on the agglomeration tendency of the bed material. For the wood/straw series Al, Fe, Ca, K and P are presented (Figure 16 - Figure 18). The bark figure also contains Mn and Mg (Figure 15). The RDF group also contains Ti, Na and Mg (Figure 19). Si clearly dominates in all bed samples and is therefore not shown in the figures.

All figures have the same scale on the y-axis, but since *wood/straw2%Al* contains such a large amount of Ca, this group is shown in two figures. One with the same scale as the rest of the figures (Figure 17) and one with a scale that shows the total amount of Ca (Figure 18).

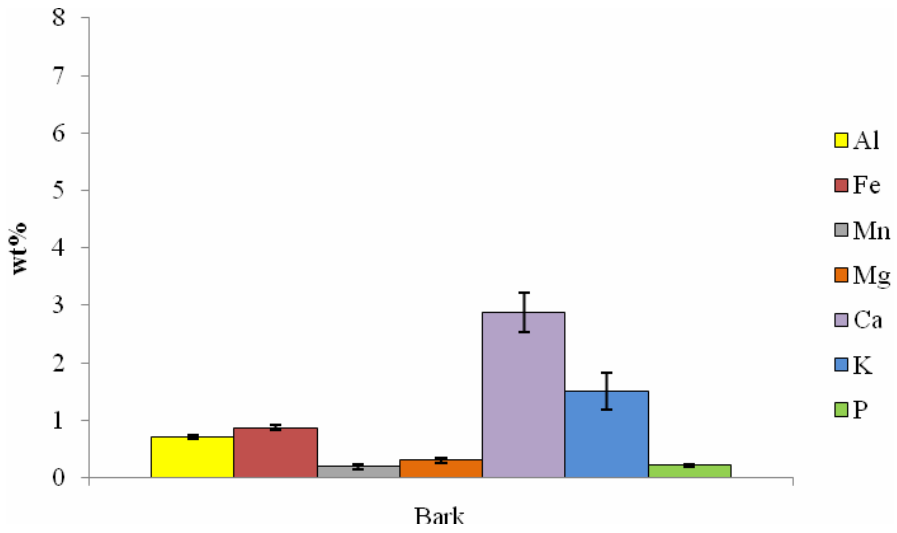

Figure 15. Chemical composition of some of the main elements in the bed sample from the combustion test using Bark.

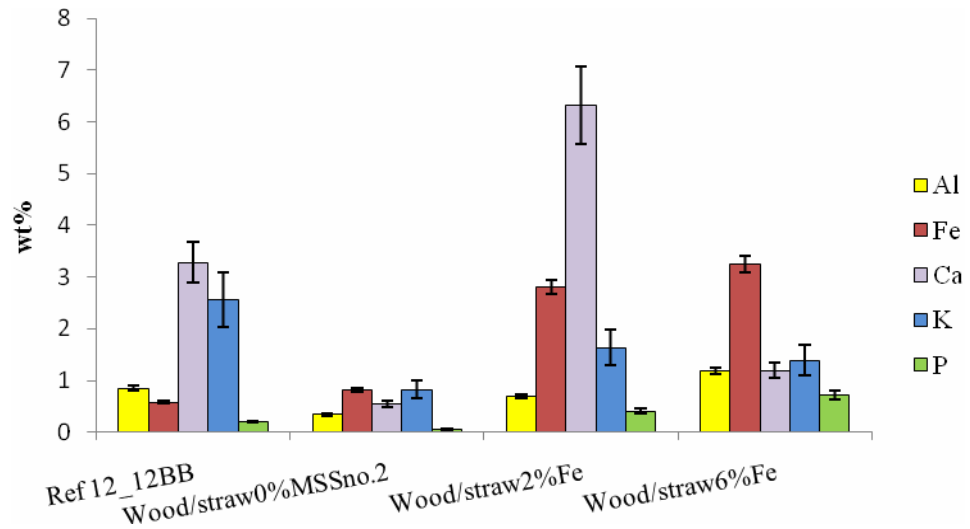

Figure 16. Chemical composition of some of the main elements in the reference case and the group of experiments with wood/straw and an addition of Fe-sludge.

The Ca content in the bed sand of the *wood/straw0%MSS* sample (0.55 wt%) was lower than the Ca content in the reference case (3.28 wt%). The Ca content varies a lot between all the bed samples. For the experiments where all the fuel was combusted it differs from 1.19 wt% (*wood/straw6%Fe*) to 15.8 wt% (*wood/straw2%Al*). The high content of Ca in *wood/straw2%Al* and *wood/straw2%Fe* compared to other wood/straw samples is remarkable. The error bars show that the deviation cannot be explained by the source of error of the test method. Some sort of calcium oxide compound present in the bed sand could be the reason to the high Ca content.

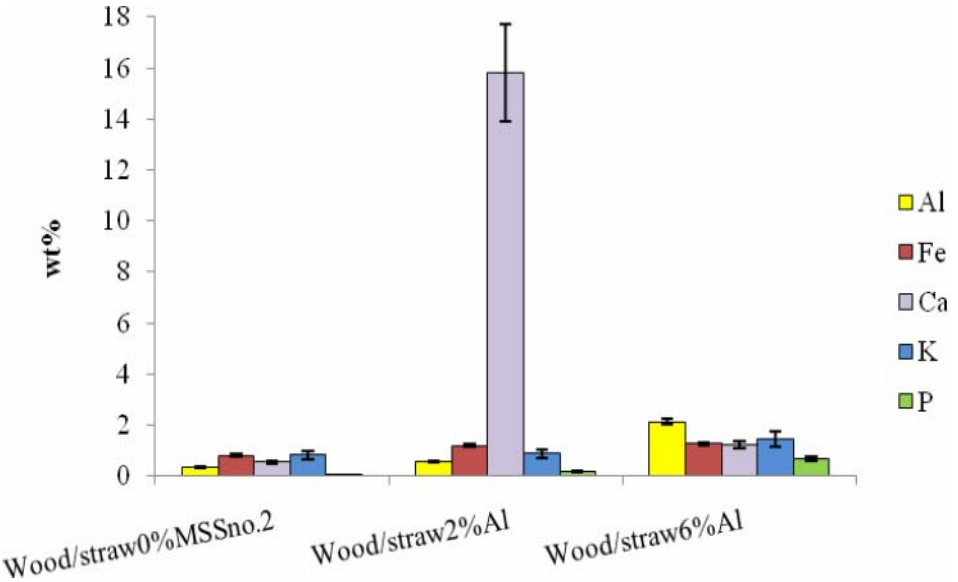

Figure 17. Chemical composition of some of the main elements in the group of experiments with wood/straw and an addition of *Al-sludge.* The Ca content in *wood/straw2%Al* is too high to fit to the table (see Figure 18).

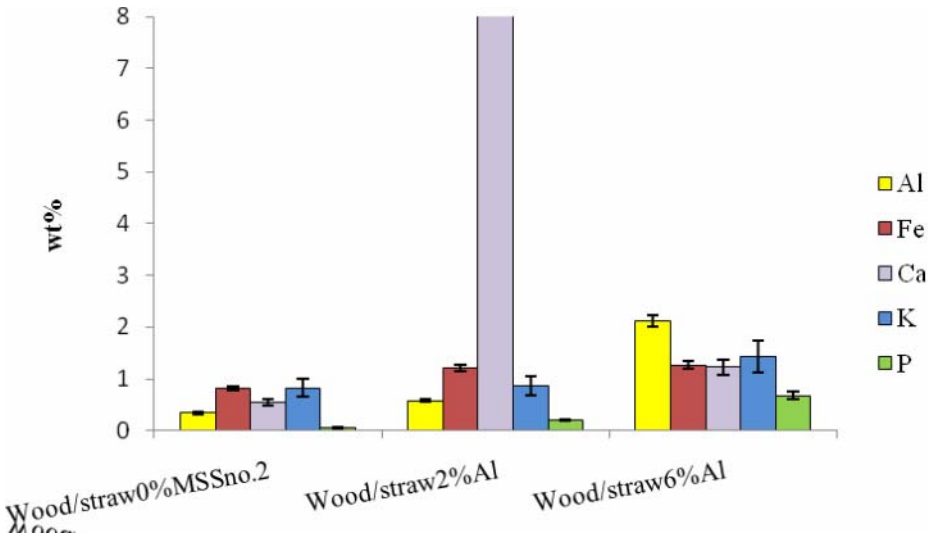

Figure 18. Chemical composition of some of the main elements in the group of experiments with wood/straw and an addition of *Al-sludge.* All Ca content is included in this figure.

The content of P, Fe and Al increases in the wood/straw samples with the addition of Fe-sludge. The addition of Al-sludge increases the content of P and Al, whereas the content of Fe seems to be constant. The content of Fe is probably affected by traces of metal originating from the laboratory equipment that has ended up in the bed sand. It is however impossible to distinguish between the contribution of Fe from the equipment and Fe originating from the combusted fuels. Besides the differing Al and Fe content, the concentration of the different ash components are approximately the same for *wood/straw6%Fe* and *wood/straw6%Al.*

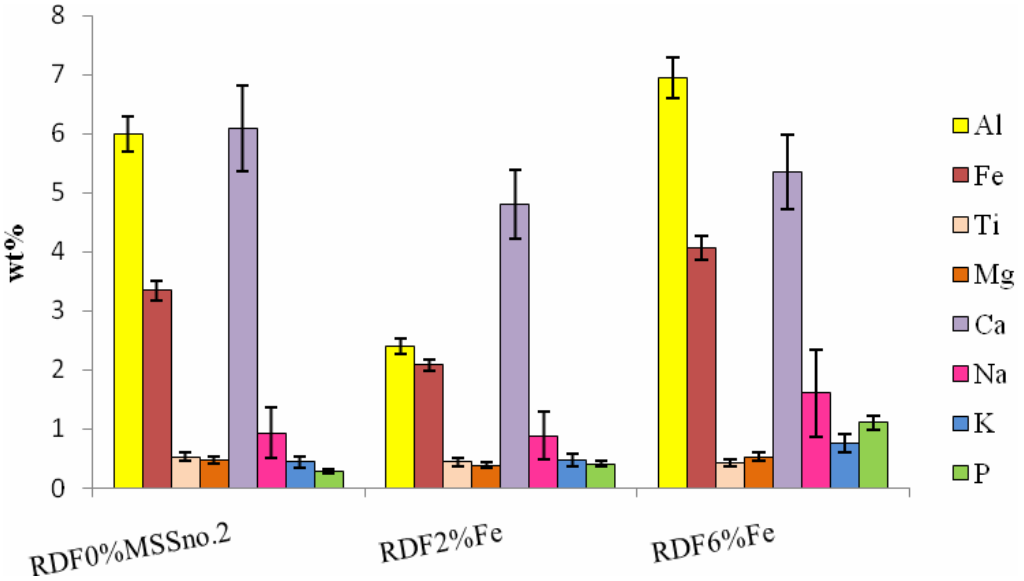

Figure 19. Chemical composition of some of the main elements in the group of *RDF Fe-sludge.*

In contrast to the wood/straw fuel, RDF is rich in Na. This is reflected in the bed sand samples after combustion. The Na content in the RDF bed sand increases with an increased amount of

combusted fuel. RDF is also rich in Ti, which is probably explained by a large fraction of paper in the fuel (Ti is part of a colour pigment used to dye paper). The fact that *RDF6%Fe* was the only RDF experiment where all fuel was combusted makes it difficult to determine the effect of an increased addition of sludge. However RDF has high ash content even without the addition of sludge and it is obvious that an increased amount of combusted fuel increases the content of ash in the bed sand (*RDF0%MSSno.2* was combusted 5 hours compared to *RDF2%Fe* that was combusted only 2 hours).

4.2.3 Results and discussion from the SEM/EDX analysis

The SEM/EDX analysis gives pictures of the analyzed sample, EDX – mappings of the element distribution and quantification of different elements in specific points. SEM/EDX analyses of the bed sand were performed after the combustion experiments (but before the agglomeration test). This means that *Bark*, *Wood/straw2%Fe*, *Wood/straw6%Fe*, *Wood/straw2%Al*, *Wood/straw6%Al* and *RDF6%Fe* were analyzed before the samples were agglomerated, while the remaining bed sand samples agglomerated during the combustion. As discussed above the sintering of the bed material during some of the combustion experiments resulted in that different amount of fuel was combusted in the different experiments. This resulted in that different amounts of ash remained in the bed for the different test runs. Pictures and mappings for all experiments are presented and discussed below. Element quantifications are used as basis of discussion and are presented in appendix I.

Bark

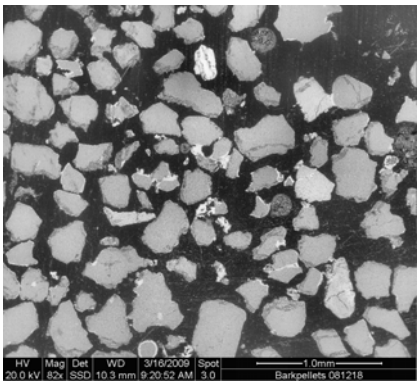

Figure 20. SEM-picture of the *bark* sample.

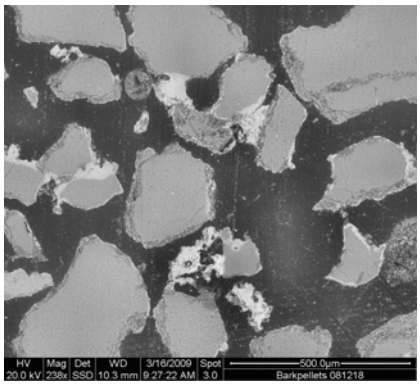

Figure 21. SEM-picture of the *bark* sample

Most sand particles in the SEM-pictures of the bark sample (Figure 20 and Figure 21) have coatings that appear as brighter areas. EDX-mapping (Figure 22) shows that the coatings consist of silicate melt rich in K and Ca. EDX-mapping together with the element quantification (Appendix I, Figure 70) also show the traces of Na, P, and Mn in the coatings.

The coating has grown thicker on some particles, which in some cases have led to adhesion of sand particles, this can be clearly seen in Figure 21.The melt bridge that adhere the particles is called necking.

The quantification analysis shows that the particle seen with a clear Al content (Figure 22) probably is feldspar from the bed sand since it corresponds to the same element content; Al, Si, O and K.

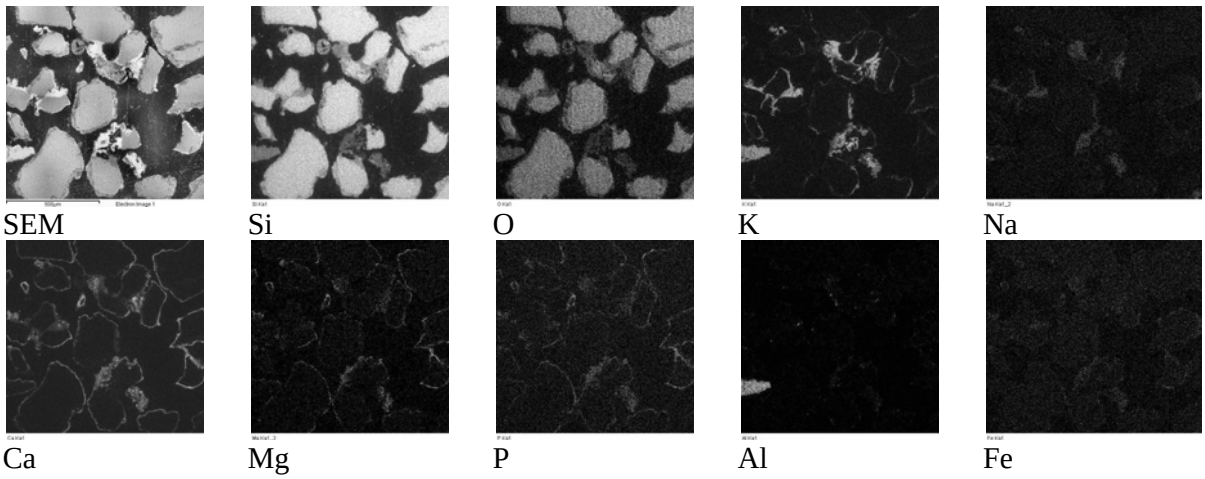

Figure 22. Pictures from EDX-mapping showing the elements in a cross-section area of the *bark* sample.

Wood/straw0%MSSno.1

SEM/EDX was performed on Wood/straw0%MSSno.1. It was considered to be enough to get a good idea of the behaviour of the bed material when combusting wood/straw without any addition of sewage sludge.

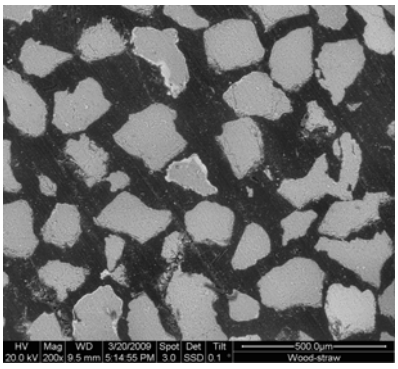

Figure 23. SEM-picture of the W*ood/straw0%MSSno.1* sample.

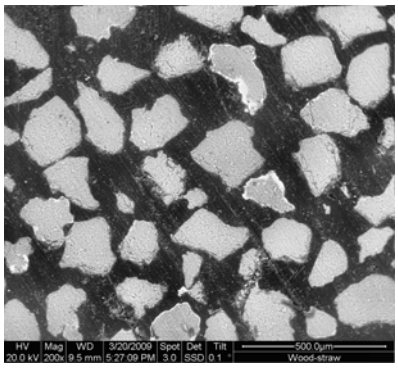

Figure 24. SEM-picture of the W*ood/straw0%MSSno.1* sample.

SEM-pictures (Figure 23 and Figure 24) and EDX-mapping (Figure 25) show that some of the sand particles in the *Wood/straw0%MSSno.1* sample have coatings. The EDX-mapping shows that the coatings consist of silicate melt rich in Ca and K. Element quantification (Appendix I,

Figure 71) shows that some coatings also contain minor amounts of Cl, Mg and P. Na can, according to the element quantification, be found in low concentrations in the coatings. Two of the particles in the mapping have thick coatings. According to element quantification these have higher concentration of Fe, Mg and P compared to the rest of the coatings.

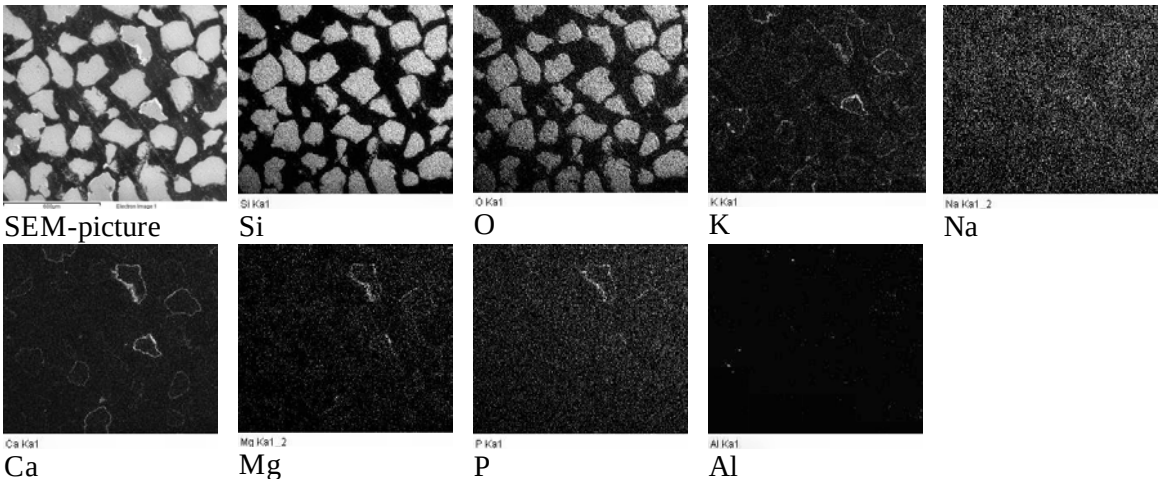

Figure 25. Pictures from EDX-mapping showing the elements in a cross-section area of the *Wood/straw0%MSSno.1* sample. Fe is not presented in the figure since the concentrations are too low to be visible.

Wood/straw2%Fe

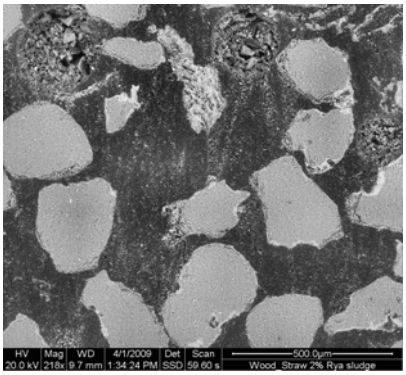

Figure 26. SEM-picture of *Wood/straw2%Fe.*

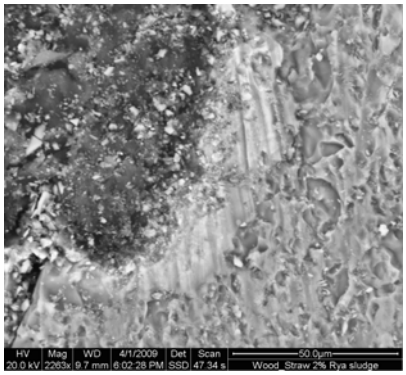

Figure 27. SEM-picture of *Wood/straw2%Fe*.

SEM-pictures (Figure 26 and Figure 27) and EDX-mapping (Figure 28) show that most of the sand particles have thin coatings. EDX-mapping shows that the coatings consist of silicate melt rich in Ca and K, but also minor amounts of Mg was found. The element quantification (Appendix I, Figure 101) shows that the analyzed coating also has a content of Na, P, Al, Fe and Cl.

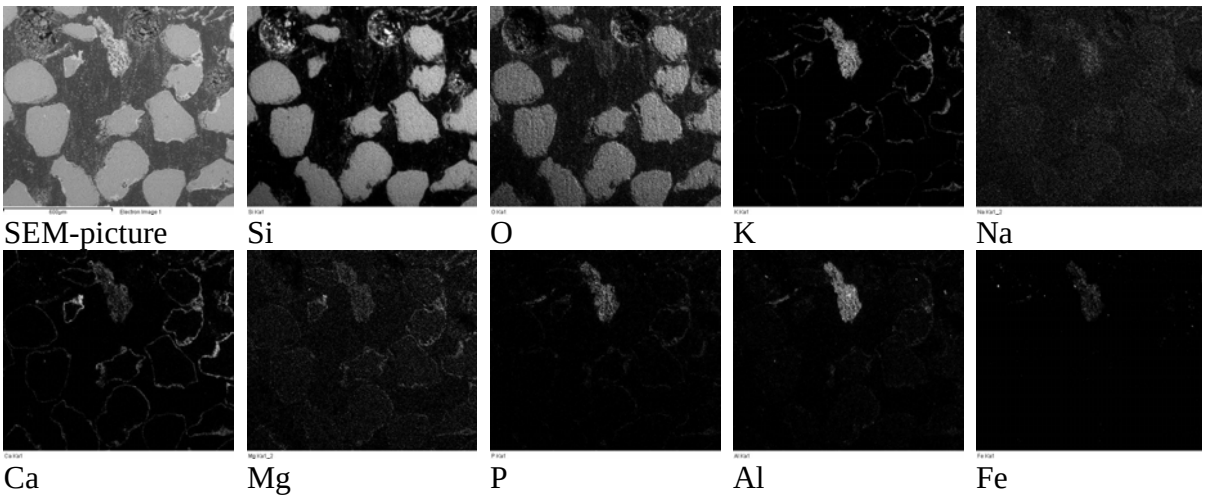

Figure 28. Pictures from EDX-mapping showing the elements in a cross-section area of the *Wood/straw2%Fe* sample.

Wood/straw6%Fe

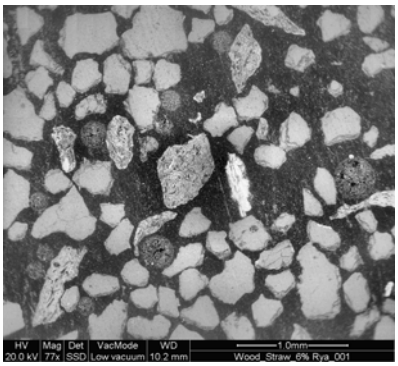

Figure 29. SEM-picture of the *Wood/straw6%Fe* sample.

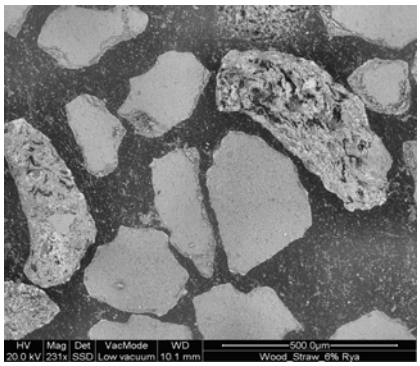

Figure 30. SEM-picture of the *Wood/straw6%Fe* sample.

SEM-pictures (Figure 29 and Figure 30) does not show any agglomerated particles. Figure 30 is a SEM-picture where porous particles that resemble raisins can be seen, these are sludge ash particles. EDX-mapping of *Wood/straw6%Fe* (Figure 31) shows more distinct coatings of silicate melt rich in Ca and K compared to *Wood/straw0%MSSno.1*. The coatings have according to element quantification (Appendix I, Figure 732) a content of Al, Fe and P which also is clearly seen in the EDX mappings (Figure 31).

To see whether the element composition of the sludge was changed during combustion, the element quantification was compared with the fuel analysis of the sludge of the sludge ash particles. It was seen that the content of K had increased and the content of Al had decreased

during combustion. The rest of the ash components in the sludge ash particle seem to have approximately the same concentration before and after combustion.

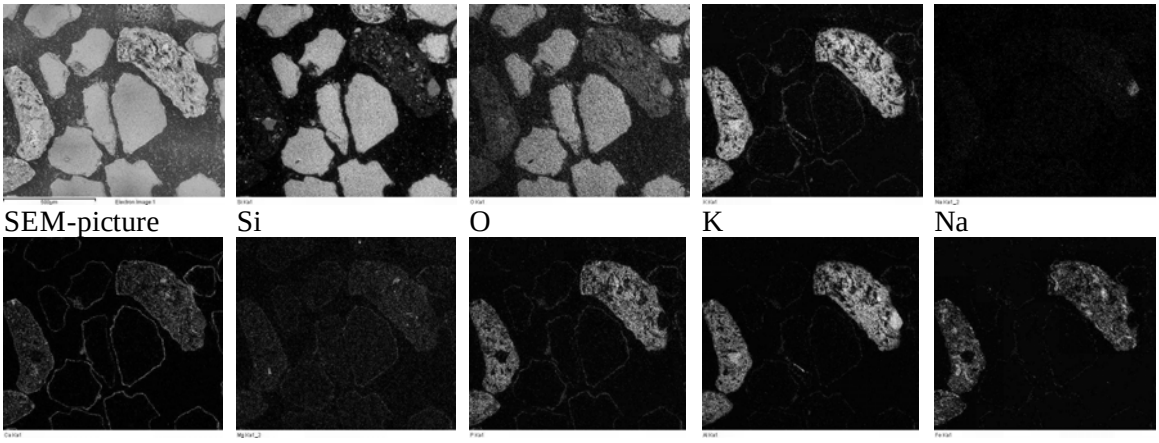

Figure 31. Pictures from EDX-mapping showing the elements in a cross-section area of the *Wood/straw6%Fe* sample.

Comparing the samples with addition of Fe-sludge

The EDX-mapping shows that there is hardly any Fe, Al or P in the coatings in the *Wood/straw0%MSSno.1* sample. The addition of sludge gave coatings in the *Wood/straw2%Fe* and *Wood/straw6%Fe* samples that contained Fe, Al and P. This can be seen in EDX-mappings and element quantifications. The content of Fe and P in the coatings increases with increased addition of Fe-sludge, whereas the content of Al seems to be approximately the same.

The element quantifications show that the content of Ca in the coatings is approximately the same in all three samples. The content of K in the coatings is similar in the *Wood/straw0%MSSno.1* and *Wood/straw2%Fe* samples but significantly lower in the *Wood/straw6%Fe* sample.

Wood/straw2%Al

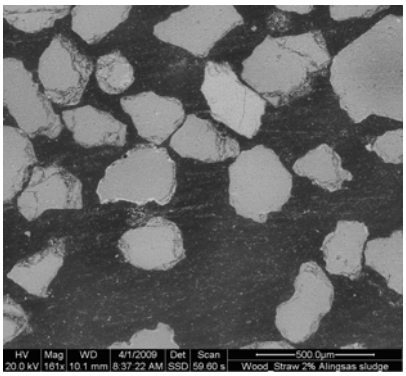

Figure 32. SEM-picture of the *Wood/straw2%Al* sample.

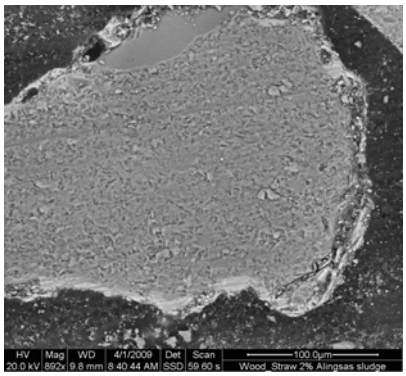

Figure 33. SEM-picture of the *Wood/straw2%Al* sample.

SEM-pictures (Figure 32 and Figure 33) and EDX-mapping (Figure 34) show coatings on the sand particles. The EDX-mapping shows that the coatings consist of silicates rich in Ca and K. Element quantifications (Appendix I,Figure 74) also show a content of Na, Al, P, Cl and Fe.

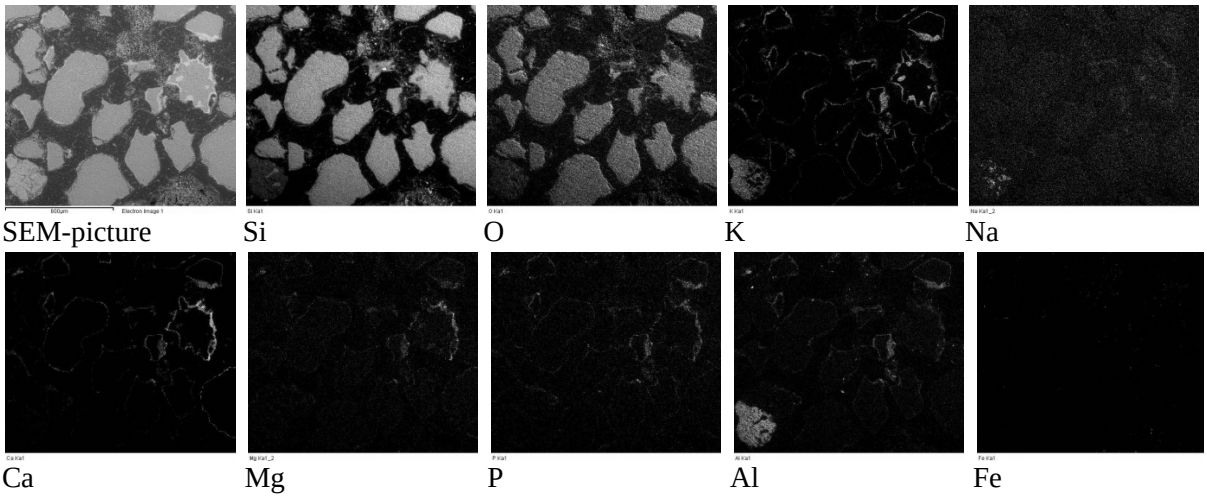

Figure 34. Pictures from EDX-mapping showing the elements in a cross-section area of the *Wood/straw2%Al* sample.

Wood/straw6%Al

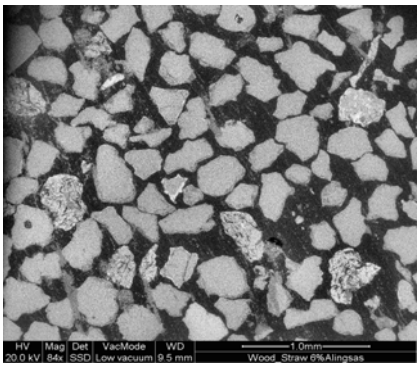

Figure 35. SEM-picture of the *Wood/straw6%Al* sample.

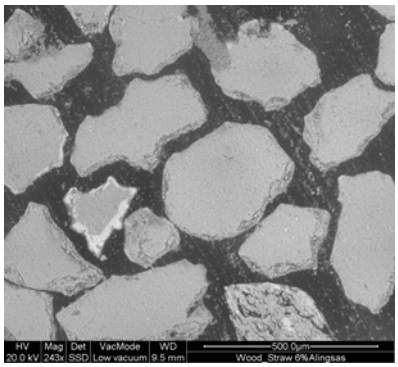

Figure 36. SEM-picture of the *Wood/straw6%Al* sample.

SEM-pictures (Figure 35 and 36) and EDX-mapping (Figure 37) show that particles of the *Wood/straw6%Al* sample have thin coatings. The EDX-mapping shows that the coatings consist of silicates rich in Ca and K. The coatings also contain P, Al, Fe and Mg.

In Figure 75 in Appendix I there are two sludge ash particles, these have been analyzed with element quantification. The result has been compared with the fuel analysis of the sludge before combustion. The comparison shows that Al-sludge particles after combustion have an increased content of K (from 1.1wt% to >6wt%) and a decreased content of Al (from 19wt% to approximately 12wt%). The rest of the ash components in the sludge have approximately the same concentration before and after combustion.

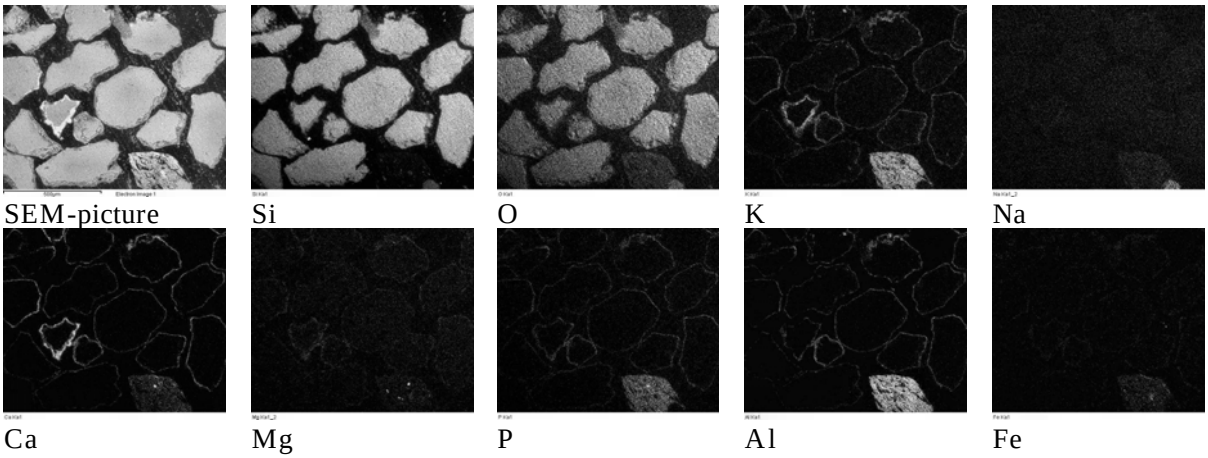

Figure 37. Pictures from EDX-mapping showing the elements in a cross-section area of the *Wood/straw6%Al* sample.

Element quantifications made in a line across the coating

Figure 38 shows a coated sand particle from the combustion experiment of *Wood/straw6%Al*. The coating seems to be built up by a dense inner coating and a more porous outer coating. Element quantification was carried out in a line across the coating to see how the element distribution changes throughout the coating, see Figure 38. The inner layer (LS1(4) - LS1(8)) is rich in K and Ca whereas in the outer layer (LS1(9) – LS1(10)) the concentration of Ca increases compared to K. In the outer layer there is a significant increase of Fe, Al and P. The theory is that the high concentration of K in the inner layer creates a sticky inner coating upon which elements from the sludge (Fe, Al and P) get trapped. The outer coating of sludge elements increases the melting point resulting in decreased stickiness and prevention of further build up of agglomerates.

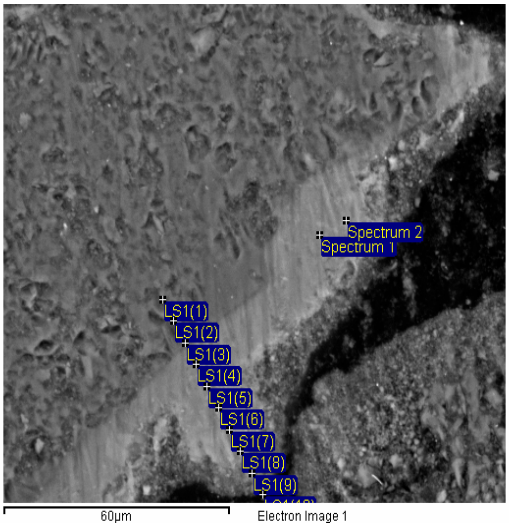

Figure 38. Figure with the points where the element quantification has been performed on the *Wood/straw6%Al* sample.

The quantification for the *Wood/straw6%Al* sample has been performed in a line across the coating of the sand particle. LS1(1) – LS1(3) are points on the surface of the sand particle and LS1(5) – LS1(10) are points where element quantifications have been performed on the coating.

Table 4. Element composition in a cross section of a coating in the *wood/straw6%Al.* "Coat" indicates that the element quantification has been performed on a coating.

Spectrum/ wt%	O	Na	Mg	Al	Si	P	Cl	K	Ca	Fe
Spec 1 coat	51.7	0.6	0.8	0.3	34.5	0.0	0.3	7.4	4.5	0.0
Spec 2 coat	51.2	0.5	0.7	0.4	30.9	0.9	0.1	5.2	9.8	0.4
LS1(1)	52.5	0.0	0.1	0.2	45.6	0.2	0.1	0.6	0.7	0.0
LS1(2)	52.2	0.0	0.1	0.1	45.7	0.2	0.0	0.8	0.9	0.0
LS1(3)	53.4	0.0	0.2	0.1	43.5	0.2	0.1	1.1	1.2	0.2
LS1(4) coat	51.1	0.6	0.8	0.3	34.6	0.3	0.0	7.4	4.5	0.4
LS1(5) coat	50.7	0.5	0.9	0.4	34.6	0.3	0.1	7.5	4.7	0.5
LS1(6) coat	50.5	0.6	0.9	0.4	33.7	0.4	0.1	7.3	5.4	0.6
LS1(7) coat	50.0	0.6	0.9	0.6	33.3	0.4	0.2	6.9	6.7	0.6
LS1(8) coat	47.1	0.3	1.1	0.7	29.6	1.3	0.1	4.6	14.7	0.6
LS1(9) coat	50.9	0.4	1.8	7.3	17.8	4.4	0.4	3.4	11.1	2.5
LS1(10) coat	50.6	0.0	1.0	5.1	24.0	3.8	0.8	3.6	8.6	2.1

Element quantification in lines has also been done on *Wood/straw2%Fe* (Appendix I, Figure 72) and *Wood/straw2%Al* (Appendix I, Figure 74). All three coatings share the same tendency: Fe, Al and P are present in the outer layers.

Both *Wood/straw2%Al* and *Wood/straw6%Al* have high concentrations of Ca and K in the inner layer. In the outer layer the concentration of Ca increases and the concentration of K decreases. In the *Wood/straw2%Fe* sample the concentration of K seems to be equal in both layers. The concentration of Ca is higher in the outer layer compared to the inner layer.

Comparison of wood/straw Al-sludge samples

The element quantifications shows that the concentrations of K and Ca in the coatings around the sand particles are similar for *Wood/straw0%MSS, Wood/straw2%Al* and *Wood/straw6%Al.* Addition of sludge increases the concentration of Fe in the coatings, but the Fe concentration do not differ remarkably between *Wood/straw2%Al* and *Wood/straw6%Al*. The concentration of Al and P in the coatings increases with an increased addition of sludge.

RDF0%MSSno.1

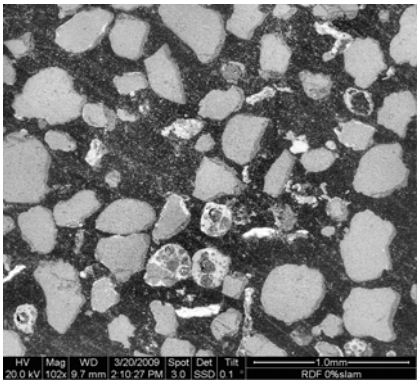

Figure 39. SEM-picture of the *RDF0%MSSno.1* sample.

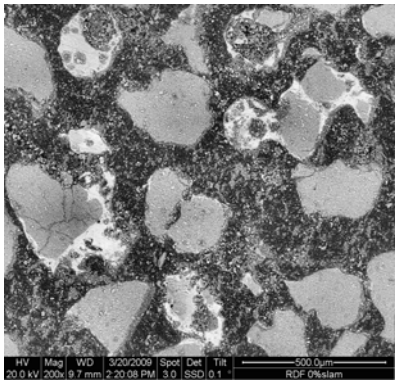

Figure 40. SEM-picture of the *RDF0%MSSno.1* sample.

SEM-pictures (Figure 39 and Figure 40) and EDX-mapping (Figure 41) show that particles in the *RDF0%MSSno.1* sample have coatings with different density. EDX-mapping shows that the coatings consists of silicates rich in Ca (up to 10 molar-%). A number of neckings can clearly be seen in Figure 40, indicating that sticky melt has been formed on the surface of the bed particles. EDX-mapping showed that the neckings contain silicate melt with Ca, but also Na, K, Mg and some Ti. Elemental quantification (Appendix I, Figure 76) shows that the neckings also contain Al and Fe.

Elemental quantification shows that the concentration of Na in the coatings is higher than the concentration of K. This corresponds to the relation Na:K in the ash composition of RDF before combustion.

There are some round-shaped particles in the SEM-picture that seem to be more porous compared to the sand particles. These particles also exist in other RDF samples. They are often coated and indicate a tendency of taking part in the formation of agglomerates. EDX-mapping shows that those particles, especially in the case of *RDF0%MSSno.1* and *RDF0%MSSno.2* contain quite a lot of Si, O, Ca and Na. It could consist of a silicate melt rich in Ca and Na. Element quantification shows that those particles have a clear content of metals, for example Mg, Al, Fe and Ti is found.

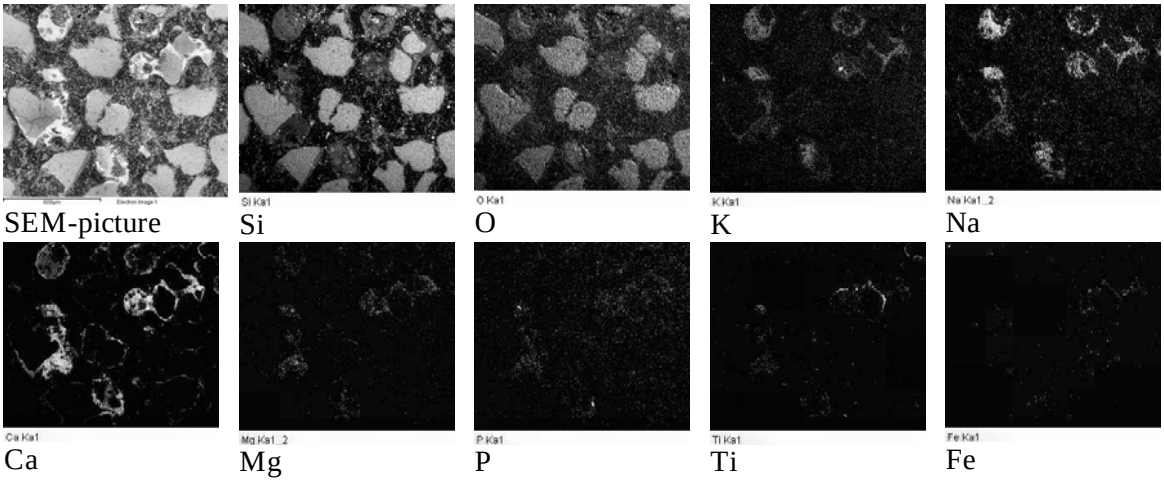

Figure 41. Pictures from EDX-mapping showing the elements in a cross-section area of the RDF0%MSSno.1 sample.

RDF0%MSSno.2

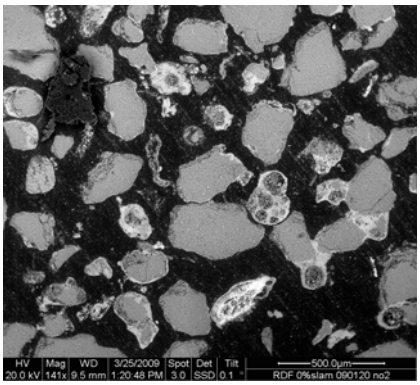

Figure 42. SEM-picture of the *RDF0%MSSno.2* sample.

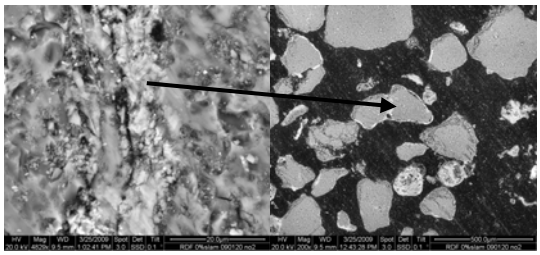

Figure 43. SEM-picture of the *RDF0%MSSno.2* sample. The picture to the left is an enlargement of a coating in the picture to the right.

In SEM- pictures Figure 42 and Figure 43 and EDX-mapping (Figure 44) it can be seen that most sand particles in the *RDF0%MSSno.2* sample have coatings with different density. Many of them are quite thick and have resulted in the formation of agglomerated bed particles. The EDX-mapping shows that the coatings consist of silicates rich in Ca. It also shows that Na, K and in some degree Mg are present in the coatings, in particular in the thicker ones.

According to the fuel analysis the ash of RDF is not very rich in P. Despite this, element quantifications of a cross section of two agglomerated particles show that P exists in small concentrations in the coatings (Appendix I, Figure 78). Also Ca, Mg, Al, Ti, Fe, K, Na and Cl exist in varying concentrations. Ca is present in high concentrations. From the element quantification it can be seen that Ca has penetrated the bed sand particle.

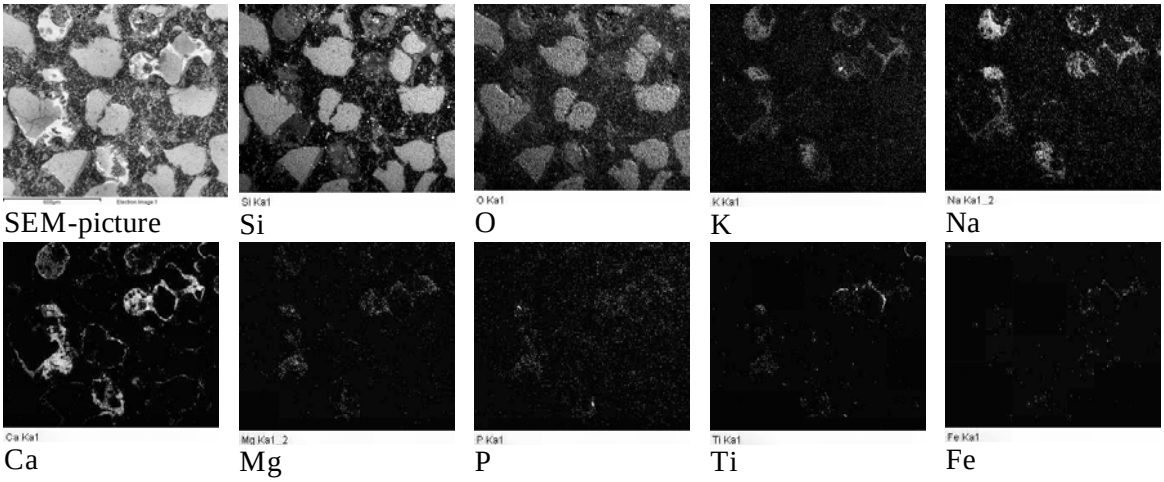

Figure 38. Pictures from EDX-mapping showing the elements in a cross-section area of the *RDF0%MSSno.2* sample.

RDF2%Fe

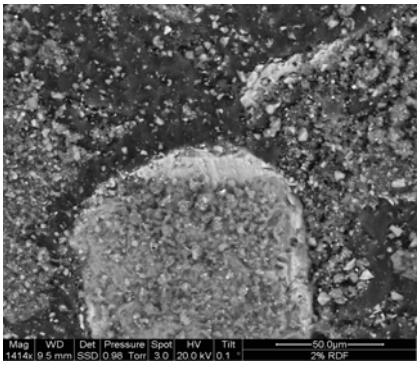

Figure 45. SEM-picture of *RDF2%Fe.*

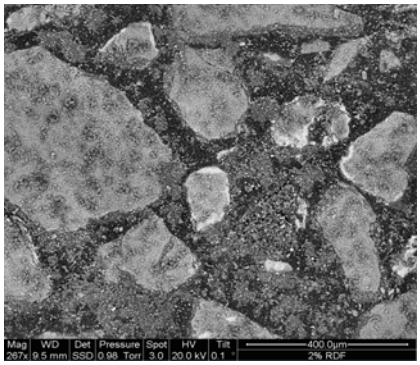

Figure 46. SEM-picture of *RDF2%Fe* showing a clearly coated bed sand particle.

SEM-pictures (Figure 45 and Figure 46) and EDX-mapping (Figure 47) show that parts of the bed sand particles in the *RDF2%Fe* sample have coatings. The EDX-mapping shows that the coatings contain silicate melt rich in Ca. Element quantification (Appendix I, Figure 79) shows that the concentration of Na in the coatings is lower compared to the Na concentration in the coatings of the *RDF0%MSS* samples. The Al and Fe content in the coatings are similar to the Al and Fe content in the coatings of *RDF0%MSS*.

The round shaped particle that is discussed in the *RDF0%MSSno.1* section is not that clearly showed for *RDF2%Fe*. EDX-mapping shows one particle that corresponds to this description. It can be recognized from its content of K, Na, Ca, Mg and P.

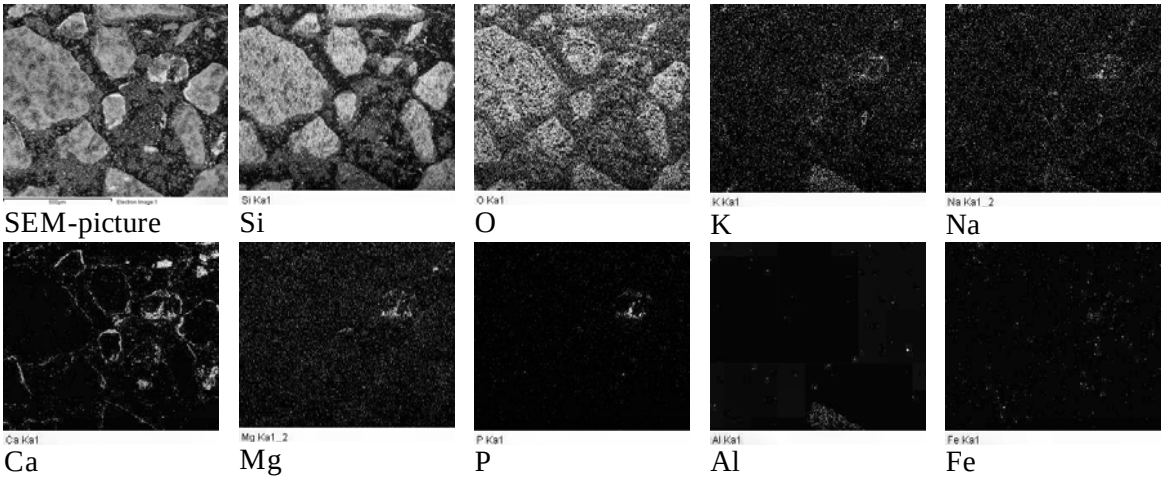

Figure 47. Pictures from EDX-mapping showing the elements in a cross-section area of the RDF2%Fe sample.

RDF6%Fe

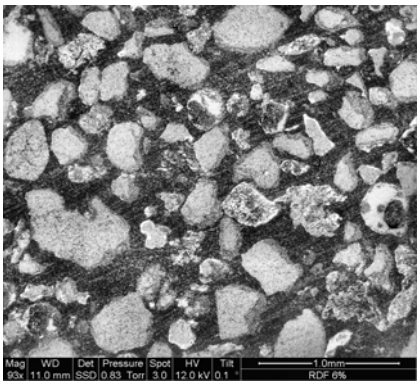

Figure 48. SEM-picture showing *RDF6%Fe.*

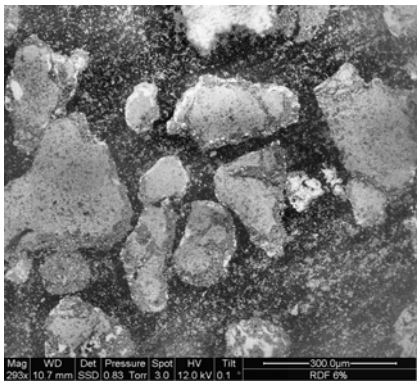

Figure 49. SEM-picture showing *RDF6%Fe.*

SEM-pictures (Figure 48 and figure 49) and EDX-mapping (Figure 50) show that the *RDF6%Fe* sample contains bed sand particles with coatings of varying density. The EDX-mapping shows that the coatings contain silicates with a varying concentration of Ca. Element quantification shows that also Na, K, P, S, Cl, Fe and Al exists in the coatings (Appendix I, Figure 80).

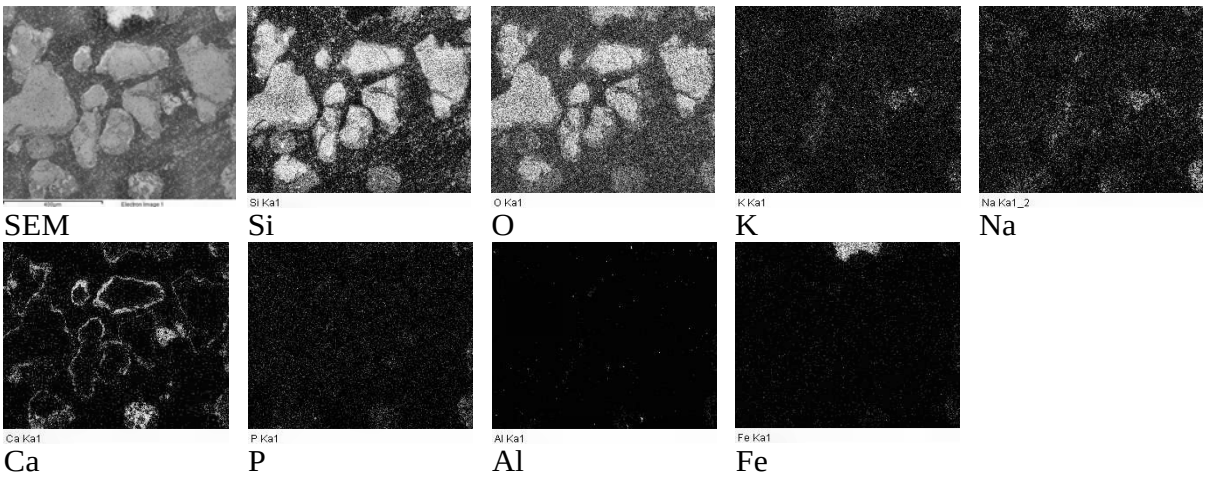

Figure 50. Pictures from EDX-mapping showing the elements in a cross-section area of the *RDF6%Fe* sample.

Comparison of RDF samples

The concentration of Ca in the coatings is high in all RDF samples, but there seems to be a small decrease of Ca in the coatings with addition of sludge. The content of K in the coatings is low (< 1wt%) in all samples. The content of Na in the coatings is high compared to K in all samples. The Na concentration in the coatings decreases with an increased addition of sludge.

It is found that the Fe concentration in the coatings is higher in the *RDF6%Fe* sample compared to *RDF0%MSS* and *RDF2%Fe*. This trend also seems to be valid for P. It cannot be decided whether this is an effect of the increased addition of sludge or comes from an increased time of combustion.

Summary of comparisons of SEM/EDX results

Some particles have denser coatings than other particles. These coatings are clearly shown in the SEM-pictures. The less dense coatings are often more clearly seen in the EDX-mapping. Some particles seem to have both types, one denser inner coating and a more porous outer coating. Theoretically, denser coatings could be reaction introduced, while porous coatings could be melt induced. Ash that reacts with the quartz bed particles or other ash particles results in dense packed phases.

The outer coating layer seems to partly consist of elements from the sludge ash. It is possible that the inner coating layer consists of a sticky film of alkali melt on which elements from the sludge get stuck. The second layer has a high content of P, Al and Fe that probably originates from the sewage sludge. The elements originating from the sludge seem to reduce the stickiness of the coating and hence reduce the bed agglomeration.

The composition of sludge ash before and after the combustion is investigated by comparing the fuel analyses of Fe- and Al-sludge with element quantification of sludge ash particles in some wood/straw samples. This comparison indicates that the concentration of Fe in sludge ash particles is constant, while the concentration of Al decreases. One theory regarding the decrease in Al is that Al that is not bound into zeolites diffuses, while Al bound to zeolites are too big to move. All fuel mixes, including RDF, has ash with a higher content of Al compared to Fe. Despite this the relation Al:Fe approximately is 1:1 (molar basis) for the wood/straw samples. Al seems to be more mobile than Fe, but it is unknown where it ends up. It could move to the coatings, but this should result in a different Al:Fe relation. However the RDF samples have higher concentration of Al compared to Fe in the coatings.
The concentration of Ca in the coatings seems to be much higher in the RDF and Bark samples than in the wood/straw samples.

4.2.4 Results and discussion regarding the agglomeration temperatures

Agglomeration tests were performed on all samples that did not agglomerate during the combustion test. The agglomeration is divided into three different categories depending on degree of agglomeration (see chapter 3.7). Some samples only show a distinct agglomeration temperature while others contain all three stages. The Bark sample, Figure 51, showed all three stages. All the performed agglomeration tests are presented in appendix F and resulting temperatures are presented in Table 5.

.

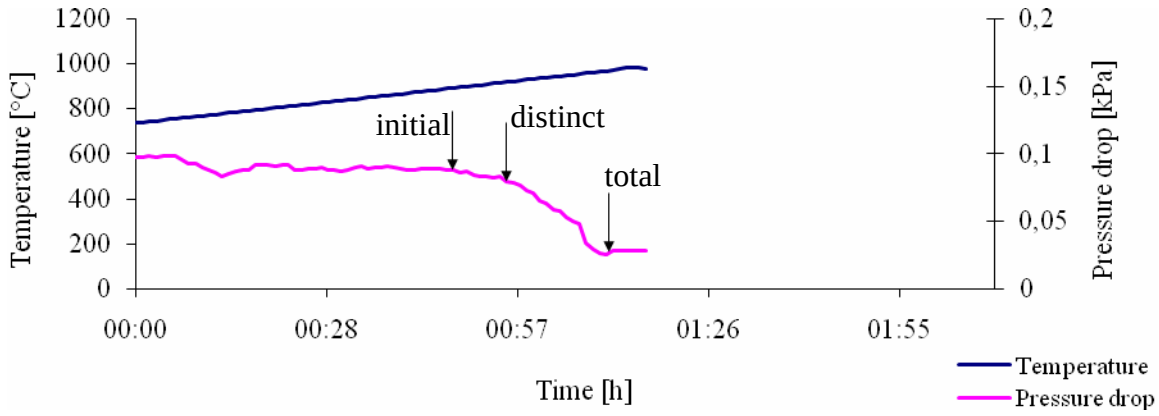

Figure 51. Agglomeration temperature for the *bark* sample; Initial agglomeration temperature 898°C, distinct agglomeration temperature 925°C, total agglomeration temperature 978°C.

Table 5. Agglomeration temperatures.

	Initial agglomeration temperature [°C]	Distinct agglomeration temperature [°C]	Pressure drop [Pa/min]	Total agglomeration temperature [°C]
Ref 12_12BB	-	860	-	-
Bark	898	926	4.32	978
Wood/straw2%Fe	-	962	4.52	1008
Wood/straw6%Fe	-	1082	4.13	1094
Wood/straw2%Al	-	1007	4.12	-
Wood/straw6%Al	-	No agglomeration	-	-
RDF6%Feno.1	905	1016	4.12	-
RDF6%Feno.2	-	1010	3.54	1081

The agglomeration test of *RDF6%Fe* was repeated. *RDF6%Feno.2* gave a maximum pressure drop of 3.54 Pa/min. Due to the norms of the agglomeration test this should not be considered as distinct agglomeration, but graphically there is an obvious slope at this pressure drop that can almost be considered equivalent to distinct agglomeration (Figure). The temperature during those two pressure drops were 1016°C for *RDF6%Feno.1* (Figure 63) and 1010°C for *RDF6%Feno.2*. The result showed a good repeatability and the method used for the agglomeration test can be considered reliable.

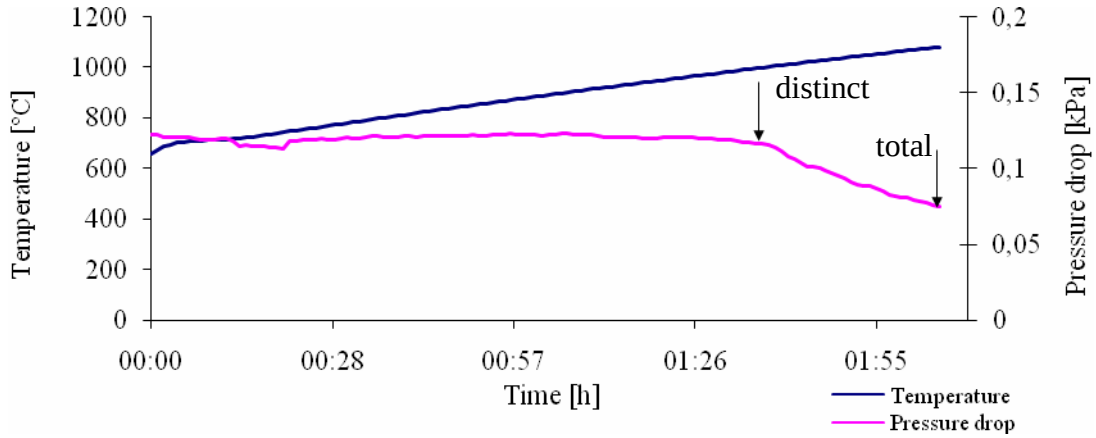

Figure 52. Agglomeration temperature for the *RDF6%Feno.2* sample; distinct agglomeration temperature 1010°C, total agglomeration temperature 1081°C.

4.2.5 Summary of the agglomeration discussion

It can clearly be seen that an addition of sewage sludge increases the agglomeration temperature. Both *wood/straw0%MSS* and *RDF0%MSS* agglomerated before the fuel batch was fully combusted. Both Fe- and Al-sludge gave positive effects with both dosages when

wood/straw was combusted. The agglomeration temperature was increased with an increased dosage of sludge. The dosage of 2% sludge gave an agglomeration temperature of 962°C for the samples with Fe-sludge compared to 1007°C for the samples with Al-sludge. The dosage of 6% sludge gave an agglomeration temperature of 1082°C for the samples with Fe-sludge, while the samples with Al-sludge did not agglomerate at all within the allowed temperature interval of the laboratory scale reactor (1100°C).

RDF0%MSS and *RDF2%Fe* agglomerated during combustion. A dosage of 6% Fe-sludge hindered the agglomeration during combustion and two agglomeration tests of the sample showed agglomeration temperatures of 1010°C and 1016°C respectively. A higher dosage of sludge is needed for the prevention of agglomeration during combustion of RDF compared to the combustion of wood/straw. This is probably due to that RDF has a higher ash and alkali content (15.4%) compared to wood/straw (1.7%) and hence higher amounts of alkali was supplied to the sand bed when combusting RDF compared to combusting wood/straw. *Bark* persisted the combustion without agglomerating and the agglomeration temperature was determined to 926°C in the agglomeration test.

4.2.6 Bed sand samples after agglomeration tests

After the agglomeration test the bed sand was taken from the reactor. Pictures of the samples and shorter descriptions are presented in appendix H.

5 Discussion and suggestions for further investigation

To make the discussion easy to follow it is divided into four smaller parts.

The combustion experiments

The amount of fuel is calculated in order to reach a Ca content of 3.28wt% in the bed sand after combustion for *wood/straw0%MSS*. The same amount of fuel was to be combusted in all experiments, which led to large variations in the relation fuel ash to bed sand. Other ways to determine the amount of fuel to be used in the combustion experiments could be to have a constant relation of ash to bed sand or to add constant amount of heat by the various fuels.

The weight of the bed sand after combustion varies between the experiments. The main reason for this is that only part of the fuel batch was combusted in some experiments and that the content of ash varies between the fuels. This results in a varying relation of ash to bed sand from case to case. This makes the results from the different experiments more difficult to compare. Also the fact that bed sand and fuel ash were carried away with the flue gases in all experiments contributes to this. A constant fluidizing gas flow should result in the same amount of carried away bed sand. It is however likely that the amount of carried away ash varies between the different experiments.

Combustion in the laboratory scale reactor gave an incomplete combustion. The residence time in the reactor might have been too short to reach a good oxidization. This together with an extra supply of excess air led to air factors that were higher than intended. However, these combustion conditions should not have affected the agglomeration tendencies of the bed sand.

Due to a computational mistake the combusted fuel batch of *bark* was too small (1.73 kg ds compared to 2.00 kg ds). The bed sand after combustion showed tendencies of being agglomerated. It is possible that the bed would have sintered during combustion if the experiment had been performed with the same amount of fuel as the rest of the experimental matrix.

Sintering tendencies during combustion

The reference case (*Ref 12h_BB)* from Agglobelägg 2 had a low agglomeration temperature (860°C) it is therefore not surprising that both *wood/straw0%MSSno.1* and *wood/straw0%MSSno.2* sintered already during the combustion in the laboratory scale reactor. The laboratory scale reactor has an uneven temperature distribution. Local high temperature maximum can exist to a greater extent in the laboratory scale reactor than in a full scale boiler. Also, the temperature in the laboratory scale reactor varied in time and the

difference between the average temperature and maximum temperature could easily be recorded to more than 50°C. This makes the bed sand more sensitive to bed agglomeration even though the average bed temperature was recorded to be fairly low.

The RDF pellets are inhomogeneous. This might result in that the ash content in the small batches of fuel that is prepared for the different experiments of RDF might not represent the theoretical average ash content. It is therefore possible that the results from the combustion experiments might be somewhat misleading.

Both *RDF0%MSSno.1* and *RDF0%MSSno.2* sintered during combustion. During the combustion of *RDF0%MSSno.1* the bed temperature was quite high and had reached 900°C when the bed sintered. The experiment was repeated with a better control of the bed temperature. When keeping the bed temperature under 880°C, it was possible to combust more of the fuel batch before the bed sintered. However the bed agglomeration could not be hindered.

Also *RDF2%Fe* sintered during the combustion. In contrary to *RDF0%MSSno.1* the bed temperature was kept under the upper limit of 880°C and the experiment was therefore not repeated. However the combustion temperature was slightly higher for *RDF2%Fe* than for *RDF0%MSSno.2*. The higher temperature during combustion of *RDF2%Fe* is the most likely reason that less of the fuel batch was combusted for *RDF2%Fe* than for *RDF0%MSSno.*2. A larger fuel batch result in a longer combustion period and higher ash content in the bed sand in the *RDF0%MSSno.2* compared to *RDF2%Fe*, which makes the samples hard to compare.

The two performed agglomeration test of the RDF6%Fe samples gave approximately the same distinct agglomeration temperatures (1010°C and 1016°C respectively). These shows good repeatability of the method and the results are considered reliable.

Analysis of the bed sand

The coating seems to be built up by a dense inner coating and a more porous outer coating. Both coatings contain a lot of Ca, but the Ca content is higher in the outer coating. The inner coating is a sticky layer rich in K while the outer coating is rich in Al, Fe and P that probably originate from the sludge. The positive effect of the addition of sludge can be explained by this outer coating that prevents the stickiness of the inner coating and hence reduce the agglomeration tendencies of the bed sand.

Addition of sludge results in a decreased amount of K in the coatings of the sand particles. K is probably captured by zeolites in the sewage sludge during combustion. An increase of K is seen in the sludge when comparing the fuel analysis of sludge before combustion with the

element quantification of the sludge ash particles after combustion. The total content of Na in the bed sand is increased with an increased addition of sludge during the combustion of RDF. In contrary, the concentration of Na in the coatings seems to decrease. This could be an indication of that the sludge also absorbs Na. Unfortunately no element quantification of the sludge ash in the RDF samples were performed, which makes it impossible to make specific conclusions.

The amount of Fe, Al and P are increased in the coatings with an increased addition of sludge (an exception is that there is no obvious difference in the amount of Al in the coatings between 2% and 6% addition of Fe-sludge to wood/straw fuel). The theory is that Fe, Al and P move from the sludge to the outer coating layers of the sand particles. However, when comparing the fuel analysis of sludge before combustion and element quantification of the sludge ash particles after combustion only a decrease in the content of Al was seen. No change in the content of Fe and P during combustion was noticed. These tendencies were seen both for Fe-sludge and Al-sludge.

It seems like P that originate from the sludge have a positive effect on preventing bed agglomeration by moving to the coatings of the bed sand. Further investigations with addition of some kind of P compound could tell more about this effect. It should be remembered that P theoretically can form silicates rich in K and P and it is known that Ca and Al plays important roles in hindering the formation of low-temperature eutectics.

Suggestions for further investigations

The addition of Al-sludge showed an overall better effect on preventing bed agglomeration compared to Fe-sludge. It would be interesting to investigate if the addition of Al-sludge to RDF shows the same tendency and hence could prevent bed agglomeration even with the lower addition of sludge.

It is known that both ion-exchanged and non-ion exchanged zeolites absorbs K both at low and high (combustion) temperatures. It would therefore be interesting to use both ion- and non-ion exchanged zeolites as additives during combustion to investigate whether any differences could be found.

A lot of different reactions take place in the reactor during the combustion which results in the formation of a lot of different compounds. SEM/EDX and chemical analysis recognizes elements that are present in the bed sand, but does not tell anything about the compounds that are formed. To further investigate reactions and resulting compounds, X-ray diffraction could be used.

6 Conclusions

Without any addition of sludge to the wood/straw base fuel the bed sintered during the combustion. Addition of 2% and 6% Fe- and Al- sludge to the wood/straw fuel prevented agglomeration of the bed material and it was possible to combust the total batch of fuel without sintering the bed.

In the agglomeration test it was seen that the higher addition increased the agglomeration temperature more than the lower. It was also seen that the Al-sludge had a better overall effect than the Fe-sludge.

RDF sintered during the combustion when no sludge was added to the fuel. An addition of 2% Fe-sludge was not enough to hinder bed sintering. An addition of 6% Fe-sludge to RDF prevented the bed agglomeration and the bed was not sintered during the combustion. Apparently RDF requires higher addition of sludge than wood/straw to be able to prevent bed agglomeration.

It is seen that the coatings are built up by two layers, one inner layer and one outer layer. The composition of the two layers differs. The inner coating is rich in K while the outer coating is rich in Al, Fe and P that probably originate from the sludge. Both coatings contain a lot of Ca, but the Ca content is higher in the outer coating. The positive effect of the addition of sludge can be explained by this outer coating. It prevents the stickiness of the inner coating and hence reduces the agglomeration tendencies of the bed sand.

The agglomeration temperature of *bark* was determined to be 926°C, which is a low agglomeration temperature. To prevent sintering when combusting bark, measures should be taken in order to increase the agglomeration temperature. Addition of sludge is an example of such measure.

The total amount of P in the bed sand samples is increased with an increased addition of sludge for all cases. The concentration of P is especially higher in the outer layers/coatings. P is most probably originating from the sludge.

The total amount of Al increases with an increased addition of sludge for the wood/straw samples. For the RDF samples the total amount of Al increases with an increased amount of combusted fuel. A tendency of a higher concentration of Al in the bed sand might be seen in the Al-sludge samples compared to the Fe-sludge samples.

The total amount of K in the bed sand was only increased to a small extent during the combustion experiments regardless of what fuel mixtures that was combusted.

7 References

1. **Gyllenhammar M. et al.**, *Measures For Simultaneous Minimization of Alkali Related Operating Problems, Phase 2.* Stockholm , Värmeforsk report no. 1037, www.varmeforsk.se, 2007.

2. **Davidsson K. et al.**, *Measures For Simultaneous Minimisation of Alkali Related Operating Problems,Phase 1.* Stockholm , Värmeforsk report no.997, www.varmeforsk.se, 2006.

3. **ÅF.**, Ångpanneföreningen, *www.energiochmiljo.se, chapter 15.4*, Online ÅF at the 1st of Sept. 2002, cited at the15th of Nov. 2008.

4. **Karnik C.**, *Bäddmaterial i Pannor av Fluidbäddtyp,* Stockholm , Värmeforsk report no.253, 1987.

5. **Glicksman L. R.**, Chapter 8: *Heat Transfer in Circulating Fluidized Beds* in *Circulating Fluidized Beds,* (Eds: J. R. Grace, A.A. Avidan and T. M Knowlton), London , Chapman & Hall, 1997.

6. **Lee Y. Y.**, Chapter 11: *Design considerations for CFB boilers* in *Circulating Fluidized Beds,* (Eds: J. R. Grace, A.A. Avidan and T. M Knowlton), London , Chapman & Hall, 1997.

7. **Knowlton T. M.**, Chapter 7: *Standpipes and Return Systems* in *Circulating Fluidized Beds,* (Eds: J. R. Grace, A.A. Avidan and T. M Knowlton), London , Chapman & Hall, 1997.

8. **Esmail R. et al.**, *Impact of the Circulating Fluidized Bed Riser on the Performance of a Loopseal Nonmechanical valve,* Ind. Eng. Chem. Res., Vol. 6, pp.1843-1850, 2007.

9. **Muschelknautz E., Greif V.** Chapter 6: *Cyclones and Other Gas-Solids Separators* in *Circulating Fluidized Beds,* (Eds: J. R. Grace, A.A. Avidan and T. M Knowlton), London : Chapman & Hall, 1997.

10. **Öhman M. et al.,** *Förbrukning av bäddmaterial i biobränsleeldade fluidbäddar p.g.a. bäddagglomereringsrisk - beläggningsbildning och möjligheter till regenerering,* Stockholm , Värmeforsk report no. 739, www.varmeforsk.se, 2001.

11. **Thunman H.** *Combustion Engineering.* Göteborg , Chalmers University of Technology, 2003.

12. **Andersson S.** *Förbränningsteknik.* Göteborg , Chalmers University of Technology, 1996.

13. **EM**, Energimyndigheten, *Biobränsle - ved och pellets,* www.energimyndigheten.se, Online EM at Nov.15th 2007, cited at Mars 3rd 2009.

14. **Jenkins B. M, et al.**, *Combustion Properties of Biomass,* Fuel processing technology, Vol. 54, pp.17-46, 1998.

15. **Theliander H., Paulsson M., Brelid H.** *Introduktion till massa och pappers-framställning,* Göteborg , Chalmers University of Technology, 2000.
16. **Valmari T.**, *Potassium Behaviour During Combustion of Wood in Circulating Fluidised Bed Power Plants.* Helsingfors , Technical Research Centre of Finland (VTT), ISBN 951-38-5570-8, 2000.
17. **Nordin A.**, *Chemical Elemental Characteristics of Biomass Fuel,* Biomass and bioenergy, Vol. 6, 5, pp 339-347, 1994.
18. **Ljungdahl B., Zintl F.**, *Alternativa bäddmaterial i FB/CFB-pannor* , Termiska Processer (TPS) report no. 803, 2003.
19. **Rönnbäck M. et al.**, *ERA-net utvärdering av utvecklingsstatus för småskalig förbränning av pelletes från nya askrika råvaror,* : Swedish Testing and Research Institute (SP), SP report 2008:31, ISSN 0284-5172, ISBN 978-91-85829-48-4, 2008.
20. **Zarrinpour A., Åmand L.E.**, *Samförbränning av avfall med biobränslen - Ett exempel med avfallspellets som utgångspunkt.* Göteborg : Chalmers University of Technology report no. A2007-001, ISSN 0281-0034, 2007.
21. **Åmand L. E., Davidsson K.**, *Co-Combustion of Lignin and Bark in the 12 MW_{th} Circulating Fluidized Bed Boiler at Chalmers University of Technology,* Göteborg , Chalmers University of Technology, FRAM 2 report no.3, 2006.
22. **GRYAAB**, Göteborgsregionens Rya AB, www.gryaab.se/processen/filmen.html, Online GRYAAB cited at the 25th of Feb. 2009.
23. **NE**, Nationalencyklopedien, http://ne.se/artikel/226611, Online NE cited at the 7th of Nov. 2008.
24. **Zevehoven-Onderwater M. et al.**, *The Prediction of Ashes from Five Different Solid Fuels in Fluidized Bed Combustion*, Fuel, Vol. 79, pp 1353-1361, 2000.
25. **Valmari, T.**, *Field Study in Ash Behaviour during Circulating Fluidized-Bed Combustion of Biomass 1. Ash formation,* Energy and fuels, Vol. 13, pp. 379-389, 1999.
26. **Raask E.**, *The Mode of Occurence and Concentration of Trace Elements in Coal,* Progress in energy and combustion science., Vol. 11, pp. 97-118, 1985.
27. **Pettersson A.**, *Characterisation of Fuels and Fly ashes from Co-Combustion of Biofuels and Waste Fuels in a Fluidised Bed Boiler A Phosphorous and Alkali Perspective,*Thesis for the degree of doctor of Engineering, Göteborg , Chalmers University of Technology, ISBN 978-91-7385-174-9, 2008.

28. **Bartels M. et al.**, *Agglomeration in Fluidized Beds at High Temperautures: Mechanisms, Detection and Prevention*, Progress in energy and combustion science, Vol. 34, pp. 633-666, 2008.
29. **Zintl F., Ljungdahl B.**, *Sintring i FB och CFB - Utveckling av prediktiv metod samt test av additiv och sameldning,* Termiska Processer (TPS) report no. -99/23, 2000.
30. **Brus E.**, *Bed Agglomeration during Combustion and Gasification of Biomass Fuels - Mechanisms and Measures Prevention.* Umeå University, ISSN 91 - 7305-676-6, ISBN 91-7305-676-6, 2004.
31. **Visser H.J.M., van Lith S., Kiel J.H.A.**, *Biomass Ash-Bed Material Interactions Leading to Agglomeration in Fluidised Bed Combustion and Gasification,* Proceedings of the 12th European conference and technology exhibition on biomass for energy, industry and climate protection, pp. 585-588, 2002.
32. **Skrifvars B., et al.**, *Ash Behaviour in a CFB Boiler during Combustion of Coal, Peat or Wood*, Fuel, Vol. 77, 1997.
33. **Zintl, F., Ljungdahl, B.**, *Sintring i FB och CFB - Utveckling av prediktiv metod samt test av additiv och sameldning* . TPS Termiska processer AB, 2000.
34. **Skrifvars B.J., Backman R., Hupa M.**, *Characterization of the Sintering Tendency of Ten Biomass ashes in FBC Conditions by a Laboratory Test and by Phase Equilibrium Calculations.* Fuel Processing Technology, Volume 56, July 1998, pp 55-67.
35. **Steenari B.M.**, *High Temperature Reactions of Straw Ash and the Antisintering Additives Kaolin and Dolomite*, Biomass and energy, Vol. 14, pp. 67-76, 1998.
36. **Mattson J.** Göteborgsregionens Rya AB (GRYAAB), Göteborg, cited at the 16th of Mars 2009.
37. **Olsson C.**, *Slamhantering*, svenskt vatten www.svensktvatten.se, Online svenskt vatten cited the 27th of Feb. 2009.
38. **Miljödepartementet**, *www.regeringen.se*,Online Regeringen at the 1st of Mars 2008, cited the 25th of Nov. 2008.
39. **Möller, A.**, *Co-Firing of Sewage Sludge with Straw in a Fluidized Bed Boiler and Further Investigations on Zeolites and Their Impact on Agglomeration,* Diploma thesis work for the degree of master of science, Göteborg , Chalmers University of Technology, 2008.
40. **Zeuthen, F., et al.**, *Aerosol Formation During the Combustion of Straw With Addition of Sorbents*, Energy and fuels, Vol. 21, pp. 699-709, 2007.

41. **Barisic V., Åmand L. E., Coda Zabetta E.**, *The Role of Limestone in Preventing Agglomeration and Slagging During CFB Combustion of High-Phosphorous Fuels,* Proccedings poster session World BioEnergy 2008 Conference & Exhibition on Biomass for Energy, pp. 259-263, 2008.

42. **van der Knijff, A., et al.**, *Improving Operations of the DRSH Sludge Incineration Plant in the Netherlands.* Proccedings of the 9th International Conference on Circulating Fluidized Beds, (Eds:J. Werther, W. Nowak, K.-E. Wirth and E.-U. Hartge), Hamburg, 2008.

43. **NE**, Nationalencyklopedien, HTTP://NE.SE/ARTIKEL/349819, Online NE cited at the 25th of Nov. 2008. HTTP://NE.SE/ARTIKEL/349819.

44. **KE**,Kemikalieinspektionen, *Zeoliter, http://apps.kemi.se/flodessok/floden/kemamne/zeoliter.htm,*Online KE 1993, Cited at the 20th of Feb.2009.

45. **Dyer, A., Heywod, B., Szyrokyj, N.**, *Cation Exchange in the Synthetic Gismondine-Zeolite MAP,* Microporous and mesoporous materials, Vol. 92, 1-3, pp. 161-164, 2006.

46. **Townsend, R. P., Coker, E. N.**, *Ion Exchange in Zeolites*, Studies in Surface Science and Catalysis, Vol. 137, pp. 467-524, 2001.

47. **Kuronen, M. et al.**, *Ion Exchange Selectivity and Structural Changes in Highly Aluminous Zeolites,* Reactive and functional polymers, Vol. 66 pp. 1350-1361, 2006.

48. **Baerlcoher, C. och McCusker, L.B.**, *Zeolite Structures*, Studies in Surface Science and Catalysis, 2005.

49. **Lin, W., Dam-Johansen, K., Frandsen, F.**, *Agglomeration in Bio-Fuel Fired Fluidized Bed Combustors,* Chemical engineering Journal, Vol. 96, pp. 171-185, 2003.

50. **Neville M., Sarofim A.F.**, *The Fate of Sodium During Pulverized Coal Combustion*, Fuel, Vol. 64, pp. 384-390, 1985.

51. **Shao et al.**, *Agglomeration Characteristics of Sludge Combustion in a Bench-Scale Fluidized Bed Combustor*, Energy & fuels, Vol. 21, pp 710-717, 2007.

52. **Fryda L.E., Panopoulos K.D., Kakaras E.**, *Agglomeration in Fluidized Bed Gasification of Biomass*, Powder technology, Vol. 181, pp. 307-320, 2008.

53. **Zevenhoven-Onderwater M. et al.**, *The Ash Chemistry in Fluidized Bed Gasification of Biomass Fuels. Part II: Ash Behaviour Prediction Versus Bench Scale Agglomeration Tests,* Fuel, Vol. 80, pp. 1503-1512, 2001.

54. **Yan, R. et al.**, *Formation of Bed Agglomeration in a Fluidized Multi-Waste Incinerator,* Fuel, Vol. 82, pp. 699-709, 2003.

55. **Brus E., Öhman M., Nordin A.**, *Mechanisms of Bed Agglomeration during Fluidized Bed Combustion of Biomass Fuels*, Energy & fuels, Vol. 19, pp. 825-832, 2005.
56. **Eriksson G.**, *Combustion Characterisation of Rape Seed Meal and Suggestions for Optimal Use in Combustion Appliances*,Stockholm, Värmeforsk report no. 1038, ISSN 1653-1248, www.varmeforsk.se, 2007.
57. **Lindström E. et al.**, *Slagging Characteristics during Combustion of Cereal Grains Rich in Phosphorous*, Energy & fuels Vol. 21, pp. 710-717, 2006.
58. **GRYAAB**, Göteborgsregionens Rya AB, *Rundtur vattenbehandling på Rya avloppsreningverk*, www.gryaab.se, Online GRYAAB cited at the 10th of May 2009. www.gryaab.se.

Appendix

A. Fuel analyses

Table 6. Fuel analysis base fuels.

	Bark pellets	Wood pellets	Straw pellets	RDF pellet	Fe-sludge	Al-sludge
Proximate analysis						
Water (wt%, raw)	9.1	6.5	8.3	5.3	72.4	77.5
Ashes (wt% ds)	3.4	0.3	4.1	15.4	48.8	42.6
Combustibles (wt%, ds)	96.6	99.7	95.9	84.6	51.2	57.4
Ultimate analysis (wt%, ds af)						
C	54.3	50.8	49.1	55.4	51.2	49.8
H	6.1	6.0	6.3	7.7	7.6	7.7
O	39.1	43.1	43.4	35.2	33.2	35.5
S	0.0	0.0	0.1	0.2	1.9	1.4
N	0.4	0.1	0.4	0.9	6.3	5.6
Cl	0.0	<0.01	0.4	0.6	0.1	0.1
Ash analysis (g/kg dry ashes)						
K	58.8	100	146.3	11.7	14.8	11.3
Na	8.8	3.3	9.8	22.7	7.2	6.1
Al	23.5	66.7	2.4	58.4	98.2	194.1
Si	108.8	33.3	222.0	159.1	144.5	126.1
Fe	11.8	13.3	2.4	20.1	147.5	47.7
Ca	250.0	233.3	78.0	181.2	43.2	40.8
Mg	23.5	33.3	17.1	11.7	10.7	7.7
P	14.7	16.7	9.8	5.2	62.7	56.3
Ti	8.8	0.3	2.4	11.0	5.5	9.9
Ba	n.a.	n.a.	2.4	1.9	0.8	0.7
Effective heat content, H (MJ/kg)						
H, dry	17.77	19.13	17.57	19.82	10.1	11.15

ds = dry solid, ds af = dry solid ash free, raw = as received, n.a. = not analyzed

Table 7. Calculated fuel analysis for the fuel mixes.

	Wood/ straw 0%MSS	Wood/ straw 2%Fe	Wood/ straw 6%Fe	Wood/ straw 2%Al	Wood/ straw 6%Al	RDF 2%Fe	RDF 6%Fe
Proximate analysis							
Water (wt%, raw)	7.1	7.1	6.9	7.0	6.8	5.3	9.33
Ashes (wt% ds)	1.7	2.6	4.5	2.5	4.1	16.1	17.40
Combustibles (wt%, ds)	98.3	97.4	95.5	97.5	95.9	83.9	82.60
Ultimate analysis (wt%, ds)							
C	50.2	50.2	50.3	50.2	50.2	55.4	55.3
H	6.1	6.2	6.2	6.2	6.2	7.6	7.7
O	43.2	43.1	42.9	43.2	43.0	35.2	35.1
S	0.0	0.0	0.1	0.0	0.1	0.2	0.3
N	0.2	0.3	0.4	0.3	0.4	1.0	1.1
Cl	0.1	0.1	0.1	0.1	0.1	0.6	0.6
Ash analysis (g/kg dry ashes)							
K	116.7	114.6	110.6	114.6	110.4	11.7	11.87
Na	5.6	5.7	5.7	5.7	5.7	22.4	21.79
Al	43.5	44.6	46.8	46.6	52.6	59.2	60.82
Si	101.2	102.1	103.8	101.7	102.7	158.8	158.21
Fe	9.4	12.2	17.7	10.2	11.7	22.7	27.77
Ca	177.4	174.7	169.4	174.7	169.2	178.4	172.89
Mg	27.5	27.1	26.5	27.1	26.3	11.7	11.63
P	14.2	15.1	17.1	15.0	16.7	6.3	8.65
Ti	1.1	1.2	1.4	1.3	1.6	10.9	10.71
Ba	n.a.	n.a.	n.a.	n.a.	n.a.	1.9	1.88
Effective heat content, H (MJ/kg)							
H, dry	18.6	18.4	18.1	18.4	18.1	19.6	19.24

ds = dry solid, ds af = dry solid ash free, raw = as received, n.a. = not analyzed

B. Pelletized fuel

Figure 53. ***Wood/straw0%MSS.***

Figure 54. ***Wood/Straw2%Fe.***

Figure 55. ***Wood/Straw6%Fe.***

Figure 56. ***Wood/Straw2%Al.***

Figure 57. ***Wood/Straw6%Al.***

Figure 58. ***RDF0%MSS.***

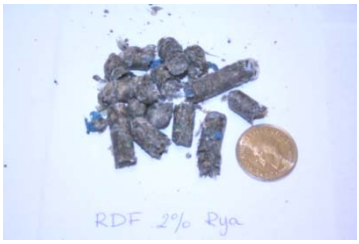

Figure 59. ***RDF2%Fe.***

Figure 60. ***RDF6%Fe.***

Figure 61. ***Bark.***

C. Calculation of air factor, m

The theoretical dry CO_2-fraction is calculated from the elementary analysis of the different fuels:

$$(CO_2)_{ot} = \frac{0.21}{1 + 2.37 \times \frac{H - 0.126O}{C + 0{,}335S}}$$

The average actual dry CO_2-fraction is measured in the combustion experiments:

$(CO_2)_t$

The air factor, m, is calculated from the theoretical dry CO_2-fraction and the average actual dry CO_2-fraction:

$$m = \frac{(CO_2)_{ot}}{(CO_2)_t}$$

D. Combustion temperature, pressure drop and concentrations of CO and CO2

This appendix presents combustion data from the experiments.

Bark

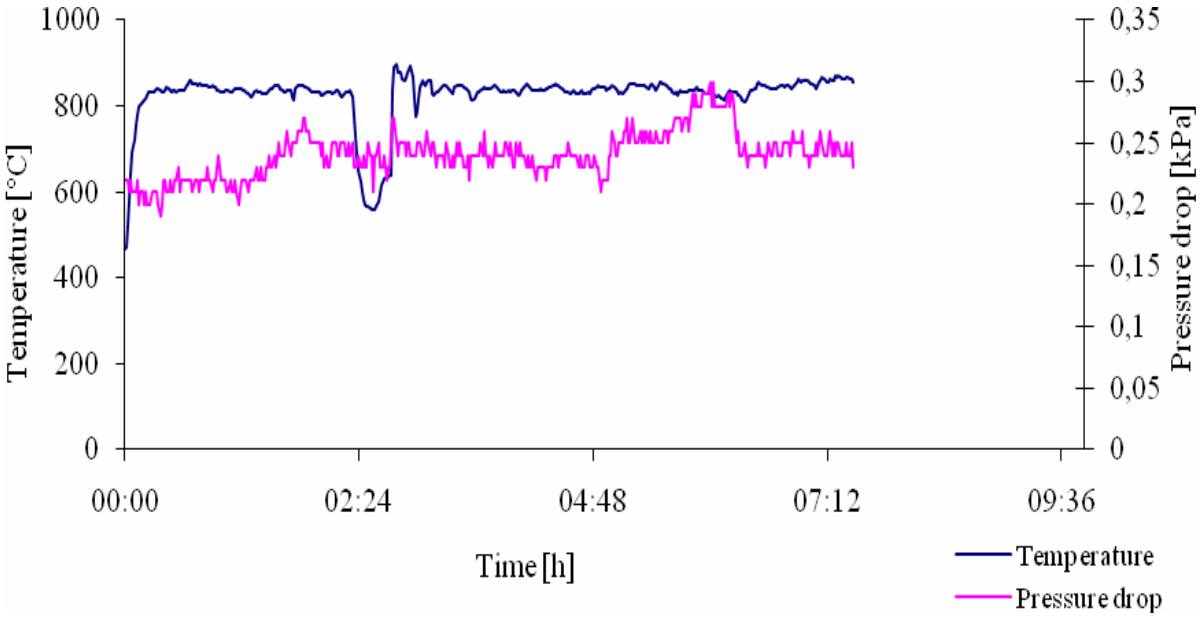

Figure 392. Temperature and pressure drop in the bed during combustion of bark pellets.

The decrease in temperature (Figure 392) and CO/CO_2 concentrations at 02:24h (Figure 403) was due to a blockage in the fuel feeding pipe.

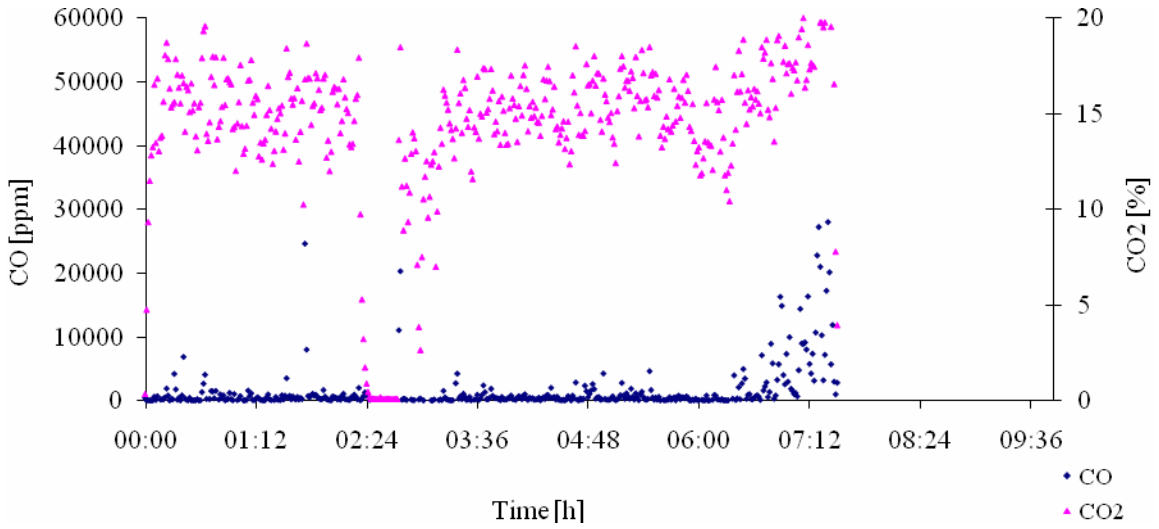

Figure 403. CO and CO_2 concentrations in the flue gas during combustion of bark pellets.

The concentration of CO_2 was approximately 15%. The CO concentration was very low.

Wood/straw0%MSSno.1

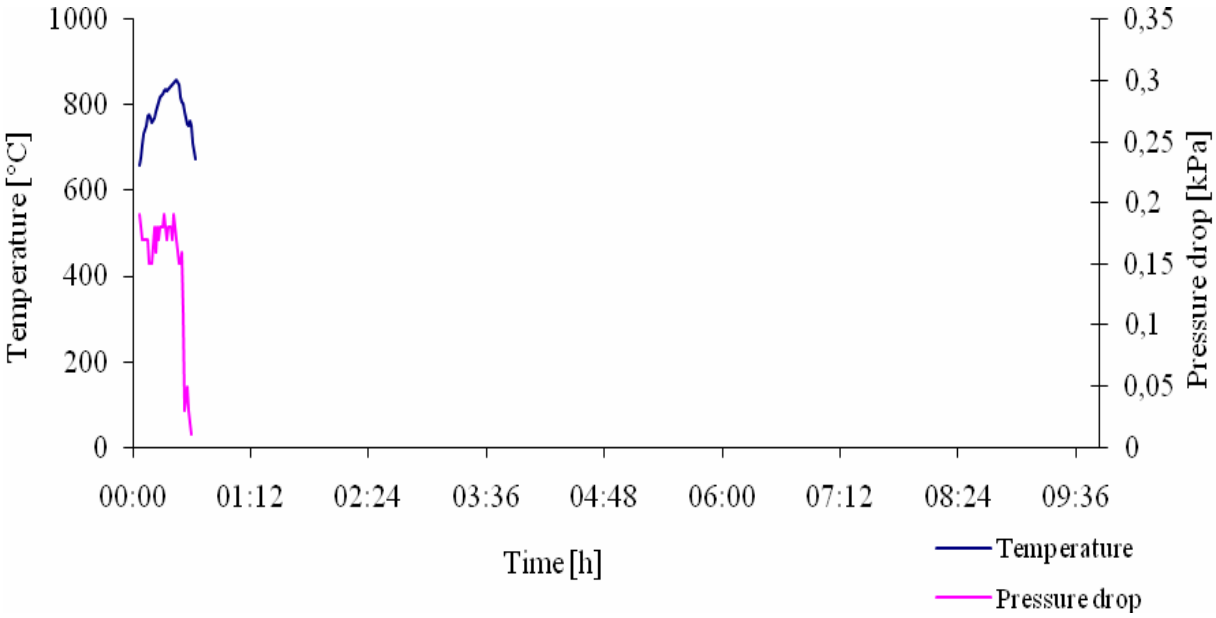

Figure 414. Temperature and pressure drop in the bed during combustion of *wood/straw0%MSSno.1*.

The bed sintered at 00:45 which can be seen as the decrease in pressure drop in Figure 414. CO/CO_2 -results are not available for the combustion of *wood/straw0%MSSno.1* due to a dysfunctional gas analysis instrument.

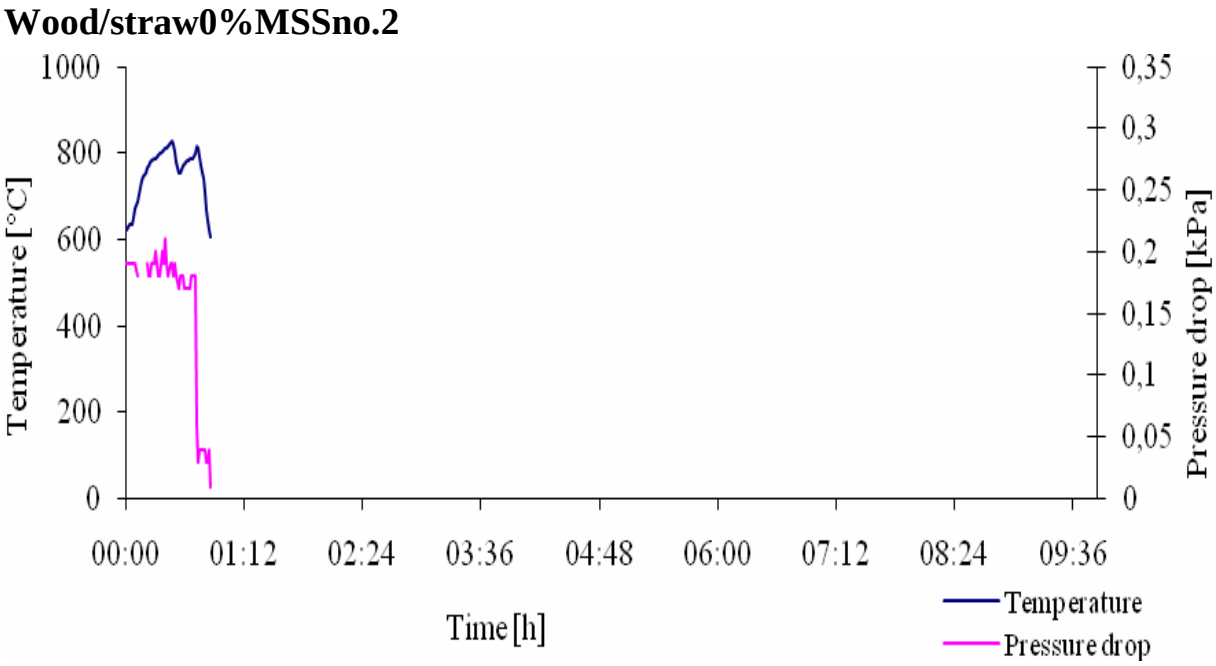

Figure 42. Temperature and pressure drop in the bed during combustion of *wood/straw0%MSSno.2.*

The *wood/straw0%MSSno.2* experiment gave a result similar to *wood/straw0%MSSno.1*. The bed sintered at 00:38 h (Figure 42). The manometer was disconnected between 00:08 - 00:12, which explains missing pressure drop data.

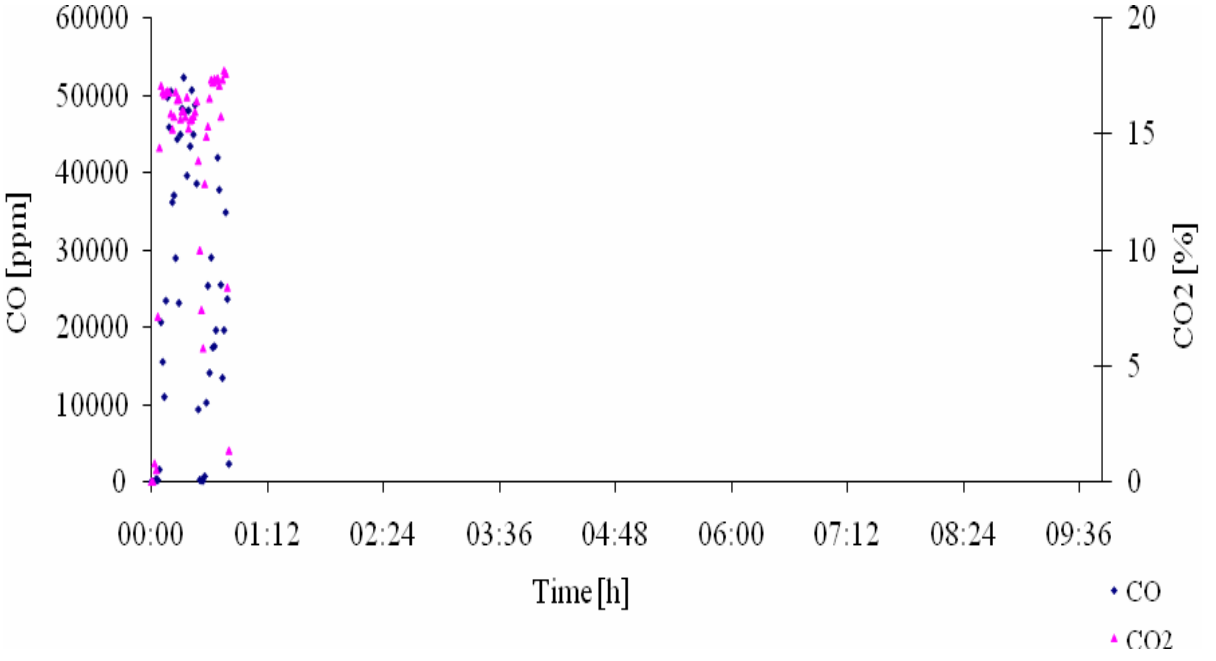

Figure 43. CO and CO_2 concentrations in the flue gases during combustion of *wood/straw0%MSSno.2.*

The concentration of CO_2 was approximately 15% (Figure 43). The concentration of CO was varying and rather high which indicates an uneven and incomplete combustion.

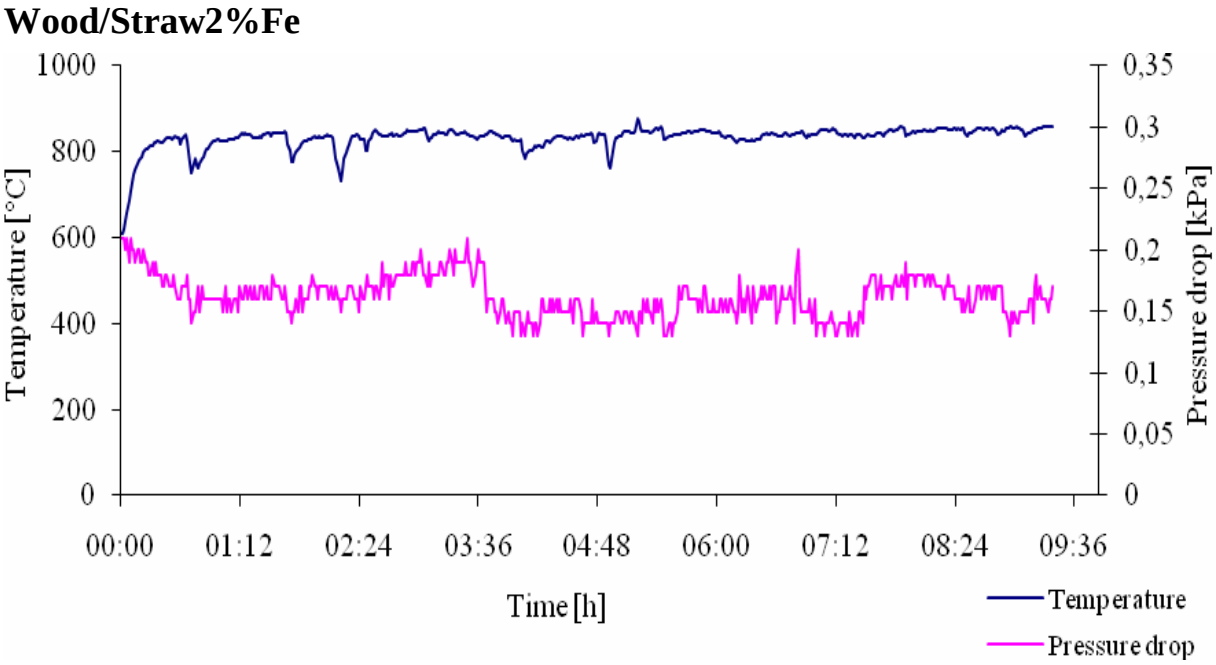

Figure 44. Temperature and pressure drop in the bed during combustion of *wood/straw2%Fe.*

The temperature was rather constant except some smaller dips due to blockage of the fuel feeding pipe (Figure 44).

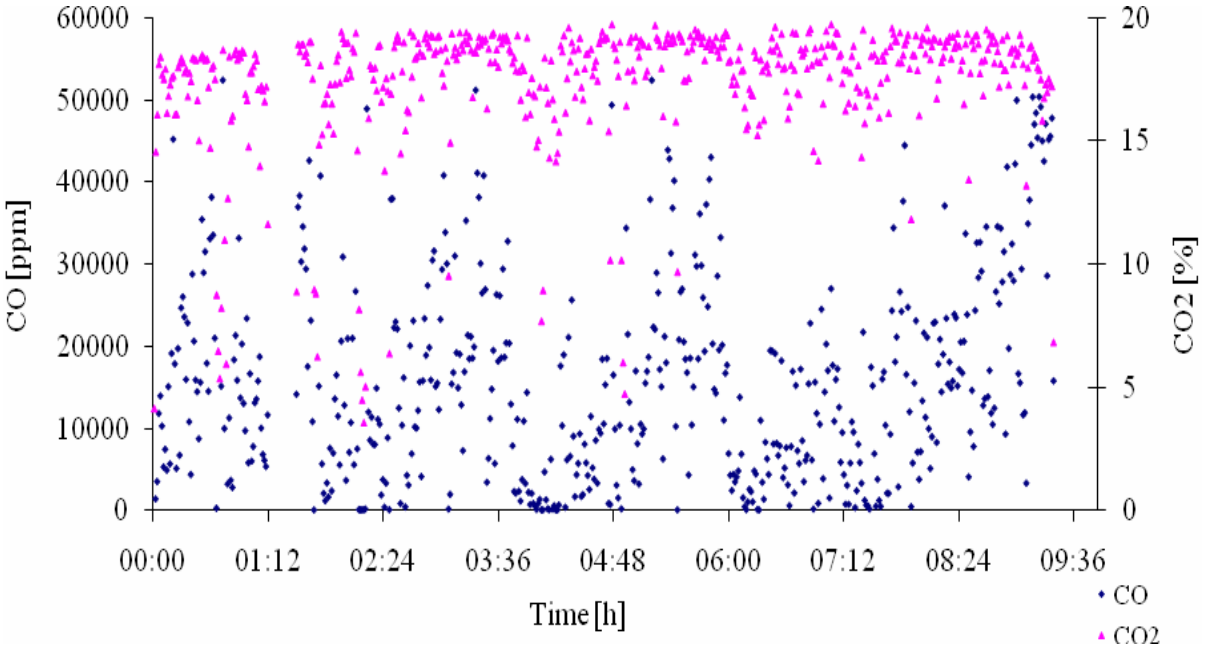

Figure 45. CO and CO_2 concentrations in the flue gases during combustion of *wood/straw2%Fe.*

The concentration of CO was very high and uneven which indicates incomplete and uneven combustion (Figure 45). The concentration of CO_2 varied between 15 - 20%.

Wood/straw6%Fe

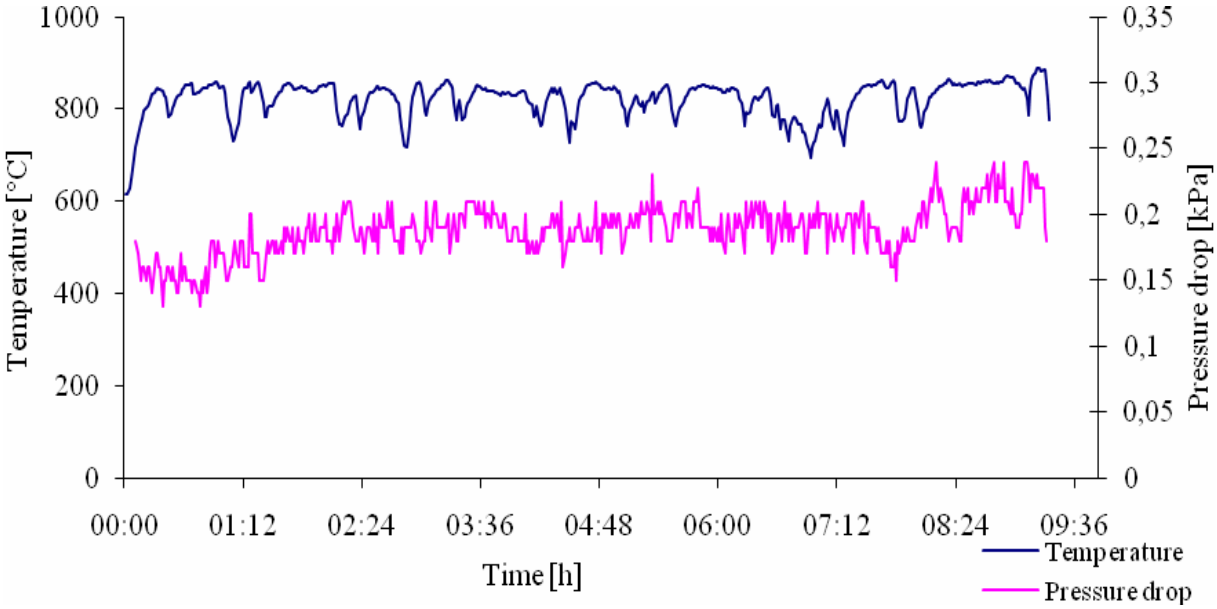

Figure 46. Temperature and pressure drop in the bed during combustion of *wood/straw6%Fe.*

The temperature profile was uneven because the fuel feeding pipe was blocked on several occasions (Figure 46). This can also be seen in the CO/CO_2-graph where the concentration of the gases varies a lot (Figure). The CO_2-concentration was between 15-20 %.

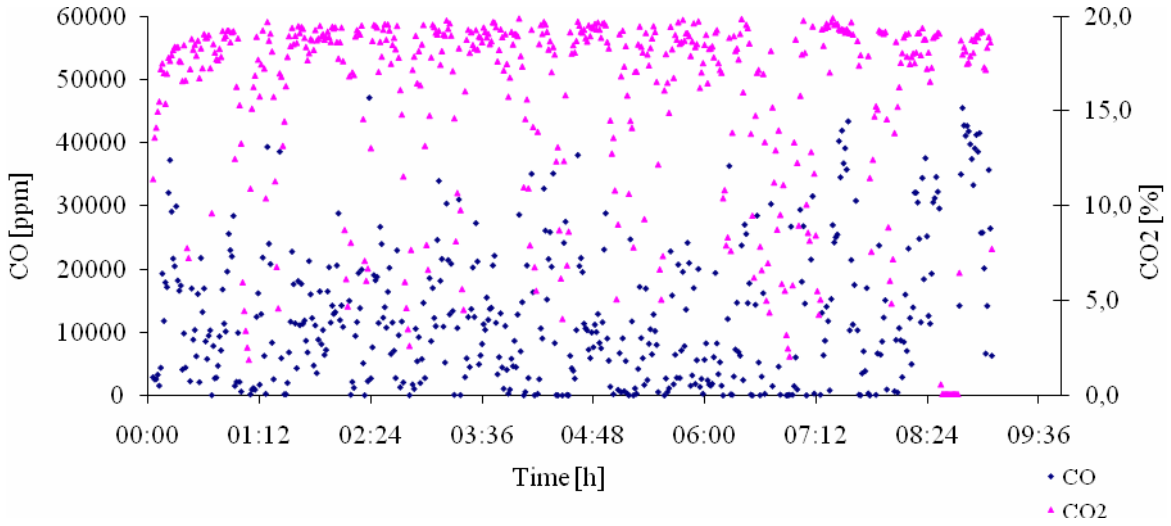

Figure 70. Temperature and pressure drop in the bed during combustion of *wood/straw6%Fe.*

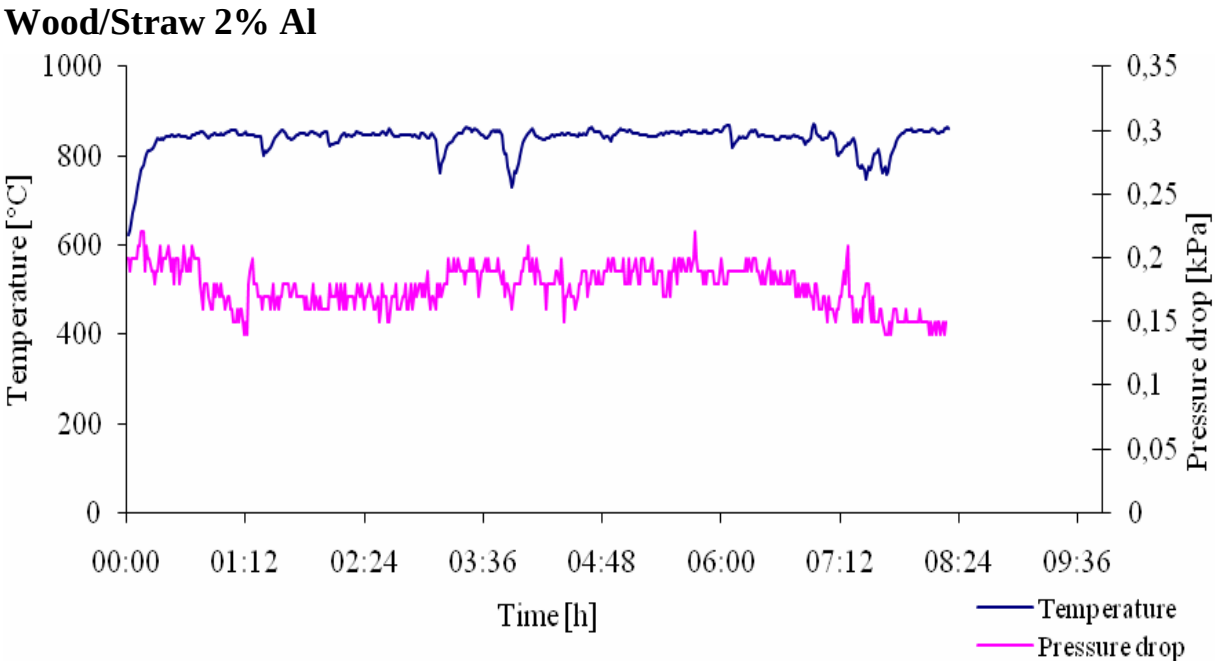

Figure 71. CO and CO_2 concentrations in the flue gases during combustion of *wood/straw2%Al.*

The temperature dips were due to blockage of the fuel feeding pipe (Figure). Reliable flue gas data is missing from combustion of *wood/straw2%Al* due to instrumental problems.

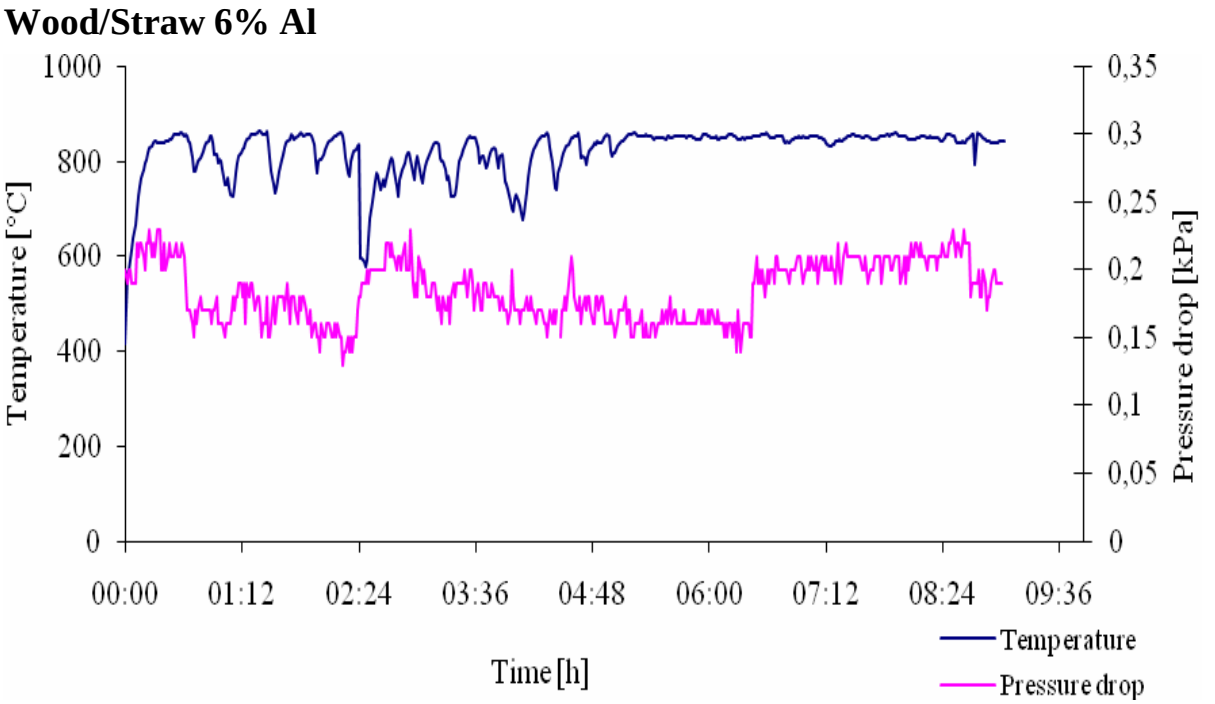

Figure 47. Temperature and pressure drop in the bed during combustion of *wood/straw6%Al.*

The uneven temperature profile was due to repeated blockages of the fuel feeding pipe (Figure 47). At 4:55 it was decided to feed the pellets by hand, which resulted in a more even combustion. Reliable flue gas data is missing from combustion of *wood/straw6%Al* due to instrumental problems.

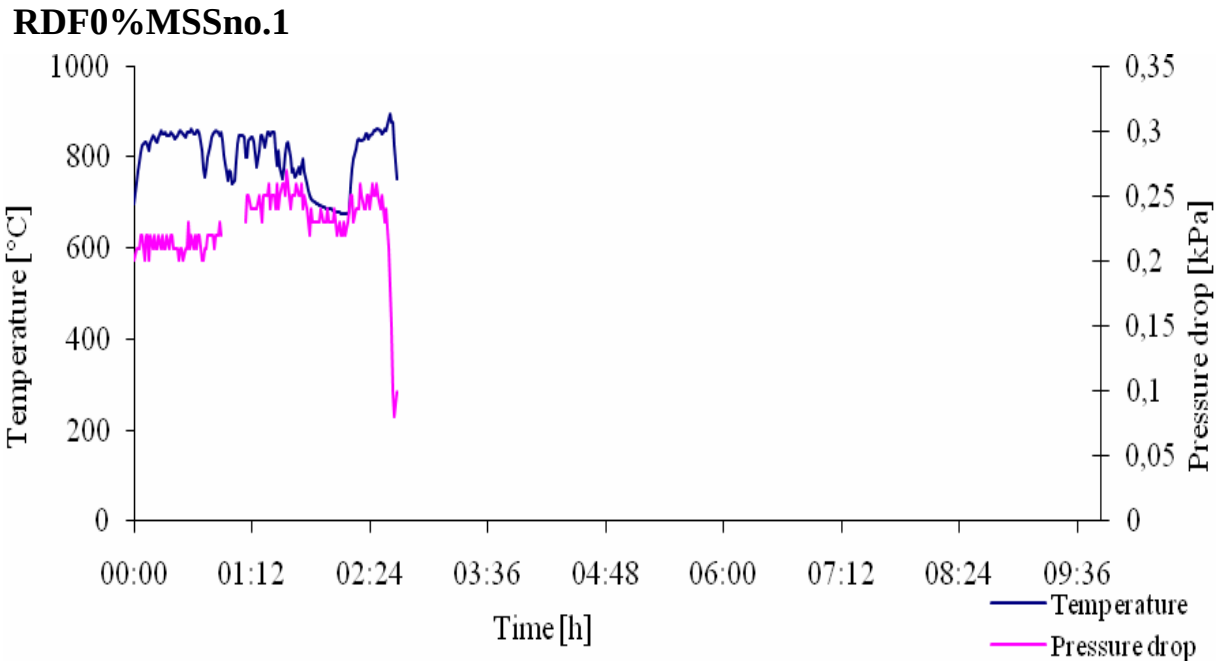

Figure 48. Temperature and pressure drop in the bed during combustion of *RDF0%MSSno.1*.

RDF0%MSSno.1 sintered at a bed temperature of 895°C (Figure 48). Missing pressure drop data is due to that the manometer was disconnected between 00:54 - 01:07.

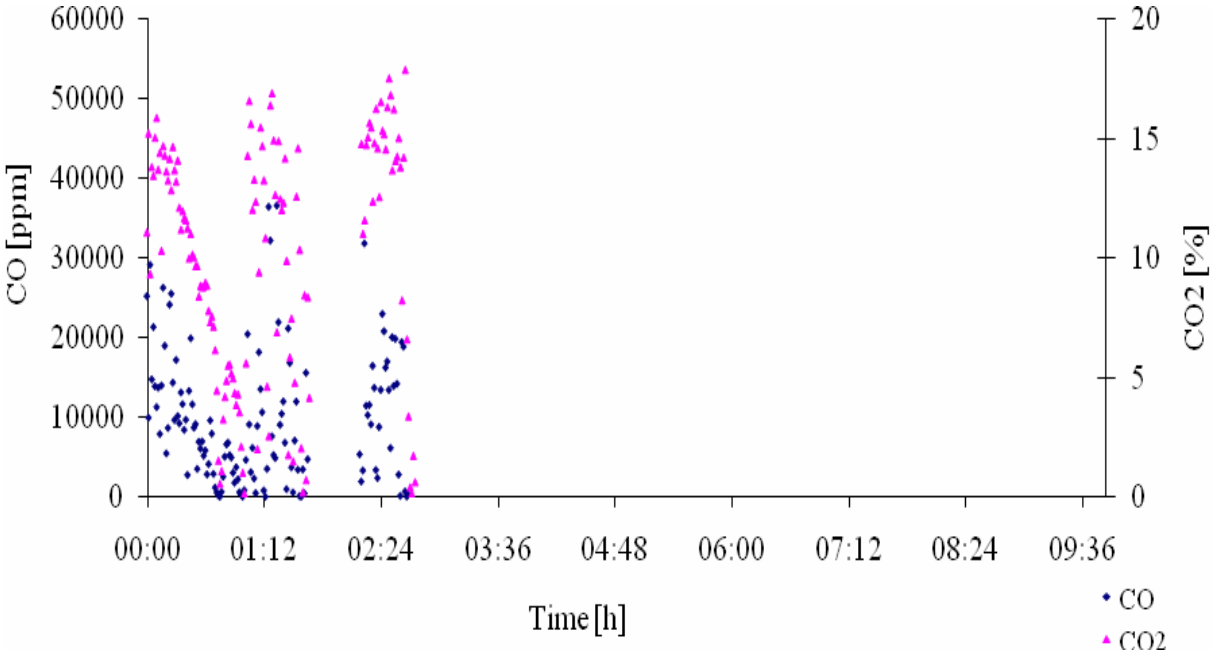

Figure 49. CO and CO_2 concentrations in the flue gases during combustion of *RDF0%MSSno.1*.

The CO/CO_2-filter was cleaned at 01:40. During cleaning the background concentration of CO/CO2 was logged, these data are not presented in the graph (Figure 49).

RDF0%MSSno.2

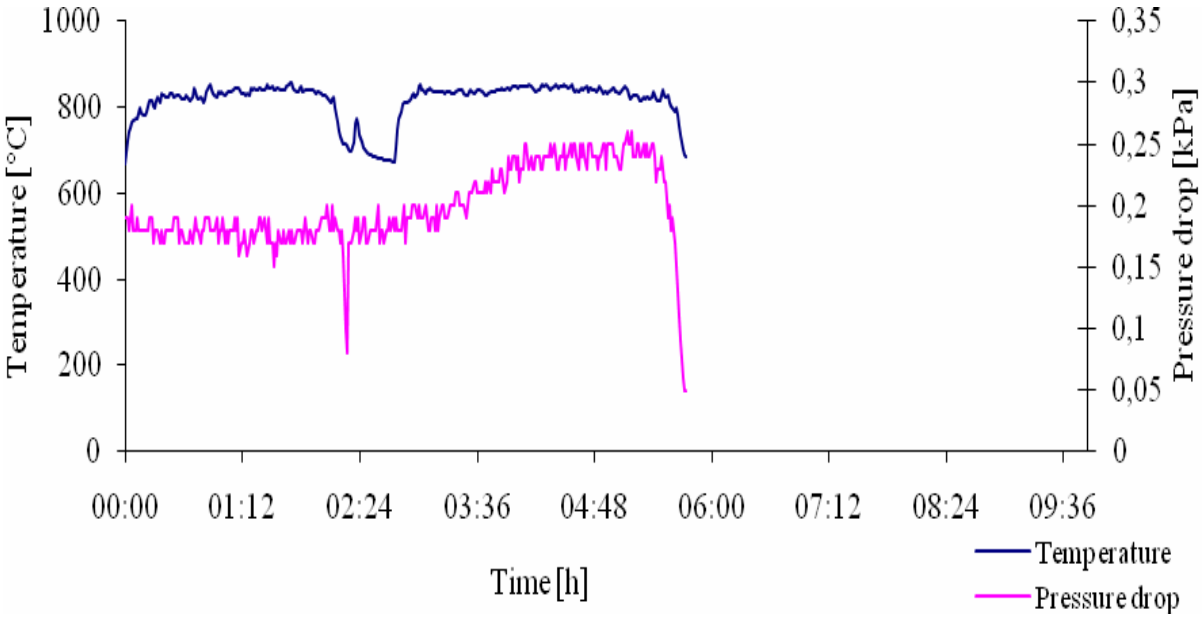

Figure 50. Temperature and pressure drop in the bed during combustion of *RDF0%MSSno.2*.

RDF0%MSSno.2 sintered at 05:45 (Figure 50). The temperature drops were due to blockages of the fuel feeding pipe.

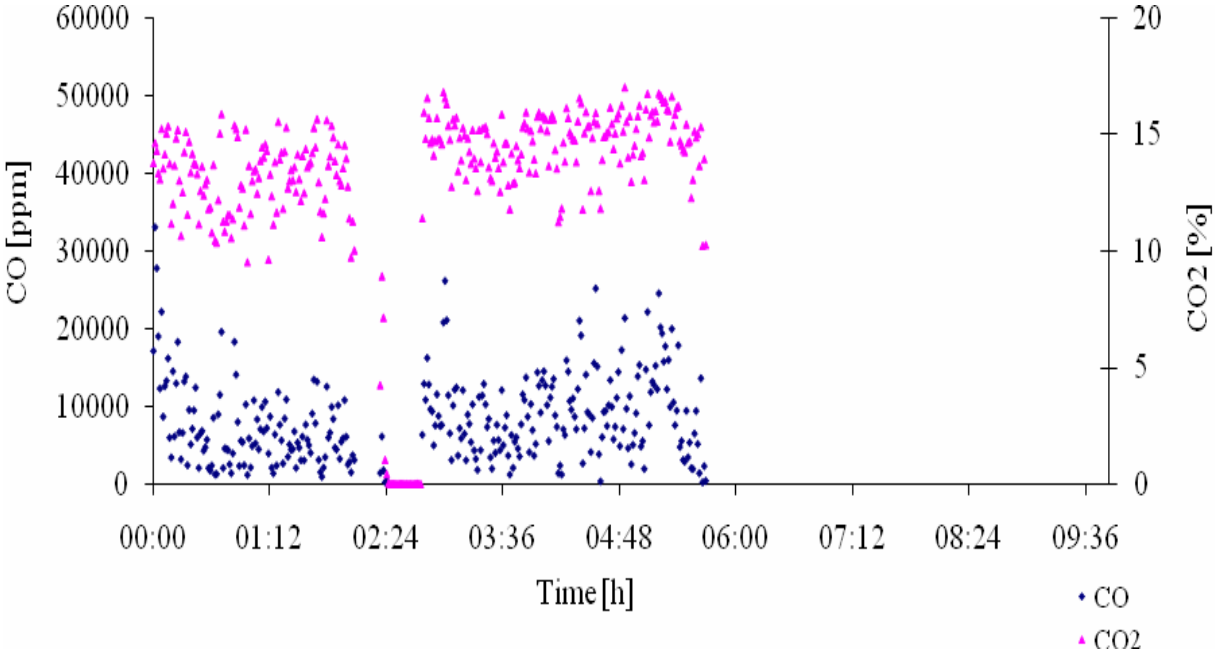

Figure 51. CO and CO_2 concentrations in the flue gases during combustion of *RDF0%MSSno.2*.

The CO/CO_2 filter was cleaned at 02:24 which results in missing CO/CO_2-data (Figure 516).

RDF2%Fe

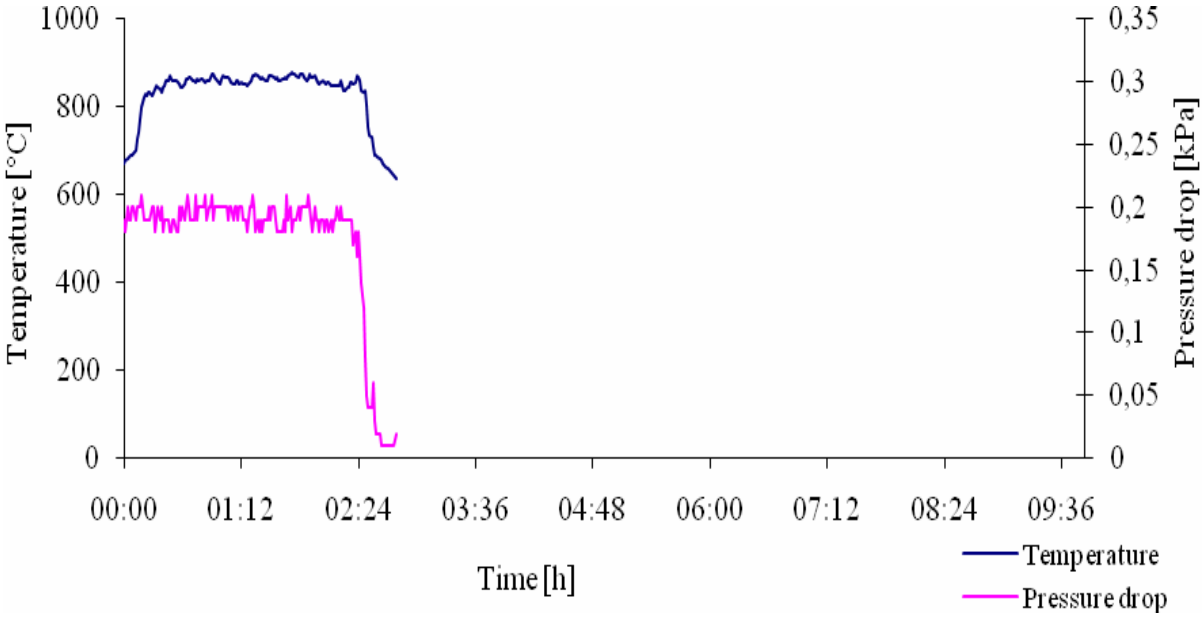

Figure 77. Temperature and pressure drop in the bed during combustion of *RDF2%Fe.*

The bed material of *RDF2%Fe* sintered at 02:30 (Figure).

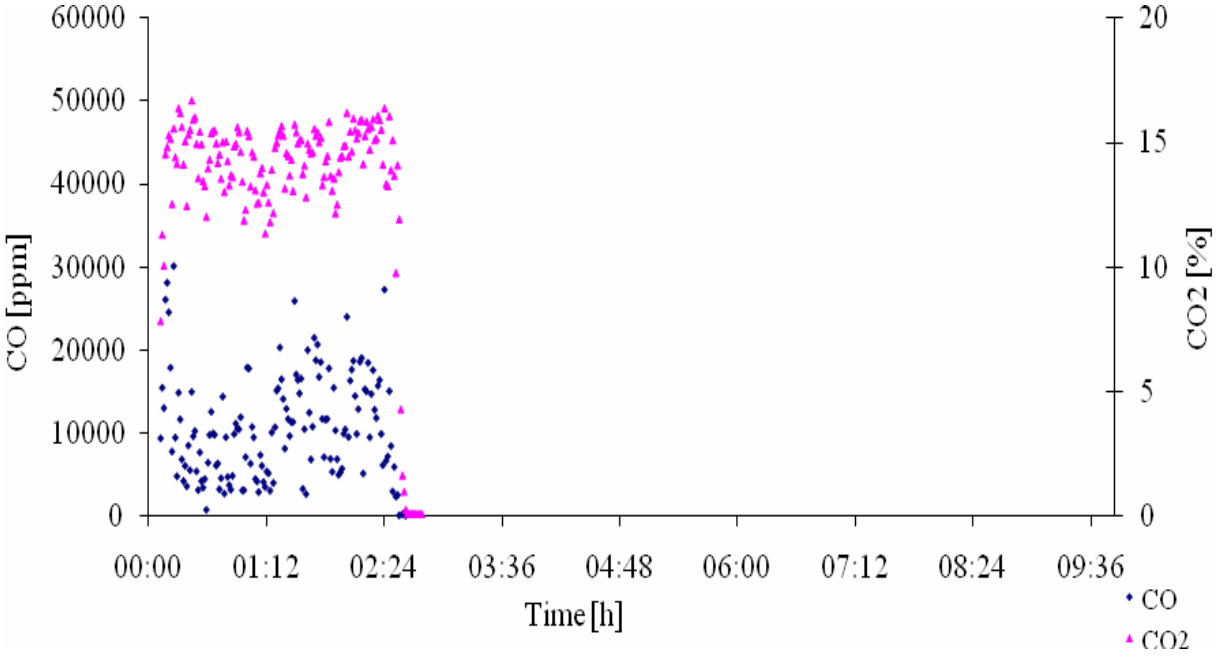

Figure 52. CO and CO_2 concentrations in the flue gases during combustion of *RDF2%Fe*

The concentration of CO_2 was around 15% (Figure 52). The concentration of CO varied between 10 000-20000 ppm.

RDF6%Fe

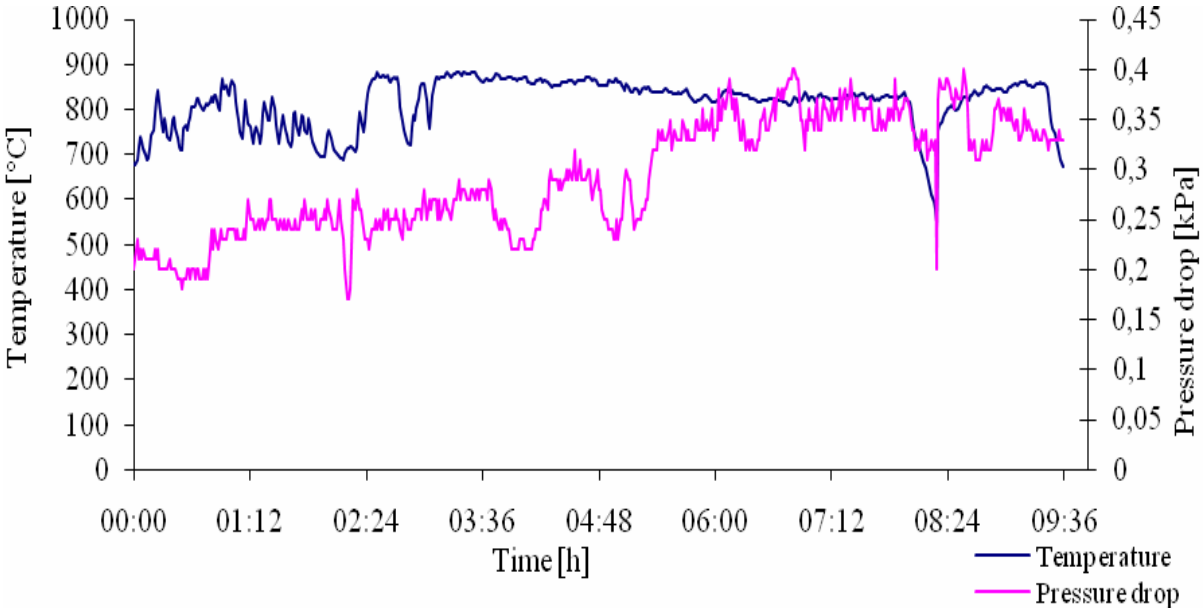

Figure 53. Temperature and pressure drop in the bed during combustion of *RDF6%Fe.*

The uneven temperature profile was due to repeated blockages of the fuel feeding pipe (Figure 53).

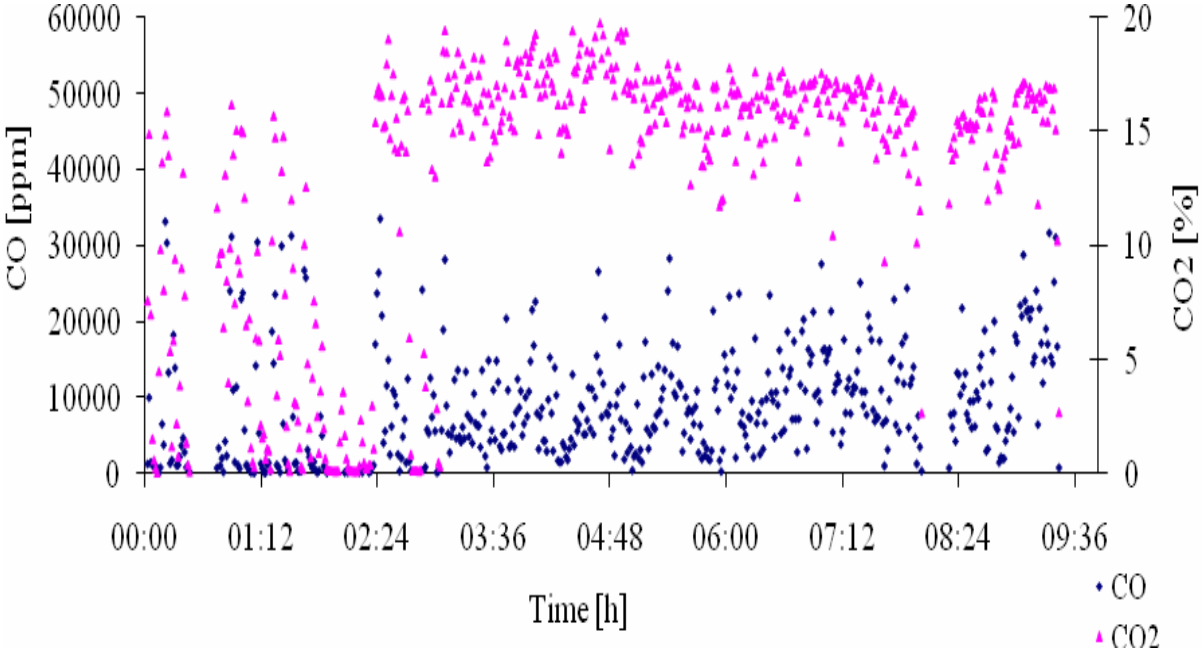

Figure 80. CO and CO_2 concentrations in the flue gases during combustion of *RDF6%Fe.*

The concentration of CO was high during the experiment (Figure). The concentration of CO_2 varied between 10 - 20 %.

E. Samples of bed sand after combustion

Figure 54. Bed sand sample after combustion of *wood/straw2%Fe.*

Figure 55. Bed sand sample after combustion of *wood/straw6%Fe.*

Figure 56. Bed sand sample after combustion of *wood/straw2%Al.*

Figure 57. Bed sand sample after combustion of *wood/straw6%Al.*

Figure 58. Bed sand sample after combustion of *RDF0%MSSno.1.*

Figure 59. Bed sand sample after combustion of *RDF2%Fe.*

F. Result from Chemical analysis of bed sand composition

Table 8. Chemical composition of the bed material for the different experiments. When two experiments for the same fuel mix have been performed *(wood/straw0%MSS* and *RDF0%MSS)* only bed sand from one experiment has been analyzed.

	S	Cl	Al	Si	Fe	Ti	Mn	Mg	Ca	Ba	Na	K	P
	wt%	wt%	wt%	wt%	wt%	wt%	wt%	wt%	wt%	wt%	wt%	wt%	wt%
Ref 12_12BB	0.1	<0.01	0.85	43.2	0.58	0.08	0.25	1.27	3.28	0.04	0.34	2.56	0.2
Bark	0.06	<0.01	0.7	47.1	0.87	0.08	0.19	0.3	2.88	0.06	0.21	1.51	0.21
Wood/straw0%MSS no.2	0.03	<0.01	0.34	44.1	0.81	0.14	0.04	0.1	0.55	0.01	0.08	0.82	0.05
Wood/straw2%Fe	0.05	0.03	0.7	34.7	2.8	0.13	0.08	0.28	6.32	0.02	0.14	1.63	0.41
Wood/straw6%Fe	0.04	<0.01	1.19	39.5	3.24	0.17	0.07	0.25	1.19	0.02	0.13	1.39	0.72
Wood/straw2%Al	0.03	0.02	0.58	27.1	1.2	0.1	0.05	0.26	15.8	0.01	0.03	0.87	0.2
Wood/straw6%Al	0.04	0.02	2.12	42.4	1.27	0.21	0.06	0.21	1.23	0.02	0.13	1.43	0.68
RDF0%MSSno.2	0.14	0.13	5.99	33.8	3.34	0.53	0.09	0.47	6.09	0.08	0.93	0.44	0.29
RDF2%Fe	0.09	0.08	2.4	36.7	2.08	0.44	0.04	0.38	4.8	0.08	0.88	0.47	0.41
RDF6%Fe	0.09	0.04	6.95	29.3	4.07	0.43	0.07	0.53	5.35	0.09	1.61	0.75	1.11

The results from the chemical analysis have large error range.

G. Result agglomeration test

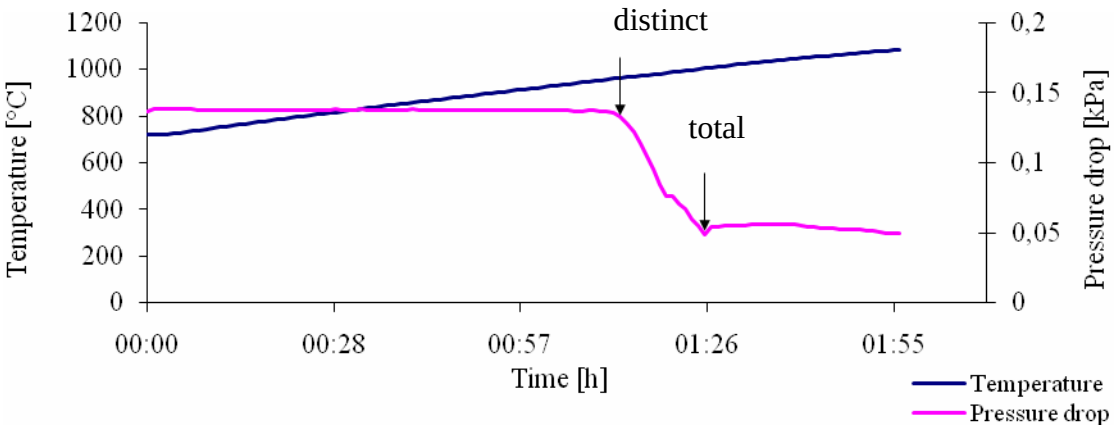

Figure 60. Agglomeration temperature for the *wood/straw2%Fe* sample; distinct agglomeration temperature 964°C, total agglomeration temperature 1008°C.

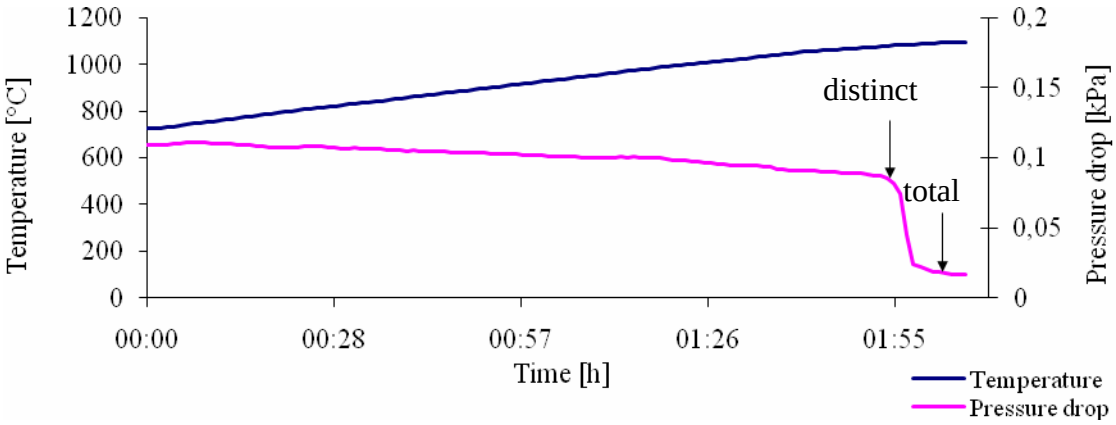

Figure 61. Agglomeration temperature for the *wood/straw6%Fe* sample; distinct agglomeration temperature 1081°C, total agglomeration temperature 1094°C.

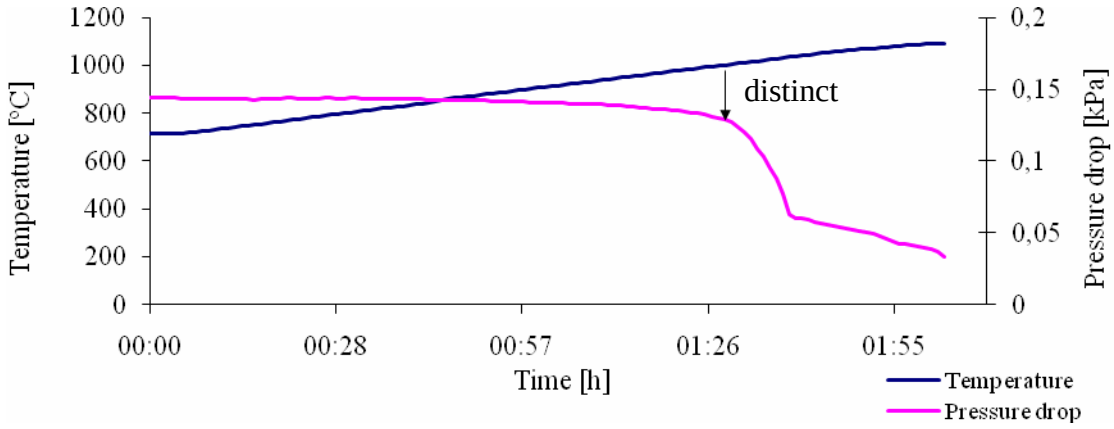

Figure 62. Agglomeration temperature for the *wood/straw2%Al* sample; distinct agglomeration temperature 1007°C.

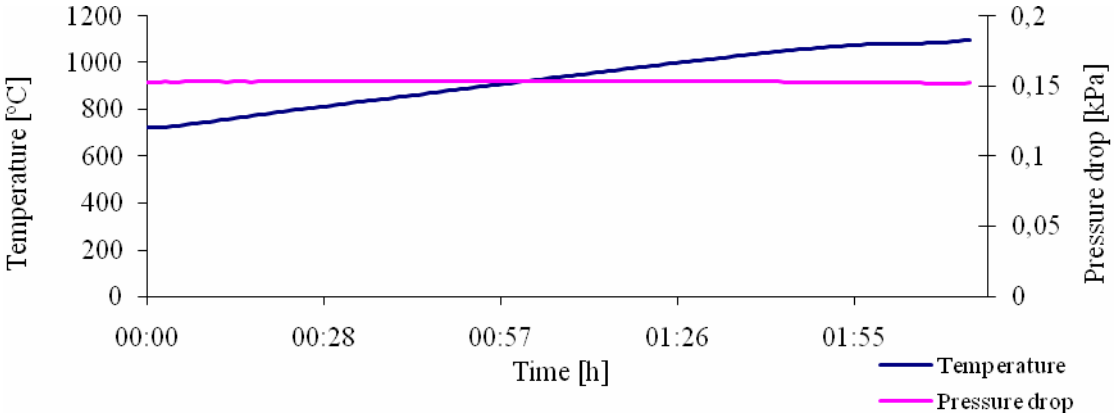

Figure 90. No agglomeration was obtained for the *wood/straw6%Al* sample.

The largest pressure drop obtained for *wood/straw6%Al* was 0.79 Pa/min. This pressure drop occurs at 848°C (0.78 Pa/min) and 1054°C (0.79 Pa/min). This pressure drop is considered not to be an indication of agglomeration or even initial agglomeration, since it is so small that it could be an uncertainty of measurements.

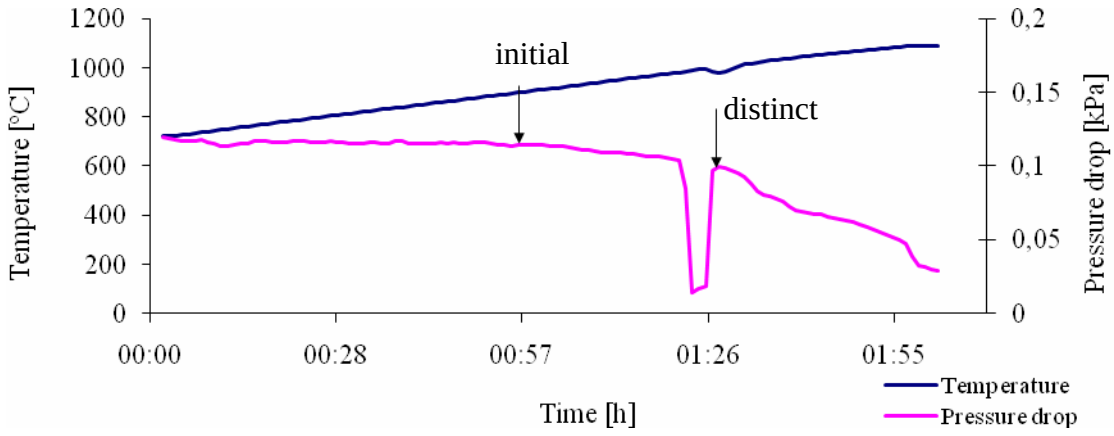

Figure 63. Agglomeration temperature for the *RDF6%Feno.1* sample; Initial agglomeration temperature 905°C, distinct agglomeration temperature 989°C.

H. Agglomerated Bed sand samples

Bark

The pressure drop indicated agglomeration at 926°C. No large agglomerates were found when the reactor was emptied, but the sand was formed in many small agglomerates, see Figure 64. The agglomeration was not obvious, but since no fluidization could be obtained even at high gas flows the sample was considered to be agglomerated. Small agglomerates can be porous enough to let air slip through without a substantial pressure drop. The bed sand has a light brown colour after the agglomeration test.

Wood/straw2%Fe

The pressure drop indicated a clearly agglomeration at 962°C. A large fragile agglomerate was found in the bed sample. The bed sand has a white colour, see Figure 65.

Wood/straw6%Fe

The pressure drop was slowly decreasing from the start before indicating a clear agglomeration at 1082°C. The agglomerate was quite fragile. The sample contains a lot of dark brown small sand agglomerates, but also several small red flakes that are not bound to the agglomerates, see Figure 66. Iron probably gives the red colour of the flakes.

Wood/straw2%Al

The pressure drop indicated a clear pressure drop at 1007°C. A large fragile agglomerate was found in the bed sample. The bed sand has a beige/white colour, see Figure 67.

Wood/straw6%Al

The pressure drop was only marginally decreased during the agglomeration test. The sample was considered to not be agglomerated. This indication was proven correct when studying the sample. The sample contains only a few sand particles that form agglomerates. The sample has a white colour, see Figure 68.

RDF6%Fe

The pressure drop indicated that *RDF6%Feno.1* was agglomerated at 1016°C and *RDF6%Feno.2* was agglomerated at 1010°C. The agglomerate that was taken out of the reactor was less fragile compared to earlier observations of wood/straw samples. The sample still contains a lot of small metallic parts. The colour is brown/black, see Figure 69.

Figure 64. Agglomerated Bed sand, *bark*.

Figure 65. Agglomerated bed sand, *wood/straw2%Fe*.

Figure 66. Agglomerated bed sand, *wood/straw6%Fe*.

Figure 67. Agglomerated bed sand, *wood/straw2%Al*.

Figure 68. Agglomerated bed sand, *wood/straw6%Al*.

Figure 69. Agglomerated bed sand, *RDF6%Rya*

I. SEM/EDX – element quantification

Bark

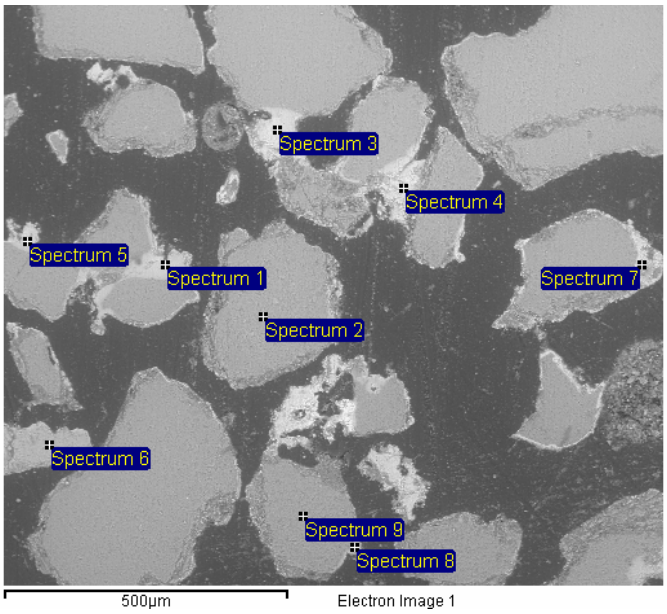

Figure 70. Figure with the points where the element quantification has been performed on the *bark* sample.

Table 9. Element quantification in the *bark* sample. "Coat" indicates that the quantification has been performed on a coating.

Spectrum/ wt%	O	Na	Mg	Al	Si	P	S	Cl	K	Ca	Mn	Fe
Spec 1 coat	50.3	1.5	0.5	0.5	28.3	0.4	0	0.1	7.4	10.4	0.3	0.4
Spec 2	57.4	0	0	0	41.9	0	0	0.1	0.3	0.4	0	0
Spec 3 coat	49	1.5	0.6	0.3	28.3	0.3	0	0.2	7.9	11.3	0.4	0.3
Spec 4	50.4	0.8	0.6	0.7	26.8	0.4	0	0.2	6.2	13.4	0.2	0.3
Spec 5 coat	50.1	1.6	0.8	0.3	30.2	0.6	0	0.2	10	5.7	0.3	0.3
Spec 6	50.9	0	0	7	30.8	0	0	0	10.7	0.6	0	0
Spec 7 coat	49.6	0.7	1.1	2	23.1	1.3	0	0.2	6	14.3	1	0.7
Spec 8 coat	53.8	0.8	0.8	0.3	29.8	0.7	0	0.2	7	6.5	0	0.2
Spec 9	56.5	0	0	0	42.6	0	0	0.2	0.3	0.5	0	0

Wood/straw0%MSSno.1

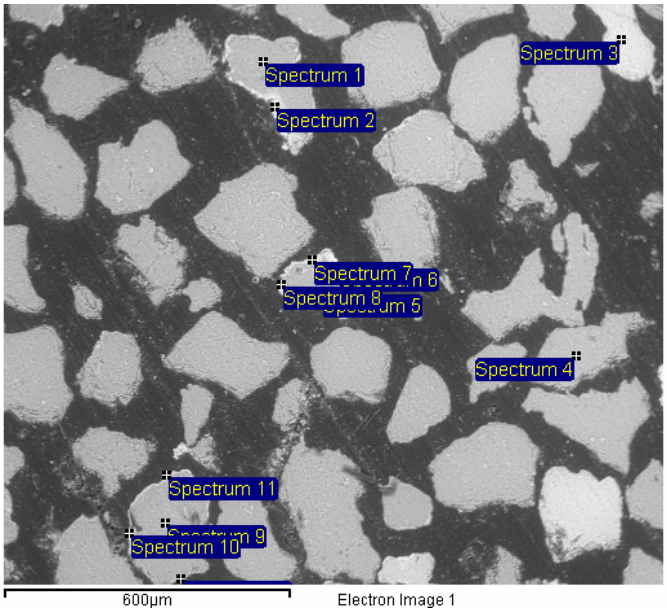

Figure 71. Figure with the points where the element quantification has been performed on *wood/straw0%MSSno.1*.

Table 10. Element quantification in the *wood/straw0%MSSno.1* sample. "Coat" indicates that the quantification has been performed on a coating.

Spectrum/ wt %	O	Na	Mg	Al	Si	P	S	Cl	K	Ca	Ti	Mn	Fe
Spec 1	56.1	0	0	0	43.4	0	0	0.2	0	0.3	0	0	0
Spec 2 coat	51.6	0.2	1.7	0	35.5	1.1	0	0.2	2.6	5.8	0	0.7	0.6
Spec 3	51.8	0.5	0	7.6	30	0	0	0.1	10	0	0	0	0
Spec 4	54	0	0	0	46	0	0	0	0	0	0	0	0
Spec 5	55.7	0	0	0	43.6	0	0	0.2	0.2	0.3	0	0	0
Spec 6 coat	52.8	0	1.9	0	26.5	0.8	0	0.3	2.1	14.9	0	0.3	0.4
Spec 7 coat	52.6	0.9	0.7	0	30.4	0.5	0	0.2	5	9.3	0	0	0.4
Spec 8 coat	52	0	1.2	0.7	26	0.8	0	0.6	2.2	13.1	0	0	3.3
Spec 9	55	0	0	0	44.8	0	0	0	0.2	0	0	0	0
Spec 10 coat	53.5	0.5	1.2	0	36.7	0.2	0	0.2	4.7	3	0	0	0
Spec 11 coat	63.4	0	0	0	31.8	0	0	1.8	0.9	2.1	0	0	0
Spec 12 coat	56	0	0.7	0	33.2	0	0	0.3	2.3	7.6	0	0	0

Wood/straw2%Fe

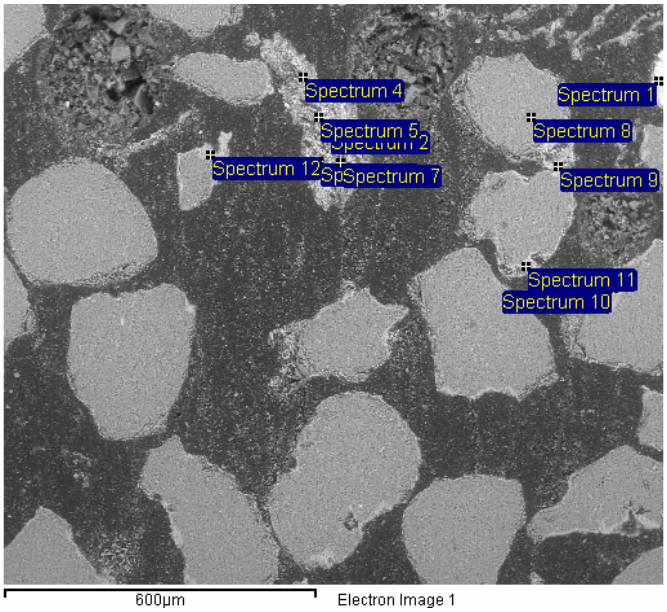

Figure 100. Picture with the points where the element quantification has been performed on the *wood/straw2%Fe* sample.

Table 11. Element quantification in the *wood/straw2%Fe* sample. "Coat" indicates that the quantification has been performed on a coating.

Spectrum/ wt%	O	Na	Mg	Al	Si	P	S	Cl	K	Ca	Ti	Mn	Fe
Spec 1	49.6	0.2	0.1	0.2	6.7	0.2	0.0	0.3	5.2	0.6	33.7	0.3	2.9
Spec 2 sludge	51.6	1.3	0.7	6.2	14.4	5.1	0.0	0.2	11.0	3.0	0.3	0.1	5.7
Spec 3	56.5	0.1	0.2	0.3	38.0	0.4	0.0	0.8	1.5	1.1	0.3	0.1	0.9
Spec 4 sludge	47.8	0.5	0.9	5.8	14.9	3.9	0.0	0.4	9.7	3.8	0.4	0.2	11.8
Spec 5 sludge	48.7	0.6	0.6	6.7	17.7	3.9	0.0	0.6	12.6	2.2	0.4	0.0	5.6
Spec 6 sludge	46.8	1.3	0.9	4.6	11.1	4.8	0.0	0.4	8.0	3.0	0.5	0.0	18.4
Spec 7 sludge	43.5	0.9	0.6	6.6	15.9	4.4	0.0	0.5	11.9	2.3	0.5	0.1	12.4
Spec 8	59.0	0.0	0.0	0.0	40.0	0.0	0.0	0.1	0.3	0.3	0.2	0.0	0.2
Spec 9 coat	49.5	0.4	0.9	0.8	29.0	2.0	0.0	0.2	8.0	6.2	0.4	0.2	2.3
Spec 10 coat	55.2	0.2	1.3	0.3	27.0	1.0	0.0	0.2	2.8	10.5	0.2	0.2	1.1
Spec 11 coat	49.9	0.4	0.7	0.9	27.3	2.0	0.0	0.2	8.5	5.8	0.2	0.1	4.1
Spec 12 coat	54.5	0.5	1.2	0.2	27.7	0.8	0.0	0.2	5.6	7.1	0.0	0.3	1.8

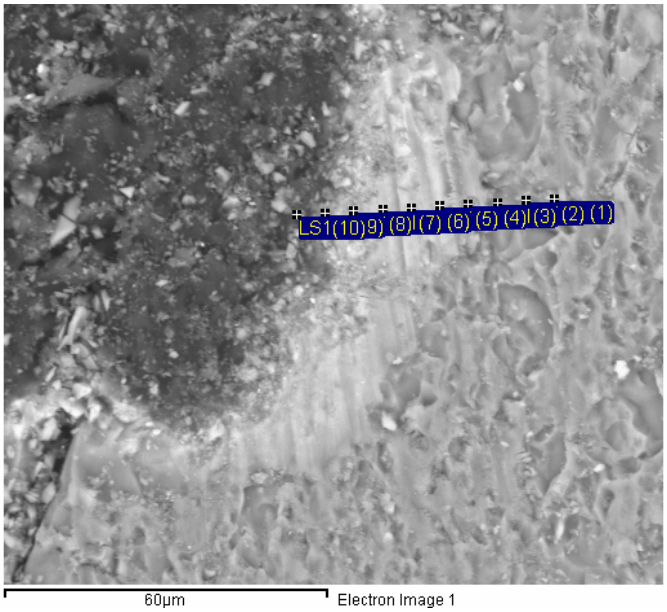

Figure 72. Picture with the points where the element quantification has been performed on the *wood/straw2%Fe* sample.

The second quantification for the wood/straw2%Fe sample has been performed in a line across the coating of the sand particle. LS1(1) - LS1(4) are points on the surface of the sand particle and LS1(5) – LS1(10) are points where element quantifications have been performed on the coating.

Table 12. Element quantification in the *wood/straw2%Fe* sample. "Coat" indicates that the quantification has been performed on a coating.

Spectrum/ wt%	O	Na	Mg	Al	Si	P	S	Cl	K	Ca	Ti	Mn	Fe
LS1(1)	51.4	0.0	0.1	0.0	47.1	0.0	0.0	0.1	0.5	0.5	0.2	0.0	0.2
LS1(2)	53.0	0.0	0.1	0.0	45.4	0.0	0.0	0.1	0.5	0.6	0.1	0.0	0.2
LS1(3)	55.9	0.0	0.1	0.0	42.5	0.0	0.0	0.1	0.6	0.6	0.1	0.0	0.2
LS1(4)	57.3	0.0	0.2	0.0	40.6	0.1	0.0	0.1	0.7	0.7	0.1	0.0	0.2
LS1(5) coat	51.6	0.5	0.9	0.0	34.3	0.2	0.0	0.2	6.1	4.9	0.2	0.4	0.9
LS1(6) coat	49.7	0.3	0.9	0.1	30.5	0.6	0.0	0.2	5.1	11.6	0.2	0.3	0.6
LS1(7) coat	48.4	0.4	1.0	0.1	32.0	0.7	0.0	0.2	7.2	8.6	0.2	0.4	0.9
LS1(8) coat	47.2	0.2	1.3	0.7	29.1	1.3	0.1	0.2	5.2	12.7	0.2	0.5	1.4
LS1(9) coat	50.0	0.2	1.2	0.8	27.7	1.5	0.0	0.2	5.6	10.7	0.3	0.3	1.7
LS1(10) coat	46.7	0.2	1.1	0.4	29.7	1.7	0.0	0.5	4.2	13.2	0.2	0.3	1.7

Wood/straw6%Fe

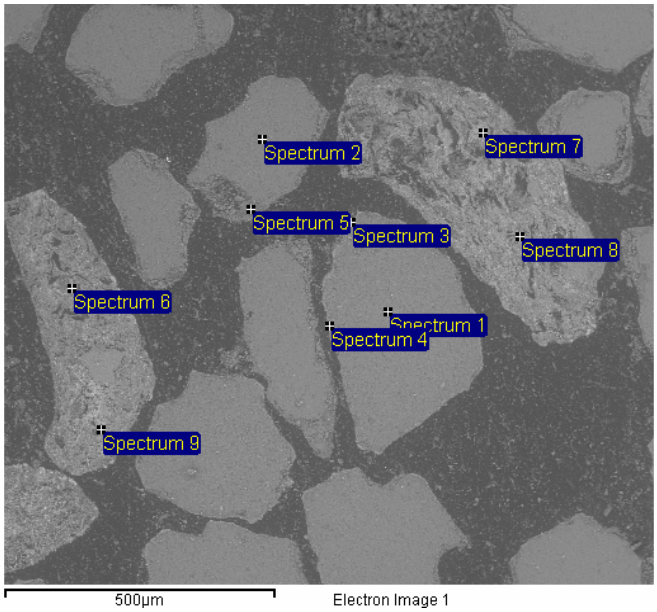

Figure 73. Figure with the points where the element quantification has been performed on the *wood/straw6%Fe* sample.

Spectrum 6, 7, 8 and 9 are placed on an ash particle that originates from sewage sludge. Spectrum 1 and 2 are quartz sand, spectrum 5 seems to be mostly quartz sand with traces of other elements. Spectrum 3 and 4 are coatings.

Table 13. Element quantification in the *wood/straw6%Fe* sample. "Coat" indicates that the quantification has been performed on a coating. "Sludge" indicates that the quantification has been performed on a sludge ash particle.

Spectrum/ wt%	O	Na	Mg	Al	Si	P	S	Cl	K	Ca	Ti	Fe
Spec 1	56.4	0	0	0	42.6	0.2	0	0.1	0.2	0.2	0	0.3
Spec 2	55.4	0	0	0	43.6	0.1	0	0.2	0.2	0.2	0	0.3
Spec 3 coat	51.5	0.1	0.8	0.9	35.6	1.2	0.1	0.3	1.6	6.1	0.1	1.8
Spec 4 coat	48.1	0.1	0.2	0.5	47	0.6	0	0.3	0.8	1.4	0	1.1
Spec 5	54.6	0	0	0.3	43.3	0.3	0	0.2	0.4	0.4	0	0.5
Spec 6 sludge	47.9	0.6	0.7	5.1	11.9	7.2	0	0.3	6.2	6.4	0.4	13.3
Spec 7 sludge	44	0.6	3.3	4.8	23.3	1.3	0	0.2	2.9	6.7	0.7	12.2
Spec 8 sludge	45.9	0.4	1.3	7.2	18.5	4.2	0.1	0.3	10.3	2.3	0.6	8.9
Spec 9 sludge	47.6	0.5	0.6	3.2	15.4	3	0	0.5	3.6	1.9	0.5	23.3

Wood/straw2%Al

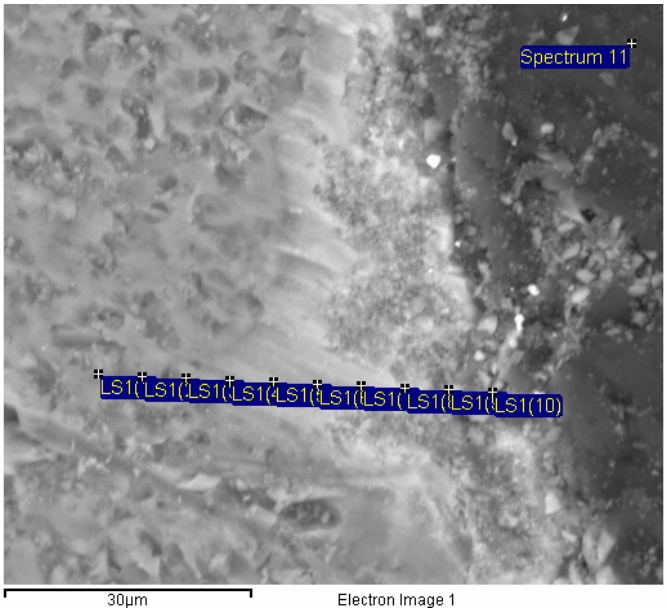

Figure 74. Figure with the points where the element quantification has been performed on the *wood/straw2%Al* sample

The quantification for the wood/straw2%Al sample has been performed in a line across the coating of the sand particle. LS1(1) - LS1(3) are points on the surface of the sand particle and LS1(4) – LS1(10) are points where element quantifications have been performed on the coating.

Table 14. Element quantification in the *wood/straw6%Al sample.* "Coat" indicates that the quantification has been performed on a coating.

Spectrum/ wt%	O	Na	Mg	Al	Si	P	S	Cl	K	Ca	Mn	Fe
LS1(1)	55.0	0.0	0.1	0.0	43.6	0.1	0.0	0.1	0.3	0.6	0.0	0.3
LS1(2)	52.2	0.0	0.1	0.0	45.9	0.1	0.0	0.2	0.5	0.7	0.0	0.3
LS1(3)	53.5	0.1	0.1	0.0	44.3	0.1	0.0	0.2	0.7	0.8	0.0	0.2
LS1(4) coat	51.0	0.3	0.6	0.0	42.0	0.1	0.0	0.1	3.0	1.8	0.7	0.4
LS1(5) coat	52.1	0.4	1.2	0.0	36.5	0.1	0.0	0.2	4.7	3.3	1.0	0.6
LS1(6) coat	51.9	0.5	1.4	0.0	34.3	0.2	0.0	0.1	5.7	4.0	1.3	0.5
LS1(7) coat	48.7	0.3	2.0	0.2	30.0	0.8	0.0	0.1	4.4	11.8	1.2	0.6
LS1(8) coat	52.5	0.2	4.5	0.8	20.8	2.8	0.2	0.2	2.0	13.7	1.1	1.2
LS1(9) coat	49.5	0.2	2.4	1.4	26.8	1.9	0.1	0.3	2.3	13.0	0.8	1.3
LS1(10) coat	43.2	0.0	2.6	0.9	27.7	2.4	0.2	0.4	1.9	17.1	1.7	1.9
Spectrum 11	58.1	0.0	0.6	0.4	31.1	0.6	0.0	3.6	1.2	3.0	0.0	1.5

Wood/straw6%Al

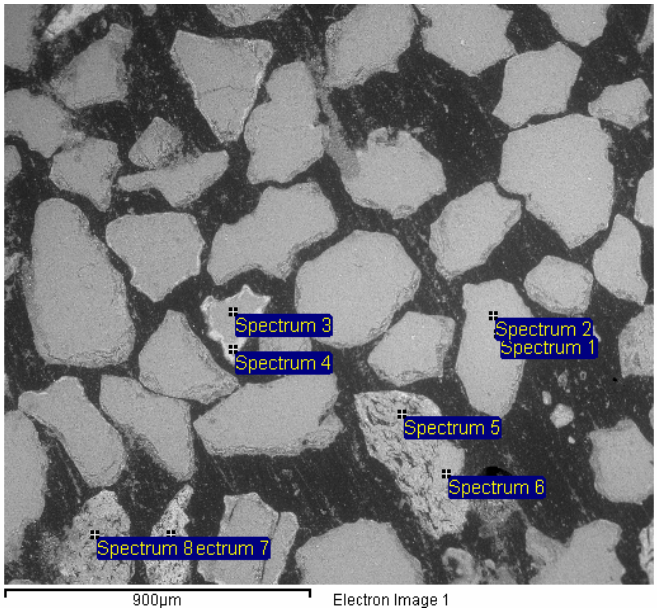

Figure 75. Figure with the points where the element quantification has been performed on the *wood/straw6%Al* sample.

Spectrum 5, 7 and 8 are ash from the sewage sludge. Spectrum 1, 2 and 3 are quartz sand and spectrum 4 is a coating.

Table 15. Element quantification in the *wood/straw6%Al* sample. "Sludge" indicates that the quantification has been performed on a sludge ash particle.

Spectrum	O	Na	Mg	Al	Si	P	S	Cl	K	Ca	Ti	Fe
Spect 1	53.4	0	0	0	46.5	0	0	0.1	0	0	0	0
Spect 2	53	0	0.1	0.2	46.1	0.1	0	0.1	0.2	0.2	0	0.1
Spect 3	54.7	0	0	0.1	44.2	0.2	0	0.1	0.4	0.4	0	0
Spect 4 coat	44.7	0.3	0.9	0.9	35.5	0.8	0	0.2	6.8	9.1	0.2	0.8
Spect 5 sludge	49.7	0.7	0.4	14.2	12	6.3	0	0.3	7.9	5.1	0.6	2.7
Spect 6	49	3.4	0	10.4	30.1	0.8	0	0.2	1.3	4.2	0	0.5
Spect 7 sludge	43.8	0.3	0.6	13	15.2	5.4	0	0.3	8.1	5.7	0.6	7.1
Spect 8 sludge	51.1	0.5	0.6	11.8	18.7	4.6	0	0.4	6	3.5	0.7	2.2

RDF0%MSSno.1

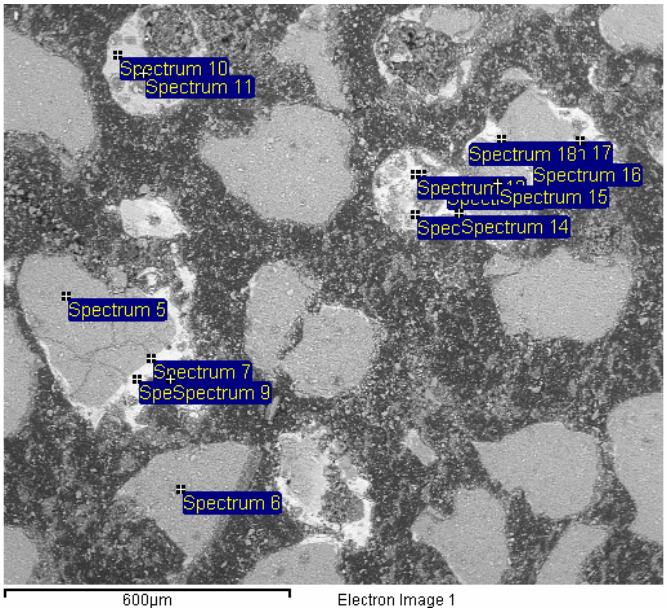

Figure 76. Picture with the points where the element quantification has been performed on *RDF0%MSSno.1*.

Table 16. Element quantification in the *RDF0%MSSno.1* sample. "Coat" indicates that the quantification has been performed on a coating.

Spectrum/ wt%	O	Na	Mg	Al	Si	P	S	Cl	K	Ca	Fe
Spec 1	48.4	0.9	0.6	4.9	22.7	0	0	0	0	20.7	2
Spec 2	52.8	0	0	6.3	22	0	0	0	0	19	0
Spec 3	50.2	1.3	0.8	5.5	20.1	0.4	0	0.4	0.3	18.7	1.4
Spec 4	54.9	0.5	0.2	0.8	38.4	0.1	0	0.6	0.3	3.4	0.5
Spec 5	54.8	0	0	0.3	44.2	0	0	0.2	0	0.6	0
Spec 6	57.5	0	0	0	41.8	0	0	0.2	0	0.5	0
Spec 7 coat	53.1	0.9	0.6	2.4	24.8	0.2	0	0	0.3	16.1	0.8
Spec 8 coat	49.5	1.3	1	3.5	21.9	0.7	0	0	0.3	18.8	1.3
Spec 9 coat	46.5	1	1	4	21.1	0.5	0	0.2	0.2	22.5	1.5
Spec 10 part	51.2	5.2	0.7	0.7	34.2	0	0	0.2	2.2	5.7	0
Spec 11 part	50.9	5.3	0.6	0.7	34.3	0	0	0.2	2.2	6	0
Spec 12 part	48.3	2.1	1.1	6.6	21	0.2	0	0.2	0.2	18.5	1.2
Spec 13 part	47.6	1.6	0.7	3.9	31	0	0	0.3	1.6	7	5.2
Spec 14 part	59.2	1.9	0.9	2	26.4	0.2	0	0.2	0.5	6.9	1.5
Spec 15	56.1	0	0	0.3	40.7	0	0	0.1	0.2	1.1	1.3
Spec 16 coat	50.7	1.6	0.5	2.8	31.7	0.3	0	0.4	1.5	5.8	3.9
Spec 17 coat	50.4	2.1	1.1	4.1	25.8	0.3	0	0.2	0.9	10.3	3.3
Spec 18 coat	52.1	2.8	1	2.4	25.2	0.4	0	0	1.2	11.8	2

RDF0%MSSno.2

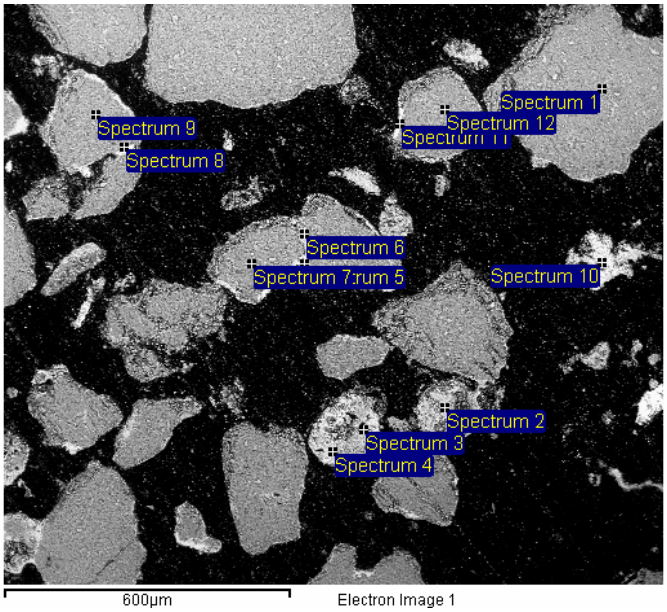

Figure 77. Picture with the points where the element quantification has been performed on *RDF0%MSSno.2*.

Table 17. Element quantification in the *RDF0%MSSno.2* sample. "Coat" indicates that the quantification has been performed on a coating. "Sludge" indicates that the quantification has been performed on a sludge ash particle.

Spectrum wt%	O	Na	Mg	Al	Si	P	S	Cl	K	Ca	Ti	Fe
Spec1	52.2	0	0	0	47.1	0	0	0.3	0	0.6	0	0
Spec2 part	46.7	1	3.9	6.7	22.6	0	0	0.2	0.9	12	1.5	4.5
Spec3 part	52.3	1.9	0.4	5.3	23.2	0.2	0	0.3	1.9	12.8	1	0.6
Spec4 part	60.7	0.7	0.3	2.5	28.4	0	0	0.6	1	5.1	0.4	0.6
Spec5 coat	52.4	1.8	1.1	2.1	23	0.3	0	0.2	0.3	15	3	0.9
Spec6 coat	53.5	1.6	0.6	1	27	0.3	0	0.2	0.6	14.2	0.6	0.5
Spec7 coat	54.8	0	0	0	44.1	0	0	0	0	0.8	0.3	0
Spec8	52.1	0.4	0	0.2	43.7	0	0	0.2	0.2	1.7	1	0.3
Spec9	52.8	0	0	0	45.5	0	0	0.4	0	0.7	0	0
Spec10 part	48.9	1.4	0.3	0.8	8.9	0	8.6	3.3	0.5	27	0	0.3
Spec11	50.1	0.6	0.8	1.2	23.4	0.5	0	0.3	0	21	1	1.2
Spec12	50.5	0	0.2	0	47.3	0	0	0.3	0	1.7	0	0

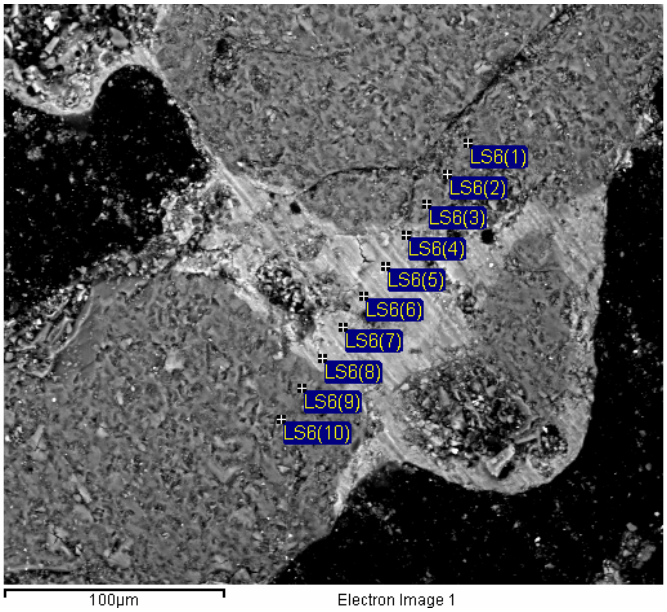

Figure 78. Picture with the points where the element quantification has been performed on *RDF0%MSSno.2.*

Table 18. Element quantification in the *RDF0%MSSno.2* sample. "Coat" indicates that the quantification has been performed on a coating.

Spectrum/ wt%	O	Na	Mg	Al	Si	P	S	Cl	K	Ca	Ti	Fe
LS6(1)	52.2	0	0	0.2	45.9	0	0	0.2	0	1.3	0	0.2
LS6(2)	51.4	0.3	0	0.2	46.2	0	0	0	0	1.5	0.2	0.2
LS6(3)	47.5	0.6	0	0.4	48.7	0	0	0	0	2.5	0	0.3
LS6(4) coat	49.3	1.9	1.1	1.9	25.3	3.2	0	0.4	0.9	14.1	0.5	1.4
LS6(5) coat	48.8	2.8	2.1	3.3	24.8	0.7	0	0	0.9	12.3	1.4	2.8
LS6(6) coat	47.4	2.2	0.9	6.4	19.9	0.5	0	0.3	0.2	18.8	1.2	1.7
LS6(7) coat	48.8	3.2	0.8	8.8	20.2	0.7	0	0.3	0.3	14.6	1.2	1.2
LS6(8) coat	46.7	1	0.9	1.8	25.3	0.3	0	0.2	0.3	19.2	1.9	2.5
LS6(9)	53.8	0	0	0.2	44.1	0	0	0	0	2	0	0
LS6(10)	54.3	0	0	0.2	43.8	0	0	0.2	0	1.5	0	0

RDF 2%Fe

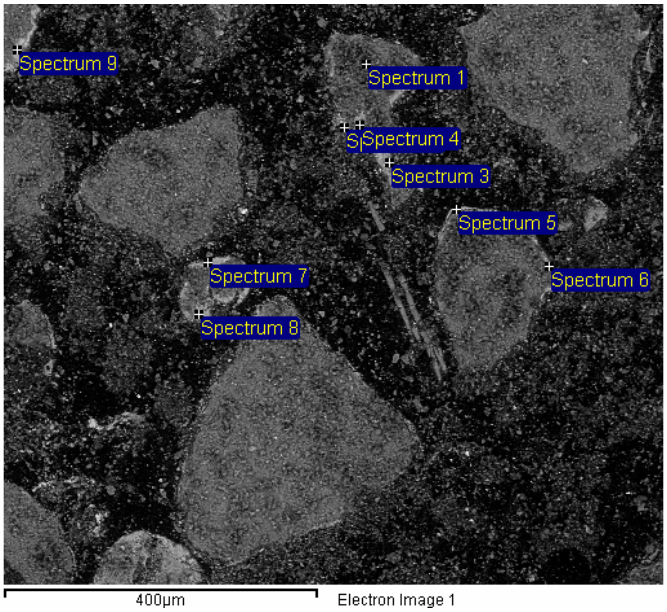

Figure 79. Picture with the points where the element quantification has been performed on *RDF2%Fe.*

Table 19. Element quantification in the *RDF2%Fe* sample. "Coat" indicates that the quantification has been performed on a coating.

Spectrum wt%	O	Na	Mg	Al	Si	P	S	Cl	K	Ca	Ti	Fe
Spec 1	41.01	0	0	0.53	55.02	0	0	0.65	0	2.16	0	0.63
Spec 2 coat	42.69	0.54	0.68	2.34	27.24	0.95	0.29	0.83	0	19.14	2.72	2.58
Spec 3 coat	53.06	0	0.55	1.12	23.81	0.39	0	0.62	0	18.39	0.94	1.11
Spec 4 coat	48.93	1.17	0.5	1.51	33.33	0	0	0.45	1.02	10.71	1.1	1.28
Spec 5 coat	43.68	0.9	0.49	1.45	26.8	0	0	0.4	0.44	18.63	5.39	1.81
Spec 6 coat	50.78	0.96	0.5	1.74	29.58	0.48	0	0.58	0.48	11.36	2.81	0.73
Spec 7 coat	48.18	1.63	1.02	2.48	24.45	0.97	0.76	0.36	0.25	15.57	1.02	3.32
Spec 8 coat	46.86	1.46	1.13	2.97	24.98	0.64	0.56	0.42	0	17.11	0.69	3.18
Spec 9 coat	51.22	0	0.38	0.28	38.83	0	0	0.85	0	7.97	0	0.47

RDF6%Fe

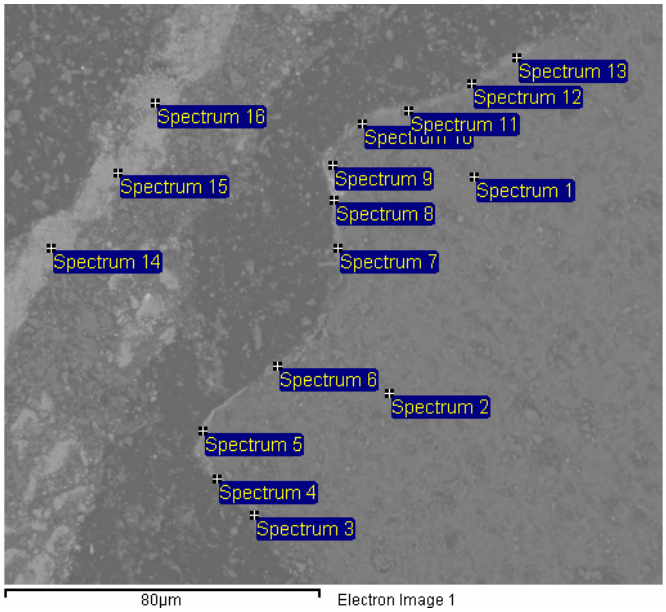

Figure 80. Picture with the points where the element quantification has been performed on *RDF6%Fe*.

Table 20 Element quantification in the *RDF6%Fe* sample. "Coat" indicates that the quantification has been performed on a coating.

Spectrum/ wt%	O	Na	Mg	Al	Si	P	S	Cl	K	Ca	Ti	Fe
Spec 1	58.65	0.25	0	0.29	39.71	0	0	0.19	0	0.91	0	0
Spec 2	57.27	0.24	0	0.45	40.97	0	0	0.22	0	0.85	0	0
Spec 3 coat	51.22	0.37	0.65	1.24	20.92	0.81	0.4	0.81	0	16.23	3.48	3.89
Spec 4 coat	50.67	0.51	0.7	2.35	21.34	1.48	0.75	0.93	0	15.8	1.12	4.36
Spec 5 coat	49.38	0.29	1.15	1.88	18.04	1.75	1.39	1.2	0	16.21	0.77	7.94
Spec 6 coat	58.27	0.33	0	0.47	36.78	0.22	0	0.34	0	3.6	0	0
Spec 7 coat	51.78	0.24	0.55	1.06	25.1	0.44	0.22	0.35	0	15.17	0.37	4.71
Spec 8 coat	53	0.28	0.74	1.12	22.17	1.17	0.44	0.9	0	14.66	0.37	5.15
Spec 9 coat	58.96	0.23	0	0.39	38.18	0	0	0.39	0	1.85	0	0
Spec 10 coat	51.93	0.28	0.33	1.19	35.75	0.49	0.24	0.49	0	4.95	0	4.35
Spec 11 coat	58.99	0.41	0	0.5	37.94	0	0	0.3	0.18	1.68	0	0
Spec 12 coat	57.88	0.21	0.25	0.49	34.99	0	0	0.21	0.26	5.71	0	0
Spec 13 coat	56.83	0.32	0	0.51	37.04	0.3	0	0.38	0	2.33	0	2.29
Spec 14 coat	45.53	0.65	0	0.97	15.06	0	0	0.31	0	2.52	0	34.96
Spec 15 coat	61.38	0.55	0	0.88	17.57	0.32	0	0.48	0	2.95	0	15.86
Spec 16 coat	45.94	0.42	0	1.03	15.38	0.38	0.28	0.42	0	7.03	0	29.13